Review

Electrochemical Approach to the Mechanistic Study of Proton-Coupled Electron Transfer

Cyrille Costentin

Chem. Rev., **2008**, 108 (7), 2145-2179 • DOI: 10.1021/cr068065t • Publication Date (Web): 11 July 2008

Electrochemical Approach to the Mechanistic Study of Proton-Coupled Electron Transfer

Cyrille Costentin*

Laboratoire d'Electrochimie Moléculaire, Unité Mixte de Recherche Université, CNRS No, 7591, Université Paris Diderot-Paris 7, 2 place Jussieu, 75251 Paris Cedex 05, France

Received September 3, 2007

Contents

1. Introduction

The coupling between electron and proton transfers has a long experimental and theoretical history in chemistry and biochemistry. To take just one example, the fact that acceptance of an electron triggers the addition of an acid or the removal of a base and vice versa for oxidations towers over all understanding of organic electrochemistry. Proton-coupled electron transfer (PCET) reactions also play a critical role in a wide range of biological processes, including enzyme reactions, photosynthesis, and respiration. A recent impressive review[1] describes PCET reactions and phenomena.

PCET is employed here as a general term for reactions in which both an electron and a proton are transferred, either in two separate steps or in a single step. Reactions in which the electron and proton transfer between the same donor and acceptor, that is, hydrogen atom transfer, are, of course, not considered here because we consider electrochemical PCET reactions in which electrons are flowing into or from an electrode while protons are transferred between acid and base.

Molecular electrochemistry, through nondestructive techniques such as cyclic voltammetry, has proved to be very useful in characterizing electron transfers and deciphering mechanisms in which chemical reactions are associated with electron transfer. Therefore, it has been a convenient tool for the mechanistic study of reactions in which electron transfer is coupled to proton transfer, that is, in which an electron leaves or enters an electrode while a proton is transferred from or to the redox species. Until recently, PCET has been mostly thought of as stepwise electron and proton transfer (ET-PT or PT-ET). We thus review in an initial section (section 2) the analysis of such stepwise mechanisms both in aprotic media and in water. In aprotic media,

Cyrille Costentin was born in Normandy, France, in 1972. He received his undergraduate education at Ecole Normale Supérieure (Cachan, France) and pursued his graduate studies under the guidance of Prof. Jean-Michel Savéant and Dr. Philippe Hapiot at the University of Paris-Diderot (Paris 7), where he received his Ph.D. in 2000. After a year as a postdoctoral fellow at the University of Rochester, working with Prof. J. P. Dinnocenzo, he joined the faculty at the University of Paris-Diderot as an associate professor. He was promoted to professor in 2007. His interests include mechanisms and reactivity in electron transfer chemistry with particular recent emphasis on electrochemical and theoretical approaches to proton-coupled electron transfer processes.

* E-mail address: cyrille.costentin@univ-paris-diderot.fr.

10.1021/cr068065t CCC: $71.00
Published on Web 07/11/2008

hydrogen bonding often precedes proton transfer. Therefore, characterization of the dichotomy between hydrogen bonding and proton transfer as associated with electron transfer is necessary to fully describe PCET processes and is thus presented first (section 2.1). In water, specific mechanistic issues on PCET arise because water itself may act as both a donor and acceptor of protons. This role may also be played by OH^- (or H_3O^+) and by the basic (or acidic) components of the buffers in which the experiments are often carried out. Moreover, proton transfers are fast and often assumed to be at equilibrium in water. Therefore, PCET in water is presented in section 2.2. Because redox couples tethered to an electrode afford an excellent means of observing heterogeneous electron transfer kinetics with no complications caused by mass transfer effects, such systems have been used to analyze the effects of proton transfer preceding or following an electron transfer (section 2.3). The vision of PCET as stepwise processes has, however, been recently questioned, and extensive work has been done on both the theoretical and experimental aspects of a competitive concerted pathway, that is, a one-step mechanism in which proton and electron transfer are concerted. We term the latter mechanism concerted proton and electron transfer (CPET). Other terms have been used in the literature to describe the same mechanism: electron transfer−proton transfer (ETPT),[2] electron−proton transfer (EPT),[3] or multiple-site electron−proton transfer (MS-EPT).[1] The specific electrochemical approach to the analysis of CPET is reviewed in section 3.

Proton transfer and its coupling to electron transfer in most biological systems is fundamental. Electrochemistry, through protein film voltammetry (PFV), has contributed widely to the establishment of how individual proton transfers occur at the molecular level and how they are coupled to electron transfer. This issue is reviewed in section 4.

2. Coupling of Electrode Electron Transfers with Proton Transfers

2.1. Hydrogen Bonding versus Proton Transfer in Aprotic Media

In well-buffered media many redox processes involve changes in proton content and provide reversible two-electron redox systems in which potentiometric or polarographic equilibrium potentials vary with pH in a straightforward Nernstian manner.[4] This behavior is conveniently summarized in potential−pH diagrams, commonly referred to as Pourbaix diagrams,[5] which show regions of existence for the various redox and protonated species. Those aspects will be detailed in section 2.2. However, understanding the environmental factors that regulate the potentials and reaction pathways of the various species appearing in a proton-coupled redox couple in natural systems requires investigation in nonaqueous media. For example, aprotic solvents are useful in mimicking the nonpolar environments in the cell where many of the biological electron transfer processes occur. Among these factors, hydrogen bonds are particularly important because they are ubiquitous in biological systems and provide essential recognition and structural and control elements needed to coordinate and run the complex molecular machinery required for life. Moreover, hydrogen bonding can be viewed as a first step toward proton transfer.

It is well-known that quinone can promote hydrogen-bonding interactions and/or proton transfer.[6] Several recent studies have been reported showing hydrogen-bonding and protonation effects on the redox behavior of quinones through electrochemical investigations. In addition to their intrinsic chemical interest, these studies are particularly important in view of the key biological functions of quinone-based couples as electron−proton transfer agents in the the oxidative phosphorylation of ADP to ATP, or photosynthesis.[7] With regard to these functions, hydrogen bonding plays an important role in the stabilization of the reduced species of quinones. In dry, neutral, aprotic media, quinones (Q) typically show two cathodic chemically reversible waves, which correspond to the formation of $Q^{\bullet -}$ and Q^{2-}, respectively. The potentials of these reductions depend on several parameters such as solvent,[8] supporting electrolyte,[6] and electrode material. In the presence of acidic additives, the course of electroreduction is remarkably complex, as was found in numerous studies of the effect of acid strength, concentration, and quinone basicity. Those studies have been interpreted on the basis of a square-scheme diagram (Scheme 1). The horizontal transformations correspond to electron exchanges, whereas the vertical transformations involve proton transfers. Additional complications, not considered in Scheme 1, involve the possible role of homogeneous electron exchange.[9]

Scheme 1

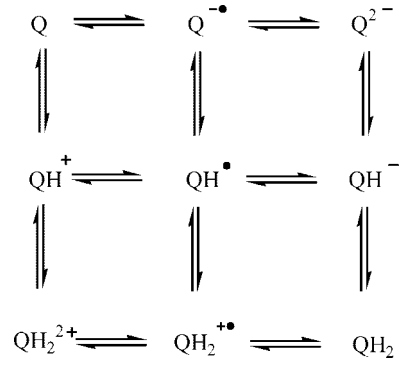

However, a remarkable systematic electrochemical study analyzing effects of weak proton donors as well as relatively strong acids on the reduction of quinone has allowed a useful classification of behaviors.[10] Prior to the description of this classification, several deviations from ideality in the reduction of quinones in dry aprotic media have to be mentioned. The most common of these are that the second wave reduction peak is shorter than predicted, and that extra current, as compared to the current obtained from simulation of two stepwise electron transfers, appears in the region between the two cathodic peaks. The origin of this last observation is still not clear. Whereas reaction involving adsorbed species has been discarded,[11] reduction of a dimer formed by the reaction between two semiquinones has been proposed.[10] With regard to the relatively small height of the second reduction peak, the assumption of a complexation reaction between a quinone and its dianion seems to be the more appropriate among several assumptions. The largest deviation from ideality has been reported for an *o*-benzoquinone, 3,5-di-*tert*-butyl-1,2-benzoquinone, for which the second voltammetric peak appears to be one-fourth as large as expected.[11] This observation has been interpreted in terms of a concerted electron and proton transfer (CPET), and it will be detailed in section 3.[12] Returning to the classification effect of acidic additives, it is worth mentioning first that the effect of these agents depends essentially on the degree of hydrogen-

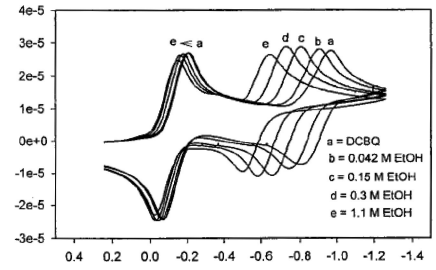

Figure 1. Cyclic voltammograms of DCBQ (see Chart 1) at different concentrations of ethanol in PhCN. Scan rate: 100 mV/s. Reprinted with permission from ref 10. Copyright 1997 American Chemical Society.

bonding interactions. Weakly basic quinones paired with strongly bonding additives behave similarly to strongly basic quinones with weakly bonding agents.

2.1.1. Effect of Weak Hydrogen-Bonding Agents on Quinone Reduction

Addition of weak hydrogen-bonding (HBa) agents such as ethanol results in positive shifts of both reduction steps of quinones. These shifts increase with additive agent concentration, but no change in electrochemical reversibility is observed (Figure 1).[10]

Protonation of quinone monoanion can be ruled out on the basis of the unfavorable pK_a value of semiquinone. Potential shifts are assigned to fast hydrogen-bonding equilibria involving mono- and dianions, whereas the hydrogen-bonding constant with the quinone itself is expected to be negligible (Scheme 2). For the sake of simplicity, only one stoichiometry is considered for each adduct, that is, 1:*n* for anions and 1:*m* for dianions.

Equilibrium constants as well as the number of agents associated per anion (*n* and *m*, respectively) may be determined from the displacements of the peaks as a function of hydrogen-bonding agent concentration according to eqs 1 and 2[13]

$$E^{0'}_{Q/Q^{\bullet-}} = E^{0}_{Q/Q^{\bullet-}} + \left(\frac{RT}{F}\right)\ln(1 + K^{(1)}_{eq}[HBa]^{n}) \qquad (1)$$

$$E^{0'}_{Q^{\bullet-}/Q^{2-}} = E^{0}_{Q^{\bullet-}/Q^{2-}} + \left(\frac{RT}{F}\right)\ln(1 + K^{(2)}_{eq}[HBa]^{m}) \qquad (2)$$

where $E^{0}_{Q/Q^{\bullet-}}$ or $E^{0}_{Q^{\bullet-}/Q^{2-}}$ and $E^{0'}_{Q/Q^{\bullet-}}$ or $E^{0'}_{Q^{\bullet-}/Q^{2-}}$ are the quinone's standard potentials in the absence and presence of hydrogen-bonding agent, respectively, and $K^{(1)}_{eq}$, $K^{(2)}_{eq}$ are the equilibrium constants for hydrogen-bonded complex formation. Several examples of *m*, *n*, $K^{(1)}_{eq}$ and $K^{(2)}_{eq}$ are listed in Table 1. The same behavior is observed when 1,4-benzoquinone (BQ) is reduced in the presence of alkylated nucleobases in DMSO.[14,15] For example, for 1-octylthymine, the maximum number of molecules associated with the semiquinone is 2 and the association constants are 298 and

Scheme 2

$$Q + e \rightleftharpoons Q^{-\bullet}$$

$$Q^{-\bullet} + n\,HBa \rightleftharpoons Q^{-\bullet}(HBa)_n \qquad fast$$

$$Q^{-\bullet}(HBa)_n + e \rightleftharpoons Q^{2-}(HBa)_n$$

$$Q^{2-}(HBa)_n + (m\text{-}n)\,HBa \rightleftharpoons Q^{2-}(HBa)_m \qquad fast$$

Chart 1

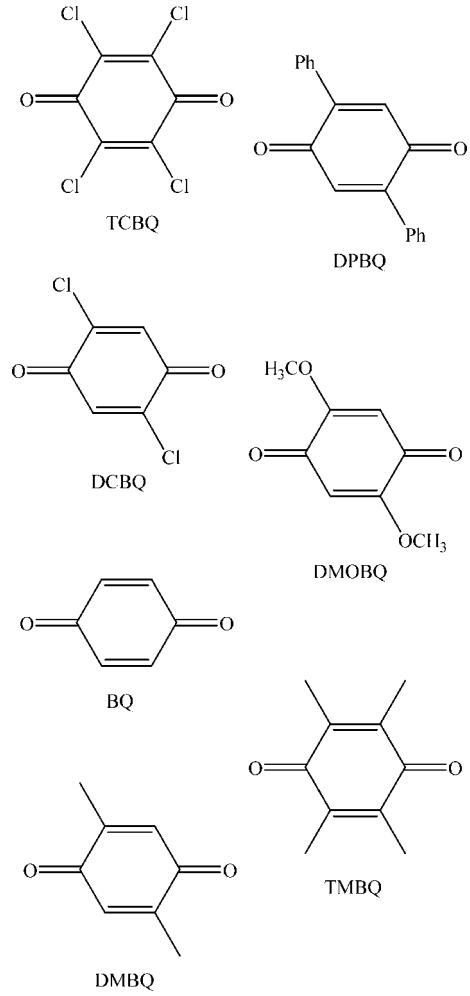

0.272 M^{-1} for the first and second molecules of 1-octylthymine, respectively.[14] The dianion is also hydrogen-bonded in the case of 9-octyladenine and 1-octylcytosine, but it is protonated in the case of 1-octylthymine. However, with this last system, a nonconventional wave shape is observed, reminiscent of that already described above for the *o*-benzoquinone, 3,5-di-*tert*-butyl-1,2-benzoquinone, and which has been interpreted in terms of a CPET.

Positive shifts in the redox potential of quinones in the presence of hydrogen-bond donors may be large, as is the case in the bonding between ureas and quinone radical anions, for which the binding constant is ca. 900 M^{-1}. To produce such strong binding it is necessary to have two carbonyls aligned in the same direction as well as two hydrogen donors on the guest that can also align in the same direction (Scheme 3).[16] Such specific interactions have been used to develop an aromatic urea sensor that could be used to detect and measure the concentration of such ureas in the millimolar range in organic media.[17]

2.1.2. Effect of Mildly Hydrogen-Bonding Agents on Quinone Reduction

A different type of behavior is observed upon the addition of a mildly hydrogen-bonding agent such as trifluoroethanol (TFE) to quinones.[10] In this case, the positive shift is accompanied by increasing height of the first peak and broadening and irreversibility of the second wave (Figure 2). As already mentioned, this change in behavior obviously

Table 1. Reduction of Quinones in Presence of Hydrogen-Bonding Agents[10]

quinone[a]	solvent	HBa	n	m	$K_{eq}^{(1)b}$	$K_{eq}^{(2)b}$
TCBQ	CH_3CN	EtOH	c	3.1	c	6.3×10^3
DCBQ	CH_3CN	EtOH	c	3.0	c	1.2×10^4
BQ	PhCN	EtOH	1.2	5.2	50	1.0×10^9
DMBQ	PhCN	EtOH	1.4	4.7	30	10^8
DPBQ	PhCN	EtOH	1.1	4.8	50	2.0×10^8
DMOBQ	PhCN	EtOH	2.03	6.5	370	2.2×10^{11}
TMBQ	PhCN	EtOH	1.3	5.5	85	8.5×10^9

[a] See Chart 1. [b] Units of $K_{eq}^{(1)} = M^{-n}$ and $K_{eq}^{(2)} = M^{-m}$. [c] Potential shift very small.

depends on the quinone basicity: for quinones with low basicity, using TFE results in the same effect as described in the previous section.

The increase in the first peak current is attributed to disproportionation of the semiquinone:[9,10]

$$2Q^{\bullet -} \rightleftharpoons Q + Q^{2-}$$

This reaction is indeed made easier by the shift in the semiquinone reduction potential caused by strong hydrogen bonding of the dianion, thus leading to a hydrogen-bonding agent *catalyzed* disproportionation (Scheme 4).

This overall disproportionation may be slow on the voltammetric time scale, but it can occur to a significant extent during a prolonged electrolysis.[12] If the dianion is a sufficiently powerful base, it is likely to be protonated:

$$Q^{2-}(HBa)_m + HBa \rightleftharpoons HQ^- + Ba^- + mHBa$$

Therefore, it has been proposed that the mechanism might better be referred as a hydrogen-bonding agent *promoted* disproportionation rather than a hydrogen-bonding agent *catalyzed* disproportionation because HBa, unlike a catalyst, is destroyed during the reaction.[12,18] Thanks to protonation of the dianion, the energetically unfavorable disproportionation of the quinone anion radical is converted into a downhill reaction. Moreover, protonation of the dianion is responsible for chemical irreversibility of the second wave.

With an even stronger hydrogen-bonding agent (or quinone of stronger basicity), a new reduction peak prior to the original first reduction may be observed at low hydrogen-bonding agent concentration (Figure 3).[10]

This new peak is attributed to the reduction of hydrogen-bonded quinone, the formation of which is confirmed by a slight red shift of the UV−vis spectrum of the quinone upon addition of a hydrogen-bonded agent. Protonation of the quinone has been rejected on the basis of its low pK_a. Note, however, that this prewave could perhaps also be due to protonation of $Q^{\bullet -}$, but this can be ruled out because the hydrogen-bonding agent is not acidic enough and the reaction is therefore thermodynamically unfavorable.

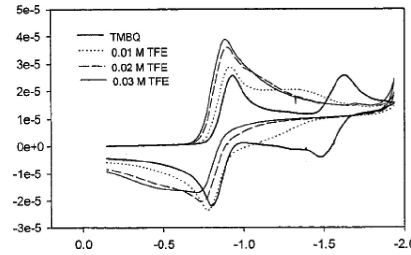

Figure 2. Cyclic voltammograms of TMBQ (see Chart 1) at different concentrations of trifluoroethanol (TFE) in PhCN. Scan rate: 100 mV/s. Reprinted with permission from ref 10. Copyright 1997 American Chemical Society.

2.1.3. Effect of Strong Acid on Quinone Reduction

In the case of a weakly basic quinone, such as chloranil (TCBQ, see Chart 1), in the presence of a strong acid (HA), such as trifluoroacetic acid, a cathodic peak prior to the first original reduction peak grows in height at the expense of the original peak (Figure 4).[10] As in the case discussed above, this suggests the presence of two reducible species in equilibrium.

Again protonation of the quinone is rejected and a hydrogen-bonded complex is preferred. Actually, the prewave can be caused by reduction of this Q(HBa) complex and/or a positive shift of quinone reduction caused by protonation of $Q^{\bullet -}$ limited by HA diffusion. The growth of the peak, up to two electrons, indeed reflects protonation of the anion radical $Q^{\bullet -}$ to yield the neutral radical $QH^{\bullet}$, which is easier to reduce than the starting molecule. As soon as it is produced, the $QH^{\bullet}$ neutral radical is reduced to QH^-, which then protonates to give QH_2. A two-electron ECE process (actually, an ECEC process) is thus triggered, which may be in competition with its homogeneous counterpart (DISP process)[19] but different from the disproportionation seen previously (Scheme 5). Note that a concerted (CPET) route for Q(HA) reduction to $QH^{\bullet} + A^-$ can also be suggested. It is thus concluded that increasing acid strength with a weakly basic quinone leads to a mechanistic switch from hydrogen bonding of the semiquinone followed by its disproportionation (Scheme 4) to semiquinone protonation triggering an ECE−DISP process (Scheme 5). Such behavior has been observed upon the addition of acids on several quinones in aprotic solvents.[16,20,21] Reduction of 1,4-benzoquinone in the presence of 9-ethylguanine in DMSO follows the same mechanism, in contrast to the behavior showed with other alkylated nucleobases.[15]

In this context, determination of the hydrogen-bonding equilibrium constant through the variation of the quinone redox potential caused by this interaction is not easy. Focusing on apparent diffusion coefficients has thus been proposed.[22] Indeed, the complex should have a smaller diffusion coefficient and consequently lead to the observation

Scheme 3

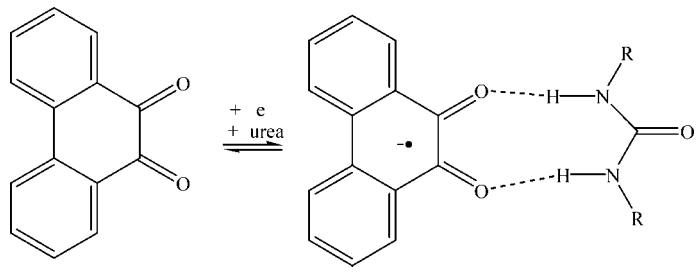

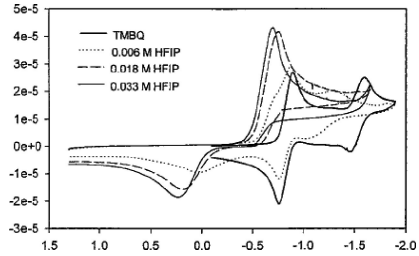

Figure 3. Cyclic voltammograms of TMBQ (see Chart 1) at different concentrations of 1,1,1,3,3,3-hexafluoro-2-propanol (HFIP) in PhCN. Scan rate: 100 mV/s. Reprinted with permission from ref 10. Copyright 1997 American Chemical Society.

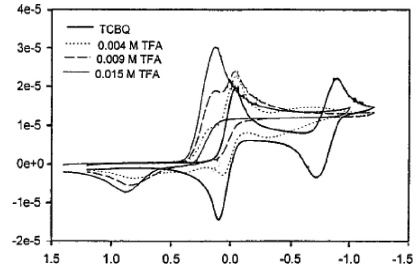

Figure 4. Cyclic voltammograms of TCBQ (see Chart 1) at different concentrations of trifluoroacetic acid (TFA) in PhCN. Scan rate: 100 mV/s. Reprinted with permission from ref 10. Copyright 1997 American Chemical Society.

of a current variation. In the absence of HA, a one-electron wave is observed for the reduction of quinone, and the peak current is given by eq 3.[23]

$$i_{p,Q} = 0.446FSC_Q D_Q^{1/2}(Fv/RT)^{1/2} \quad (3)$$

In the presence of HA, a two-electron wave corresponding to an ECE−DISP mechanism leads to eq 4.[24]

$$i_{p,Q+HA} = 0.992FSC_Q D_{Q+HA}^{1/2}(Fv/RT)^{1/2} \quad (4)$$

Scheme 4

$$Q + e \rightleftharpoons Q^{-\bullet}$$

$$Q^{-\bullet} + n\,HBa \rightleftharpoons Q^{-\bullet}(HBa)_n$$

$$2\,Q^{-\bullet}(HBa)_n \rightleftharpoons Q + Q^{2-}(HBa)_n + n\,HBa$$

$$Q^{2-}(HBa)_n + (m-n)\,HBa \rightleftharpoons Q^{2-}(HBa)_m$$

Scheme 5

$$Q + HA \rightleftharpoons Q(HA)$$

$$Q(HA) + e \rightleftharpoons Q^{-\bullet}(HA)$$

$$Q^{-\bullet}(HA) \longrightarrow QH^{\bullet} + A^-$$

$$QH^{\bullet} + e \rightleftharpoons QH^-$$

and / or

$$QH^{\bullet} + Q^{-\bullet}(HA) \rightleftharpoons QH^- + Q(HA)$$

$$QH^- + HA \longrightarrow QH_2 + A^-$$

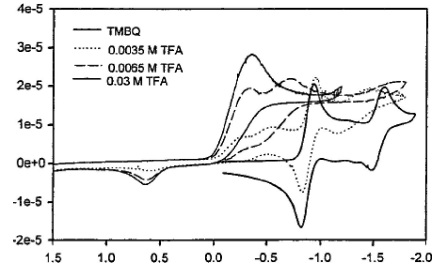

Figure 5. Cyclic voltammograms of TMBQ (see Chart 1) at different concentrations of TFA in PhCN. Scan rate: 100 mV/s. Reprinted with permission from ref 10. Copyright 1997 American Chemical Society.

Chart 2

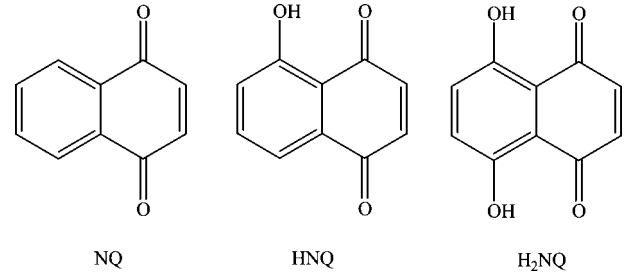

Thus, from the apparent number of electrons, n_{app}, the diffusion coefficient of the complex can be estimated as given in eq 5.

$$n_{app} = 2.2\frac{D_{Q+HA}^{1/2}}{D_Q^{1/2}} \quad (5)$$

Provided that an empirical correlation between the diffusion coefficient and molecular weight has been done, the stoichiometry of the complex can be deduced. Then, evaluation of the association equilibrium constant between Q and HA is possible from the peak current measured over a range of HA concentrations. As an example of this procedure, it was determined that 1,4-benzoquinone and benzoic acid can associate with a 1:1 stoichiometry and an association constant between 10 and 15 M^{-1}.[25]

Addition of a strong acid to a more basic quinone, for example, TMBQ (see Chart 1), leads to another prior cathodic peak at a more positive potential (Figure 5).[10] This is attributed to the reduction of the protonated quinone. At high concentration of acid, most of the quinone is protonated and only the more positive peak is observed. It is thus concluded that increasing acid strength and/or quinone basicity leads for this quinone to a switch from hydrogen-bonded complex formation to proton transfer prior to reduction.

To conclude, as concerns the actual knowledge of the dichotomy between hydrogen bonding and proton transfer coupled to electron transfer, it can be noted that the above-mentioned investigations give a remarkable picture of quinone reduction in aprotic media, but that neither a kinetically based mechanism analysis nor a rate constant determination has been reported. Work remains to be done to fill this gap.

2.1.4. Effect of Intramolecular Hydrogen Bonding on Quinone Reduction

In the specific case of α-phenolic quinones, the possibility of intramolecular hydrogen-bonding stabilization of electro-

chemically generated quinone radical anions provokes a shift of the reduction potentials toward less negative potentials. This effect may have an impact on the mechanistic behavior of α-phenolic quinone reduction in the presence of an external proton donor. This has been analyzed through cyclic voltammetry studies of 1,4-naphthoquinone (NQ), 5-hydroxy-1,4-naphthoquinone (HNQ), and 5,8-dihydroxy-1,4-naphthoquinone (H_2NQ) (Chart 2), both in the absence and in the presence of methanol and acetic acid.[26]

It has been demonstrated that the positive shift of the reduction potentials in the absence of proton donor is caused by intramolecular hydrogen bonding in the quinone anion radical, whereas the inductive effect of the OH groups is marginal. In the presence of methanol, the dianion is stabilized through intermolecular hydrogen bonds, and the corresponding association constants are determined from the potential shift. The H_2NQ dianion exhibits the lowest association constants, thus suggesting that intramolecular hydrogen bonds interfere before the establishment of intermolecular interactions with methanol. In the presence of a stronger proton donor, such as acetic acid, protonation of the anion radical occurring with NQ (ECEC process) is inhibited with H_2NQ even at high concentrations of acid. This effect can be understood as an effect of the radical anion and dianion, which are formed in the first and second electron transfer steps, being highly stabilized by the presence of intramolecular hydrogen bonds. However, acetic acid has an effect on the H_2NQ anion reduction wave: a shift toward positive potentials is observed upon addition of this acid, pointing to the intervention of strong association processes between the dianion and the acetic acid. This behavior is not exclusive to the naphthoquinone family and is also found in the case of anthraquinones. From a chemical point of view, the absence of protonation is a result of negative charge stabilization by intramolecular hydrogen bonds, whereas strong association could be the result of the establishment of double hydrogen bonds, in which case the participation of the C═O and O—H groups of the carboxyl of acetic acid could be important. Finally, the case of HNQ is intermediate in the sense that protonation does not occur, but intermolecular hydrogen bonding is strong enough so that disproportionation of the semiquinone is facilitated, thus leading to a two-electron wave corresponding to the disproportionation promoted by a hydrogen-bonding agent, as discussed previously.

The case of α-hydroxyquinone (QOH) is different. The study of this family is important because many of the compounds containing this functionality possess important biological activities.[27–29] The electrochemical study of α-hydroxyquinone shows that its behavior does not follow a typical two-monoelectronic reversible charge transfer process such as occurs for quinones in aprotic medium.[30,31] Rather, it is consistent with a reduction mechanism involving self-protonation processes.[32] This is caused by the higher acidity of a hydroxyl function at an α-position in front of the first electrogenerated anion radical (Scheme 6).

Four regimes may be envisioned. The ECE regimes correspond to the second electron transfer at the electrode, whereas the DISP regimes correspond to a homogeneous second electron transfer. Two ECE subcases are further distinguished according to the position of the equilibrium in the self-protonation reaction. If this is in favor of $HQOH^{\bullet}$, the ECE_{rev} case is obtained, whereas ECE_{irr} is obtained in the converse situation. Two DISP subcases are also distinguished. In the DISP1 case, the protonation of $QOH^{\bullet-}$ is the rate-determining step, whereas in the DISP2 case, protonation remains at equilibrium, and homogeneous second electron transfer is the rate determining step. Note that another mechanism where a dianion produced through a prior disproportionation step is the actual deprotonation agent is conceivable but can be ruled out because the disproportionation step is thermodynamically unfavorable. The experimental behavior of peak potential as a function of scan rate allows the second-order regime (DISP2) to be distinguished from first-order regimes (ECE_{irr}, ECE_{rev}, and DISP1).[32] It has been shown that ECE/DISP1 operates for 2-hydroxy-1,4-naphthoquinone and perezone, whereas a DISP2 mechanism occurs for horminone (Chart 3). Distinguishing between ECE_{rev} and ECE_{irr}-DISP1 is in principle possible on the basis of peak width[32] but was not discussed in this study. Note that ECE_{irr} and DISP1 cannot be distinguished under "pure kinetic" conditions, that is, when a mutual compensation of the chemical and diffusion processes occurs so that a stationary state is reached for intermediate species, the gradient of which is confined within a reaction layer adjacent to the electrode.

Scheme 6

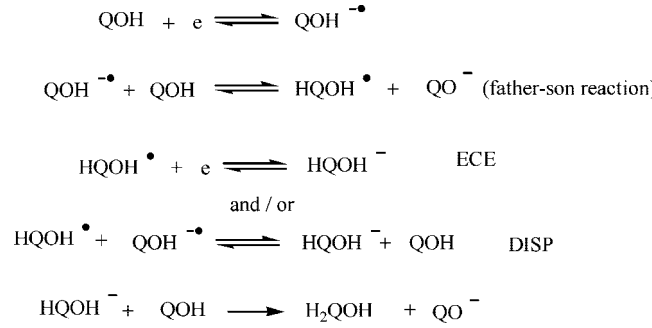

Chart 3

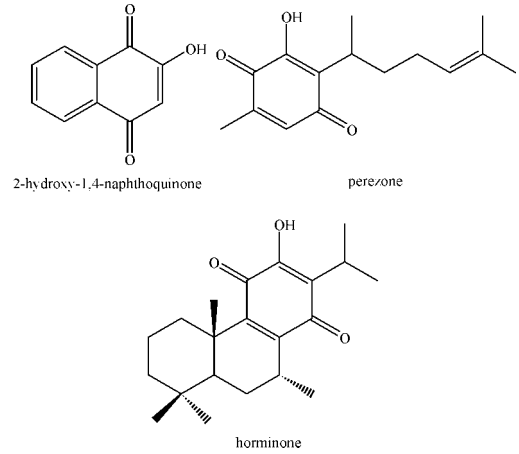

2.1.5. Oxidation of Hydroquinone, Phenols, and Related Compounds

As detailed above, the reduction pathways of the quinone/hydroquinone interconversion have been studied extensively. However, the corresponding oxidation mechanism of hydroquinones in aprotic solvents has not been extensively studied, with the main contribution to date being pioneer works.[33,34] A recent investigation has focused on the role of acids and bases in hydroquinone oxidation, including the role of hydrogen bonding.[35] In neat acetonitrile, a two-electron anodic wave is observed corresponding to an ECEC

Scheme 7

$$QH_2 - e \rightleftharpoons QH_2^{+\bullet}$$

$$QH_2^{+\bullet} \rightleftharpoons QH^{\bullet} + H^+$$

$$QH_2^{+\bullet} + QH^{\bullet} \rightleftharpoons QH_2 + QH^+$$

$$QH^+ \rightleftharpoons Q + H^+$$

mechanism wherein the cation radical that is formed by the first electron transfer is deprotonated by the solvent itself. Variation of the peak potential with the scan rate (40 mV/decade) is consistent with a transition from a mechanism controlled by the follow-up reaction (deprotonation) to a mechanism in which the first electron transfer is the rate-determining step.[36] In the presence of acid, deprotonation is thermodynamically less favorable and therefore slower. The cation radical can thus diffuse, and a DISP2 mechanism (Scheme 7) prevails. In this mechanism, deprotonation is at equilibrium and the rate-determining step is the homogeneous second electron transfer, as is consistent with the peak potential variation with the scan rate (20 mV/decade) and peak width (40 mV).[37]

The oxidation mechanism is also sensitive to the presence of both weak and strong hydrogen-bonding agents such as DMSO and acetate ion. At small concentrations of DMSO, a new less anodic wave appears, and as the DMSO concentration is increased, the intensity of the new wave and the negative shift increases while the original wave disappears. This behavior could be similar (although symmetrical) to that which has been described for weakly basic quinone reduction in the presence of strong acid, where the prewave was attributed to a hydrogen-bonded complex, which was easier to reduce than the quinone itself (Scheme 5). However, NMR studies indicate a very small association constant between hydroquinone and DMSO, suggesting that the new wave cannot be attributed to the oxidation of such a complex. It is rather interpreted as a faster deprotonation of the radical cation through a more facile proton transfer to DMSO than to acetonitrile. One could in fact argue that both effects occur, as is obviously the case at high DMSO concentration. A similar behavior is seen with the use of dimethylformamide or acetamide as hydrogen-bonding acceptor.

More important modifications occur when acetate ions are used (Figure 6). At stoichiometric concentration, a broad wave is observed at low anodic potentials corresponding to a negative shift of about 1 V. Proton transfer from hydroquinone to acetate ion has been discarded as the explanation for this on the basis of its having an unfavorable equilibrium constant ($\Delta pK_a \approx -5$). How, then, can we explain such a huge potential shift? In a similar system involving the role of carboxylate groups as hydroquinone substituents of hydroquinone, it has been shown that an intramolecular concerted electron and proton transfer occurs.[38] Such a process will be discussed in section 3. In the present case, the concerted mechanism has been rejected on the basis of the inconsistency between a large peak width and a slight variation of the peak potential with the scan rate (43.2 mV/decade). It is thus concluded that a strong hydrogen-bonding interaction between hydroquinone and acetate ion is responsible for the potential shift. However, no convincing arguments have been developed. Moreover, the argument against a concerted mechanism is based on the analysis of the wave as corresponding to a concentration of acetate ion being 2-fold the concentration of hydroquinone (see Figure 6). However, this wave is obviously composed of two overlapping waves, which makes a peak potential and peak width analysis difficult. Thus, the oxidation mechanism of hydroquinone in the presence of acetate ion remains unclear. This study points out a typical difficulty in the analysis of PCET processes in hydroquinone/quinone-like systems in both basic and protonic media, where the occurrence of two electron and two proton transfers can make the mechanistic analysis tricky. Fortunately, other systems such as phenolic compounds may not present this drawback.

The electrochemical oxidation of phenols has been widely investigated for a long time, and numerous investigations of specific phenols have been reported.[39] However, phenolic compounds still attract attention. For example, vitamin E (TOH) is one phenolic compound for which chemical activity is related to antioxidant properties. There are four structurally related phenolic compounds (the α-, β-, γ-, and δ-tocopherols, Chart 4) labeled vitamin E, and they are known to have different biological activities, although little is known of the chemical reasons for these differences. Nonetheless, the interest in these compounds focuses on their oxidized forms in connection with the role of $TO^{\bullet}$ as a chain-breaking antioxidant.

Recent studies on the oxidative electrochemistry of vitamin E have been reviewed.[40] This electrochemistry involves a sequence consisting of two electron and one proton transfers similar to other phenolic compounds, which display a richness of voltammetric responses depending on the media and nature of substituents in the 2-, 4-, and 6-positions.[39,41,42] Studies have been focused on organic solvents because they are likely to be closer to the natural environment of vitamin E, which exists in vivo in hydrophobic cell membranes.[43] The electrochemical approach gives insight into the detailed mechanism as sketched in Scheme 8, where the vertical transformations correspond to proton transfer and the horizontal transformations involve electron exchange. The oxidation peak is a two-electron wave interpreted as an ECE mechanism leading to the phenoxonium cation TO^+ (green pathway in Scheme 8). The principal feature in the electrochemical responses in pure aprotic media of vitamin E as compared to other phenols is that a reverse reduction peak is observed close to the oxidation process with a peak separation of about 400 mV.[44] This chemical reversibility

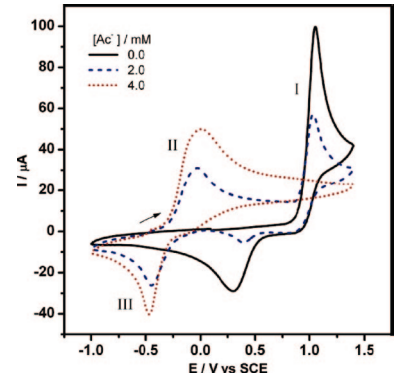

Figure 6. Cyclic voltammograms in acetonitrile + 0.2 M n-Bu_4NPF_6, on glassy carbon electrode at 0.1 V/s: (black) hydroquinone 2 mM; (blue) hydroquinone 2 mM + tetrabutylammonium acetate 2 mM; (red) hydroquinone 2 mM + tetrabutylammonium acetate 4 mM. Reprinted with permission from ref 35. Copyright 2007 Elsevier.

Chart 4

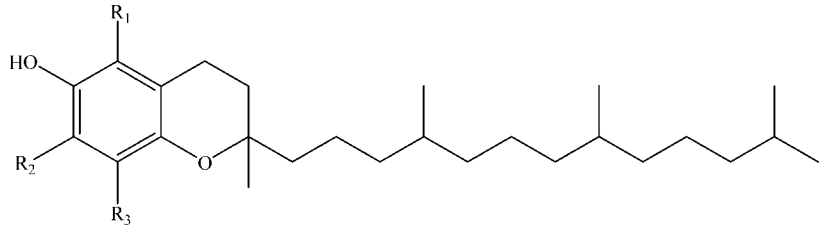

	R_1	R_2	R_3
α-	CH_3	CH_3	CH_3
β-	CH_3	H	CH_3
γ-	H	CH_3	CH_3
δ-	H	H	CH_3

Scheme 8

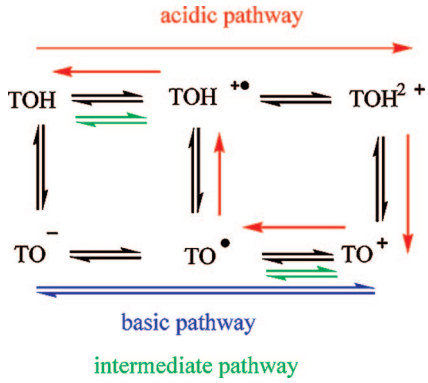

Scheme 9

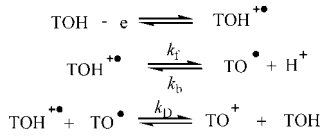

occurs because the phenoxonium cation TO^+ is stable for several hours at low temperature even though it is unstable in the presence of nucleophiles. (It has been reported to react with water to form 9-hydroxy-α-tocopherone, which then rearranges to the corresponding quinone.)[45]

The shape of the cyclic voltammograms observed both in pure acetonitrile and in dichloromethane varies considerably as the solvent or temperature is changed. This variability is assumed to be a result of the kinetic influence of the protonation/deprotonation step. Moreover, the voltammetric responses seen using Pt or glassy carbon electrodes differ because of specific solute−electrode interactions. Nonetheless, kinetic parameters were estimated from digital simulation of cyclic voltammograms recorded on Pt at 243 K.[46] Some doubt may be cast on this analysis because for $TOH^{\bullet+}$ it leads to a disfavored ($K_{eq} = k_f/k_b = 10^{-7}$ M) and slow deprotonation ($k_f = 10^3$ s^{-1}), which is incompatible with the ECE mechanism considered. A disproportionation mechanism would be preferred (Sheme 9). As already mentioned, criteria exist to analyze the ECE−DISP competition, and they could be used in this instance to assess the mechanism.[47] The slowness of $TOH^{\bullet+}$ deprotonation is indeed confirmed in acidic conditions obtained through the addition of CF_3SO_3H or CF_3COOH, which makes the cation radical stable enough so that the cyclic voltammogram appears as a one-electron chemically reversible oxidation process. The cation radical can then be further oxidized at higher potential to form the unstable TOH^{2+} dication, which deprotonates to give TO^+. In situ spectroscopic measurements also show the identity and stability of the phenolic cationic compounds. The reverse reduction reaction presumably follows another pathway corresponding to the reduction of TO^+ to $TO^{\bullet}$, which is then immediately protonated to form $TOH^{\bullet+}$, but this mechanism has not been established unambiguously (red pathway in Scheme 8). Conversely, in basic conditions, the observed behavior for TOH is typical of most phenols, which are easily deprotonated to form phenolate anions that are easier to oxidize than their corresponding phenols (blue pathway in Scheme 8). Voltammetric studies thus appear to be very useful in establishing the presence of cationic phenolic intermediates during TOH oxidation. The issue of the biological relevance of such intermediates is beyond the scope of this review, but it has been discussed elsewhere.[40]

Scheme 10

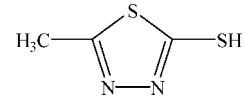

Many compound families other than hydroquinones, quinones, or phenols may involve proton-coupled electron transfers. For example, double bonds between two carbons, as in anthracene, or between one carbon and a heteroatom, possibly conjugated with other unsaturated moieties in the molecule, are susceptible to the two electron−two proton reactions shown in Scheme 1. The oxidation of synthetic analogues of dihydronicotamide adenine dinucleotide (NADH) is also a typical example of such processes whereby a proton is exchanged together with electrons.[48] These examples, that is, anthracene and NADH, are relatively simple systems in the sense that the starting molecule is neither protonated nor deprotonated in the prevailing media. Thus, mechanistic details can be obtained from cyclic voltammogram analysis[49] or simulations using available software.[50] The use of simulation programs in deciphering the intimate coupling of proton and electron transfers may, however, be delicate when there are many available pathways.[51] As an example, one can mention the investigation of redox behavior of a thiadiazole, in particular of 2-mercapto-5-methyl-1,3,4-thiadiazole (Scheme 10), which is a

Scheme 11

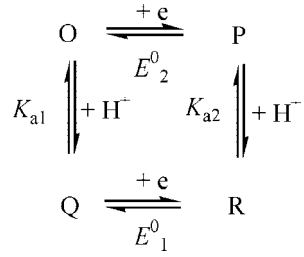

component of the cathode materials that have properties needed for secondary lithium batteries.[52]

In a neutral aprotic medium, this thiadiazole is oxidized to give a dimer, and in the course of this process protons are released. These protons influence the dimer reduction on the reverse scan because that reduction occurs at a more positive potential (by ca. 0.3 V) than the reduction observed when the neutral dimer is the starting point. This leads to the conclusion that the dimer is involved in a protonation/deprotonation equilibrium. That this equilibrium is displaced toward complete protonation is verified by running experiments in the presence of strong acid. Conversely, in strongly basic medium, the thiadiazole is fully deprotonated and thus easier to oxidize. This leads to the neutral dimer in agreement with the reduction observed when the neutral dimer is the starting point. In the presence of weak bases, there is no bulk, stoichiometric deprotonation of the thiadiazole. However, a new anodic wave appears at a less positive potential than the reduction of the neutral thiadiazole. This is interpreted as a CE mechanism in which the preceding reaction (deprotonation) is rapid enough to maintain equilibrium. Despite the good agreement between experiments and simulations using this mechanism, one could argue that other pathways might be plausible: (i) rapid and equilibrated deprotonation of the cation radical, that is, the EC mechanism, followed by dimerization of the neutral radical, and (ii) formation of a hydrogen-bonded complex between the thiadiazole and the weak base, with this complex then being easier to oxidize than the starting thiadiazole as was discussed in the case of the reduction of quinone in the presence of weak acidic agent. This reduction could follow a concerted (CPET) route. Intimate bonding between the thiadiazole and the weak base has been demonstrated by showing that introducing a steric hindrance into the base which does not affect its pK_a still does inhibit the effect on the oxidation potential of the thiadiazole. This important result clearly demonstrates that bases are not simply acting as buffer systems that provide thermodynamic sinks for protons and, thus, again highlights the interplay between hydrogen bonding and proton transfer in aprotic media.

2.2. Proton-Coupled Electron Transfer in Water

In protic media such as water, specific mechanistic issues arise for PCET. Water may act as the proton acceptor along with OH^- and the basic components of any buffers used. Water may also act as the proton donor along with H_3O^+ and the acidic components of any buffers used. Moreover, proton transfers are fast and often assumed to be at equilibrium in water.

2.2.1. pH-Dependent Redox Couples

A general equation for a pH-dependent redox couple is

$$\mathrm{Ox} + n\mathrm{e} + m\mathrm{H}^+ \rightleftharpoons \mathrm{Red}$$

The measured equilibrium potential E_{eq}, where [Ox] = [Red], is predicted by the Nernst equation to have a pH dependence according to eq 6

$$E_{eq} = E^0 - \frac{RT}{nF}\ln\left(\sqrt{\frac{D_O}{D_R}}\right) - \frac{RT\ln 10}{mF}\mathrm{pH} \qquad (6)$$

in which D_O and D_R are the respective diffusion coefficients of the oxidized and reduced species, m is the number of protons, n is the number of electrons exchanged, and E^0 is the formal potential. The diffusion coefficients are often assumed to be equal. The standard redox potential is given by eq 7.

$$E^0_{Ox,H^+/Red} = \frac{\mu^0_{Ox} + m\mu^0_{H^+} - \mu^0_{Red}}{nF} \qquad (7)$$

There, the μ^0 values are the standard chemical potentials and are related to the chemical potentials by eq 8

$$\mu = \mu^0 + RT\ln a = \mu^0 + RT\ln(\gamma[\,]) \qquad (8)$$

in which the γ values are the activity coefficients and [ ] is the concentration. With the exception of water, all standard states are defined by extrapolation of the ideal conditions at 1 M. For water, the standard state is the pure liquid. The μ^0 values do not include a contribution from the entropy of mixing of the reactants and, therefore, do not contain reactant concentration terms. The formal potential E^0 is given by eq 9

$$E^0 = \frac{\mu^0_{Ox} + m\mu^0_{H^+} - \mu^0_{Red}}{nF} + \frac{RT}{nF}\ln\left(\frac{\gamma_{Ox}\gamma^m_{H^+}}{\gamma_{Red}}\right) \qquad (9)$$

and therefore does not depend on pH if activity coefficients are assumed to be independent of pH.

The dependence of the measured equilibrium potential with pH is conveniently summarized in a potential−pH diagram, commonly referred to as a Pourbaix diagram, showing regions of existence of various redox and protonated species. The simplest system for a PCET corresponds to a one electron−one proton process, represented by the square scheme in Scheme 11. O is the oxidized deprotonated form, P is the reduced deprotonated form, Q is the oxidized protonated form, and R is the reduced protonated form. Proton transfers are assumed to be at equilibrium, so the thermodynamic parameters include the two acid dissociation constants, K_{a1} and K_{a2}, and two formal potentials, E^0_1 and E^0_2. From electrostatic arguments, it is deduced that K_{a1} is greater than K_{a2}. These parameters are used to construct the potential−pH diagram (Figure 7).

The horizontal line in the acidic pH region represents the pH-independent redox process Q/R in which both oxidized and reduced species are protonated. Similarly, the horizontal line in the basic pH region represents the pH-independent redox process O/P in which both oxidized and reduced species are deprotonated. The diagonal line corresponds to the pH-dependent redox process O/R, where oxidation and reduction are coupled to protonation and deprotonation. The slope of this line is about 60 mV/pH unit. Thus, thermodynamically, the one electron−one proton process behaves like

a simple one-electron redox couple with a pH-dependent reversible formal apparent potential E^0_{app} as given by eq 10, and it is easily characterized by electrochemical methods such as cyclic voltammetry:[53]

$$E^0_{app} = \frac{E^0_1 + E^0_2}{2} + \frac{RT}{F} \ln\left(\left(\frac{K_{a1}}{K_{a2}}\right)^{1/2}\left(\frac{[H^+] + K_{a2}}{[H^+] + K_{a1}}\right)\right) \qquad (10)$$

To observe the full pH dependence, it is necessary for the O/R couple to fall between the potentials for the oxidation and reduction of water in that pH range. Moreover, because the pH dependence occurs over the range of pH between pK_{a1} and pK_{a2}, it is desirable for the pK_{a1} to correspond to the acidic region (pH >1) and the pK_{a2} to correspond to the basic region (pH <14).

On the one hand, one would like to study such one electron−one proton processes. This can be achieved with many transition metal complexes that are stable in two or more consecutive oxidation states. Therefore, there are myriad examples of reversible PCET processes for transition metal compounds.[54] On the other hand, oxidation or reduction of main group compounds generally results in the formation of highly reactive species and, therefore, to obtain reversible PCET, it is necessary to transfer electrons in multiples of two. A typical example is the quinone/hydroquinone system. Biological systems commonly employ two electron−two proton redox couples, as with the electron transport chain and phosphorylation in which electron transfer drives proton transfer against a proton gradient to generate ATP from ADP. The complete description of potential−pH diagrams corresponding to two electrons and one or two proton process is lengthy but presents no difficulty.[55,56]

2.2.2. Metal−Ligand Systems

The need for multielectron change in many biological reactions necessitates complex pathways and the transfer of more than one electron to or from the catalysts. Charge compensation is required to avoid large increases in stepwise redox potentials to achieve redox potential leveling. This is especially important for biological redox couples in nonpolar membrane environments, where charge compensation by the surrounding dielectric is low compared to water. Charge compensation can occur through proton expulsion, thus leading to proton-coupled electron transfer.

Many biological or artificial catalysts are transition metal complexes. Such molecular catalysts, particularly ruthenium complexes such as the blue μ-oxo Ru dimers, *cis*,*cis*-$[(bpy)_2(H_2O)Ru^{III}ORu^{III}(OH_2)(bpy)_2]^{4+}$,[57,58] or the μ-oxo-bridged terpyridyl complex $[(tpy)(H_2O)_2Ru^{III}]_2O^{4+}$ have been designed for the widely studied water oxidation (see Chart 5 for ligand nomenclature).[59]

For these types of complexes, there is a large pH range in which electron transfers are accompanied by proton transfer, and those redox properties are well characterized by electrochemical investigations. Extension of the μ-oxo Ru dimer water oxidation to metal oxide surfaces based on a phosphonate-modified complex, $[(tpy\text{-}PO_3H_2)(H_2O)_2Ru^{III}]_2O^{4+}$, has been recently described, and it was shown that this compound retains its PCET and water oxidation on TiO_2.[60] Typical pH dependence of the measured equilibrium potential E_{eq} is reproduced in Figure 8. Such studies make it possible to guess at the proton composition of Ru^V-O-Ru^V species that have even limited catalytic activity. Recently, a dinuclear

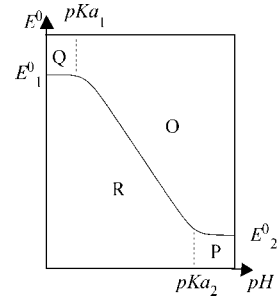

Figure 7. (Solid line) Equilibrium potential as a function of pH for a 1e-1H system (see Scheme 11). (Dotted lines) Separation of regions of existence of various protonated species.

Chart 5

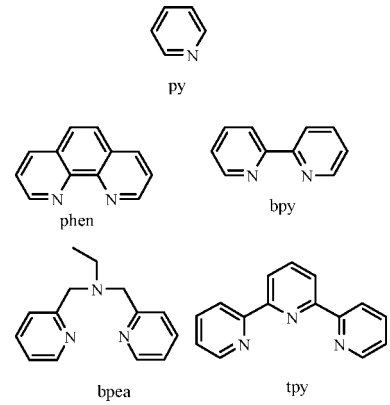

Ru complex, $[(terpy)_2(H_2O)Ru^{II}(bpp)Ru^{II}(OH_2)(terpy)_2]^{4+}$, which is capable of oxidizing water to dioxygen but which does not contain the Ru−O−Ru motif, was reported and electrochemically characterized through a Pourbaix diagram.[61,62] The catalytic performance of this complex is remarkably superior to that of the blue dimer.

Complexes of ruthenium based on bridging pyridyl-type ligands have also been of interest because of the rich oxidative properties of the Ru^{IV}═O species. Reaction mechanisms for the oxidation of several substrates by Ru^{IV}═O have been established, and catalytic oxidation systems have been described.[63,64] The schematic pathway followed to reach high oxidation states is exemplified in the following equation:

$$L_5Ru^{II}-OH_2 \overset{-H^+ - e}{\rightleftharpoons} L_5Ru^{III}-OH \overset{-H^+ - e}{\rightleftharpoons} L_5Ru^{IV}=O$$

Because loss of the electron is coupled to loss of a proton in each of the above steps, the overall charge of the complex does not change, and those redox couples can occur within a narrow potential range. Monoaqua complexes, such as $[(bpy)_2(py)(H_2O)Ru^{II}]^{2+}$,[65] $[(tpy)(bpy)(H_2O)Ru^{II}]^{2+}$,[66] $[(tpy)(tmen)(H_2O)Ru^{II}]^{2+}$,[67] and many others,[68] have been studied. They show two sequential one electron−one proton oxidations in the pH range of 1−7. Similar behaviors are observed with osmium complexes.[66] There are, however, some cases when disproportionation of the Ru^{III} complex is thermodynamically favorable, which leads to a two-electron process.[68,69] Cyclic voltammetric oxidation of most Ru^{II} complexes proceeds through a simple and fully reversible first step. However, the second oxidation step, in which the Ru^{III} complex is oxidized to the Ru^{IV}═O complex, yields notably smaller currents than the first step. This phenomenon was first qualitatively attributed to a slow disproportionation of Ru^{III} complex (top of Scheme 12).[70] However, a detailed

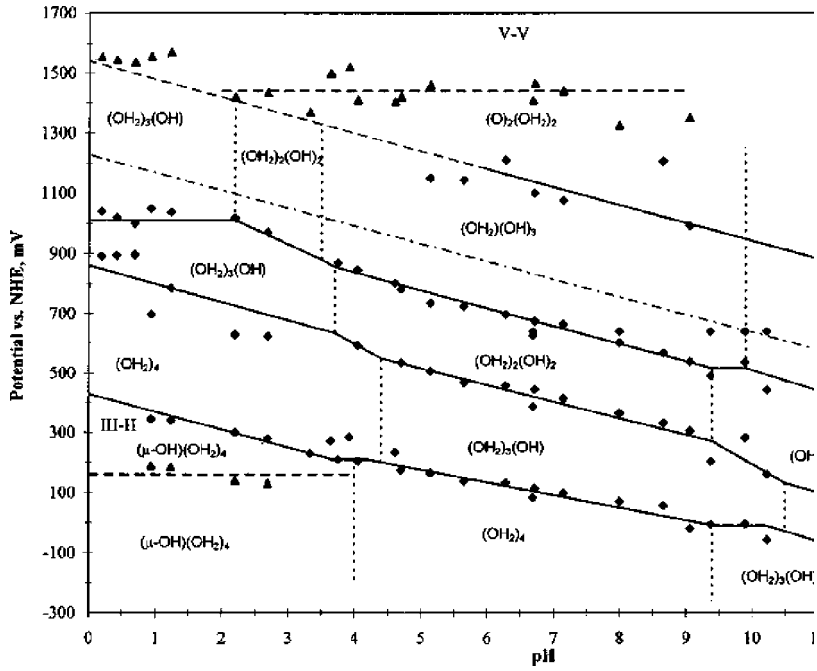

Figure 8. Equilibrium potential as a function of pH for a μ-oxo $Ru(OH_2)_2$ system. Reprinted with permission from ref 59. Copyright 1998 American Chemical Society.

Scheme 12

top

$$L_5Ru^{III}\text{-}OH + L_5Ru^{III}\text{-}OH \rightleftharpoons L_5Ru^{IV}{=}O + L_5Ru^{II}\text{-}OH_2$$

bottom

$$Ru^{III} \xrightarrow{k} Ru^{III*}$$

$$Ru^{III*} \overset{-e}{\rightleftharpoons} Ru^{IV}$$

electrochemical study of $[(tpy)(bpy)(H_2O)Ru^{II}]^{2+}$ has shown that plateau currents observed at a rotating graphite disk electrode are incompatible with this mechanism.[71]

Alternative mechanisms have been explored. Experimental data fit with an irreversible first-order step preceding Ru^{III} oxidation in which the observed rate constant k varies linearly with $[OH^-]$ in basic solution and $[H_3O^+]$ in acid solution (bottom of Scheme 12). It is suggested that the pathway followed is either the hydroxide-assisted breaking of one of the ruthenium−terpyridine bonds in $[(tpy)(bpy)(OH)Ru^{III}]^{2+}$ or a proton-assisted ligand exchange reaction to give an intermediate that is more reactive toward oxidation. There is, however, no independent evidence that ring opening occurs on the time scale of the electrochemical experiment, and comparison with homogeneous results leads to apparent discrepancy. Indeed, the homogeneous reduction of $[(bpy)_2(py)Ru^{IV}O]^{2+}$ and $[(bpy)_2(py)(HO)Ru^{III}]^{2+}$ by $[(bpy)_3Os^{II}]^{2+}$ has been studied,[72] taking into account disproportionation of the Ru^{III} complex, which had been studied by itself previously.[73] The kinetics are complex but can be fit to a double-square scheme involving stepwise electron and proton transfer without involvement of any ring opening reaction. The apparent discrepancy between the solution and electrochemical results is thus not understood. Several arguments may be developed. The homogeneous reduction

Scheme 13

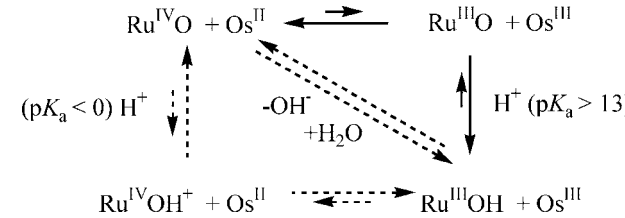

of $[(bpy)_2(py)Ru^{IV}O]^{2+}$ by $[(bpy)_3Os^{II}]^{2+}$ has been interpreted as an electron first/proton second stepwise transfer on the basis of pK_a values, making $Ru^{IV}{=}OH^+$ inaccessible (Scheme 13). As a consequence, the reverse reaction, that is, $[(bpy)_2(py)(HO)Ru^{III}]^{2+}$ oxidation by $[(bpy)_3Os^{III}]^{2+}$, follows the reverse pathway starting with slow deprotonation, thus competing with $[(bpy)_2(py)(HO)Ru^{III}]^{2+}$ disproportionation. However, the stepwise nature of the reduction mechanism was asserted on the basis of the absence of a pH dependence of the overall rate constant, ruling out a pathway involving concerted proton and electron transfer (diagonal pathway on Scheme 13) because it is claimed that this mechanism would introduce a pH dependence through its free energy change, which is said to vary as −59 mV/pH unit. This assertion may certainly be questioned. A recent debate has emerged on this issue; that is, how should the rate constant for a CPET pathway in water be expressed? Does a classical rate constant derived from Marcus theory, if valid, take into account a pH-dependent free energy? This point will be discussed in detail in section 3, but, from fundamental grounds, standard free energy has to be considered, and it is obviously pH-independent.[74,75]

Moreover, in a potential CPET pathway, the reactants are $Ru^{IV}O$, Os^{II}, and water, so that even the apparent second-order rate constant should be pH-independent.[74] Now, with regard to the electrochemical study, it can be argued that there may be a role for a catalytic surface effect arising from protonation−deprotonation coupled to electron transfer. This kind of effect has been described on a carbon

Scheme 14

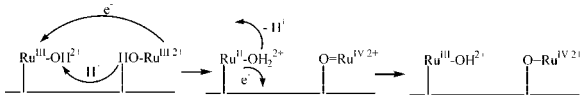

electrode in the course of oxidative studies of bisaquo complexes.[76] Consequently, both the available electrochemical and homogeneous studies are unable to clearly establish the mechanistic pathway of $Ru^{III}OH$ to $Ru^{IV}=O$ oxidation. Another electrochemical study has examined $Ru^{III}OH$ complex oxidation using an ITO surface coated by $[(tpy)(4,4'\text{-}(PO_3H_2)_2bpy)(H_2O)Ru^{II}]^{2+}$.[77] There is kinetic evidence that Ru^{III} oxidation involves intimate proton-coupled electron transfer. It is proposed that the direct Ru^{III} oxidation does not occur but instead that a disproportionation takes place within an association complex of the Ru^{III} reactant, and this is followed by Ru^{II} oxidation (Scheme 14). Note that this observation is in disagreement with previously mentioned experiments on freely diffusing reactants,[71] which indicate that disproportionation of Ru^{III} complex does not occur. A large kinetic isotope effect is measured, and its range is higher for highly loaded surface than for a dilute surface in the presence of $[(tpy)(bpy)(H_2O)Ru^{II}]^{2+}$ added to the external solution. This is interpreted as an indication of a concerted electron and proton transfer that requires specific orientations between reactants for tunneling of the proton to occur.

Types of ligand other than water may involve single one electron−one proton coupled transfer at the M^{II}/M^{III} (M = metal) stage. As an example, benzotriazole or benzimidazole has been used with ruthenium or iron as metal.[78]

The aqueous electrochemistry of diaquo complexes involves four successive one electron−one proton couples as is described for *cis*- and *trans*-$[(bpy)_2(H_2O)_2M^{II}]^{2+}$ (M = Ru, Os) and *trans*-$[(py)_4(O)_2Re^{V}]^{+}$.[79−82] This loss of four protons permits five oxidation states to be accessible within a potential range of only 0.6 V (Figure 9). To put the latter point into perspective, in acetonitrile, the span in potentials for the Ru^{IV}/Ru^{III} $Ru(bpy)_2Cl_2^{2+/+}$ to the Ru^{III}/Ru^{II} $Ru(bpy)_2Cl_2^{+/0}$ couple is 1.66 V.

As already seen through many examples, electrochemical techniques are very useful for characterizing PCET in water on thermodynamics grounds. Deciphering a mechanism requires kinetics information as described in the investigation of $[(tpy)(bpy)\ (H_2O)Ru^{II}]^{2+}$ oxidation.[71] However, electrochemical investigations using solid electrodes are sometimes complicated by effects arising from the nature of the electrode surface. Those effects have to be detected to avoid erroneous conclusions being drawn from voltammetric studies. When activated, glassy carbon electrodes do not behave as a simple outer-sphere electron donor or acceptor. The possibility of the deliberate modification of glassy carbon electrodes via electrochemical activation toward proton-coupled electron transfer was investigated for various substrates, but particularly $[(bpy)_2(H_2O)_2Ru^{II}]^{2+}$.[76] Oxidative treatment of glassy carbon electrodes has an effect on the Ru^{IV}/Ru^{III} couple corresponding to a huge increase in the heterogeneous charge transfer rate and a significant kinetic isotope effect. A much smaller effect occurs for the Ru^{III}/Ru^{II} couple, presumably because electron transfer is faster. XPS data obtained for treated electrodes show that the activation procedure results in the formation of oxidized carbon-based groups that are confined to within 20 nm of the electrode surface. The existence of a kinetic isotope effect suggests the possible intervention of concerted proton and electron transfer pathways utilizing surface chemical sites on the electrodes. It is proposed that Ru^{IV}/Ru^{III} have a greater inhibition to outer-sphere electron transfer than Ru^{III}/Ru^{II} arising from the enhanced vibrational trapping and a lack of significant proton affinity by the $Ru^{IV}=O$ group. With slow outer-sphere electron transfer, a complex but facile proton-coupled electron transfer pathway may be utilized instead, using chemical sites at the electrode surface:

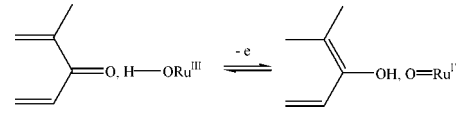

The same effect is observed on deprotonated indium tin oxide surfaces.[83] Such pathways have obvious analogues in both the homogeneous and surface disproportionation of Ru^{III} complexes.[73,77]

Many molecular catalysts for water oxidation are based on the ruthenium complex, but it is well-known that O_2 evolution in photosystem II (PSII) occurs at a manganese cluster.[84,85] A recent structure of PSII shows that the oxygen-evolving complex (OEC) consists of an oxo-bridged Mn_3Ca cubane-like cluster with an appended manganese site linked by a μ-oxo bridge.[86] The appended manganese may be a site for oxidative cycling between Mn^{II} and Mn^{V}. The key intermediate in the critical bond-forming step of water oxidation is a preorganized oxo/hydroxyl intermediate in which a nucleophilic hydroxide attacks an electrophilic oxo of a high-valent manganese:

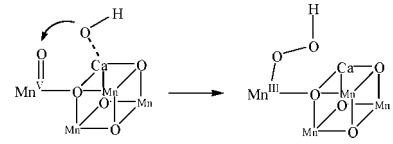

Therefore, synthetic manganese complexes have been extensively studied as structural models for the OEC or other active site of metalloenzyme-like catalase.[87−89] One severe constraint for the application of synthetic complexes as functional mimics is that in the natural OEC all four oxidation steps for the manganese cluster are compressed into about 0.3 V. This narrow potential is a result, as already mentioned, of deprotonation reactions that provide charge compensation to the oxidation steps. Thus, synthetic manganese complexes also involve proton-coupled electron transfer. The first example described in the literature is a di-μ_2-oxo-$Mn^{III}Mn^{IV}$ complex, $[(bpy)_2Mn(O)_2Mn(bpy)_2]^{3+}$, showing a potential−pH dependence corresponding to a one electron−one proton process for the $Mn^{III}Mn^{IV}/Mn^{III}Mn^{III}$ couple, whereas the other redox couple ($Mn^{III}Mn^{III}/Mn^{II}$-Mn^{II}) is unaffected by the change in pH.[90] Other complexes have been shown to exhibit the same behavior and have also clarified the role of the ancillary ligands.[91,92] As in the case of $[(tpy)(bpy)(H_2O)Ru^{II}]^{2+}$ or $[(bpy)_2(H_2O)_2Ru^{II}]^{2+}$ oxidation, the electrode surface has an effect on the oxidation pathway.[83] On oxidative-activated glassy carbon, indium oxide, and edge-oriented pyrolytic graphite electrodes, the state of protonation of the surface appears to be connected to the ability of the surface to catalyze the proton transfer and the degree to which adsorption plays a role. In addition, a kinetic isotope effect of magnitude of 4.6 has been measured, which also suggests a concerted proton−electron transfer pathway.[93] Unlike the bpy analogue, the electro-

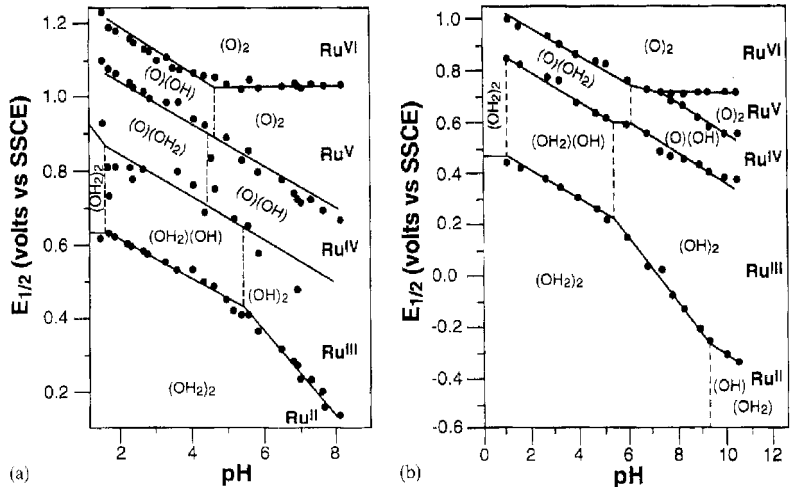

Figure 9. Equilibrium potential as a function of pH for a $Ru(OH_2)_2$ system: (a) *cis*-$[(bpy)_2(H_2O)_2Ru^{II}]^{2+}$; (b) *trans*-$[(bpy)_2(H_2O)_2Ru^{II}]^{2+}$. Reprinted with permission from ref 54. Copyright 1998 Elsevier.

chemistry of $[Mn_2^{III/IV}O_2(phen)_4]^{3+}$ undergoes two proton-coupled electron transfers in water ($Mn_2^{III/IV}/Mn_2^{III/III}$ and $Mn_2^{III/III}/Mn_2^{III/II}$); both of the μ-oxo groups protonate concomitantly with electron transfer, thus showing the role of ancillary ligands on the basicity of oxo groups.[94] Tetranuclear manganese−oxo aggregates, such as $[Mn_4O_6(bpea)_4]^{4+}$, also involve PCET, but unlike $[(bpy)_2Mn(O)_2Mn(bpy)_2]^{3+}$, the reaction is not influenced by the electrode surface.[95] It is thus evident that the mechanistic details of PCET for manganese−oxo complexes are still poorly understood.

Despite the extensive work done on metal−ligand complexes involving PCET, notably by Meyer and co-workers, many issues remain to be resolved before a full understanding of the intimate coupling between electron and proton transfers can be reached. As already indicated in the above discussion, kinetic studies are necessary, and electrochemical kinetic investigations already performed are detailed in section 2.2.4.

2.2.3. Organic Systems

The electrochemical reduction or oxidation of organic compounds in aqueous medium is characterized by two particular features. First, practically all of the organic substances are absorbable, to a lesser or larger extend. Second, rapid protonation (or deprotonation) of intermediates leads to reactions involving more than one electron. The effect of adsorption has been described quantitatively. When adsorption is strong, it can be detected from voltammogram shapes, observation of prewave, etc. However, if adsorption film is moderate, the electrochemical reaction is apparently the same as a typical heterogeneous reaction but has an apparent rate constant higher than a typical heterogeneous rate constant.[96,97] (Note that "heterogeneous" is not defined here as opposite of "homogeneous" but indicates an electron transfer between an electrode and a freely diffusing species as opposed to a surface reaction involving an electron transfer between an electrode and a species strongly adsorbed onto or attached to an electrode.)

Carbonyl compounds are typical examples of systems involving two electron−two proton transfers in aqueous media. The reduction mechanism of the C═O group has been extensively studied by Laviron and co-workers on various substrates (represented by YRCOZ, where Y and Z are various substituents): methyl isonicotinate,[98] *p*-diacetylbenzene,[99] isonicotinic acid,[100] isonicotinamide,[101] 1-methyl-4-carboxy pyridinium,[102] and thionicotinamide[103] have been investigated. The reduction follows an "E"C_1C_2"E" mechanism. The first two electron−two proton transfer ("E") leads to an intermediate P. This intermediate can be written as a molecule in which the carbon of the initial C═O group bears a minus charge and which can be protonated on different sites. The following first-order chemical reaction (C_1) is an internal proton transfer. It is faster than C_2, which involves the loss of a group ZH (ZH = MeOH, H_2O, NH_3,...). The aldehyde then obtained (YRCHO) is further reduced via a two electron−two proton transfer ("E") as sketched in Scheme 15.

Scheme 15

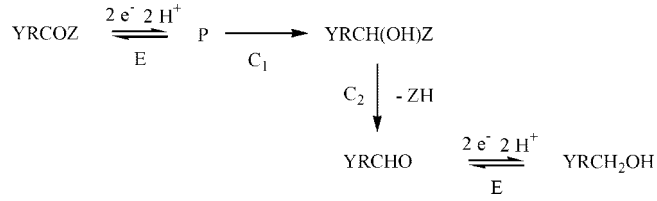

This type of mechanism also occurs during the reduction of a double bond between two carbons conjugated with quickly protonable sites as in the case of 1,2-di(4-pyridyl)ethylene.[104] An intermediate is the first form from a two electron−two proton transfer with protonation on a neighboring atom (here nitrogen) rather than on the carbon atom of the double bond, and this is then followed by a slow proton transfer to the carbon.

Analysis of the reduction of aromatic nitro compounds by the proton-coupled electron transfer mechanism was also challenging because it involves four electrons and four protons to give hydroxylamine. This reduction occurs via two successive nine-member square schemes linked by the dehydration of the intermediate dihydroxylamine (Scheme 16). The reaction path was determined on several systems: 4-nitropyridine,[105] 4-nitropyridine *N*-oxide,[106] *p*-nitrobenzophenone,[107] and nitrobenzene.[108]

In each of the above-mentioned examples, several two electron−two proton transfer sequences are separated by chemical reactions such as internal proton transfer and loss

Scheme 16

$$RNO_2 \overset{2\,e^-,\,2\,H^+}{\rightleftharpoons} RN(OH)_2 \overset{-\,H_2O}{\longrightarrow} RNO \overset{2\,e^-,\,2\,H^+}{\rightleftharpoons} RNHOH$$

of a group. Transposition can also occur.[109] In the case of the quinone/hydroquinone system, there is only a two electron−two proton transfer sequence, and the microscopic mechanistic pathway was investigated with electrochemical methods long ago,[110,111] as is detailed in the following section. Studies on catechols and their corresponding *o*-quinones at carbon electrodes have shown similar two electron−two proton reversible behavior.[112] Ascorbic acid is also oxidized in a two-electron process, but the oxidation of ascorbate is accompanied by a rapid hydration reaction.[113]

Voltammetric studies involving proton-coupled redox systems are usually conducted in buffered solution and in the presence of an excess of added supporting electrolyte. However, there are two reasons to undertake electrochemical studies at low buffer concentration: (i) to eliminate the possible interference of buffer capacity in electroanalysis in vivo and (ii) to evaluate the role of buffer components as proton donors or acceptors in mechanistic pathways. Dopamine and ascorbic acid oxidation have been qualitatively investigated at low buffer concentration.[114] At neutral pH, when the concentration of the basic component of the buffer is high enough to neutralize protons produced by the electrochemical oxidation of QH_2, the following pathway is available and a single two-electron wave is observed.[113]

$$QH_2 \overset{-H^+}{\rightleftharpoons} QH^- \overset{-e}{\rightleftharpoons} QH^\bullet \overset{-H^+}{\rightleftharpoons} Q^{\bullet -} \overset{-e}{\rightleftharpoons} Q$$

The peak position is determined by the initial CE sequence leading to $QH^\bullet$ radical. The pK_a of the $QH^\bullet$ radical is approximately 4, so that it is deprotonated at neutral pH. The resulting $Q^{\bullet -}$ is then easily oxidized because $Q^{\bullet -}/Q$ standard potential is more negative than the peak potential, whereas $QH^\bullet/QH^+$ standard potential is more positive. When the amount of the basic component of the buffer is not sufficient to neutralize protons produced by the electrochemical oxidation, two oxidation peaks appear. This is attributed to an acute change of pH at the surface of the electrode. Indeed, when the proton acceptors are depleted by neutralization of protons produced by the electrochemical oxidation of dopamine, the proton concentration at the surface of the electrode increases rapidly, making the remaining electron transfer, that is, oxidation of the remaining QH_2 or $QH^\bullet$, more difficult.

A recent study[115] has reassessed the role of proton transfer and hydrogen bonding in the unbuffered aqueous electrochemistry of quinones and shown that the behavior of quinones can be compared to that in aprotic solvents in the presence of an added acid or hydrogen-bonding agent. This study also demonstrates the important role of the hydrogen bond in water.

2.2.4. Kinetics

Establishing the microscopic pathway for electron and proton-coupled transfer in buffered aqueous media in the framework of square schemes requires a kinetic analysis, and electrochemical methods such as cyclic voltammetry are useful for such an analysis. General theoretical expressions have been established for the kinetics under the conditions that protonation reactions are at equilibrium and disproportionation and dimerization are absent.[55,56,116] For both four- and nine-membered square schemes, expressions are available for both adsorbed or freely diffusing reactants. We focus here on freely diffusing reactants. Kinetic analyses have been performed on organic systems involving two electron−two proton sequences. A description of the corresponding nine-membered square scheme can be constructed for a reduction as shown in Scheme 17, and transposition to oxidation is straightforward.

This description consists of two ladder schemes, each equivalent to a simple one-electron reaction, having apparent rate constants $k_{h1,app}$ and $k_{h2,app}$ and apparent standard potentials $E^0_{1,app}$ and $E^0_{2,app}$. The transfer coefficient of each reaction is 0.5 if the symmetry coefficients of the elementary electron transfer rate constants are 0.5, which is usually the case for organic compounds. The apparent standard potentials $E^0_{1,app}$ and $E^0_{2,app}$ are given by eqs 11 and 12,[56]

$$E^0_{1,app} = E^0_2 + \frac{RT}{F}\ln\left(\frac{\dfrac{K_{a4}}{[H^+]} + 1 + \dfrac{[H^+]}{K_{a2}}}{\dfrac{K_{a3}}{[H^+]} + 1 + \dfrac{[H^+]}{K_{a1}}}\right) \quad (11)$$

$$E^0_{2,app} = E^0_5 + \frac{RT}{F}\ln\left(\frac{\dfrac{K_{a6}}{[H^+]} + 1 + \dfrac{[H^+]}{K_{a5}}}{\dfrac{K_{a4}}{[H^+]} + 1 + \dfrac{[H^+]}{K_{a2}}}\right) \quad (12)$$

in which all constants are defined as in Scheme 17 and apparent rate constants are given by eqs 13 and 14.

$$k_{h1,app} = \frac{k_{e1}\left(\dfrac{[H^+]^2}{K_{a1}K_{a2}}\right)^{1/2} + k_{e2} + k_{e3}\left(\dfrac{K_{a3}K_{a4}}{[H^+]^2}\right)^{1/2}}{\left(\dfrac{[H^+]}{K_{a1}} + 1 + \dfrac{K_{a3}}{[H^+]}\right)^{1/2}\left(\dfrac{[H^+]}{K_{a2}} + 1 + \dfrac{K_{a4}}{[H^+]}\right)^{1/2}} \quad (13)$$

$$k_{h2,app} = \frac{k_{e4}\left(\dfrac{[H^+]^2}{K_{a2}K_{a5}}\right)^{1/2} + k_{e5} + k_{e6}\left(\dfrac{K_{a4}K_{a6}}{[H^+]^2}\right)^{1/2}}{\left(\dfrac{[H^+]}{K_{a2}} + 1 + \dfrac{K_{a4}}{[H^+]}\right)^{1/2}\left(\dfrac{[H^+]}{K_{a5}} + 1 + \dfrac{K_{a6}}{[H^+]}\right)^{1/2}} \quad (14)$$

Two limiting cases may occur: In the first case, in which $E^0_{1,app} \gg E^0_{2,app}$, the two stages are distinct and can be studied separately. In the second case, in which $E^0_{1,app} \ll E^0_{2,app}$, there is a strong overlap of the two stages, so that the process is equivalent to a simple two-electron reaction with an apparent equilibrium potential $E^0_{app} = (E^0_{1,app}+E^0_{2,app})/2$, and if the first stage is rate controlling, the transfer coefficient is equal to 0.25 and the corresponding measurable rate constant is $k^*_{h1,app} = k_{h1,app}\sqrt{\rho}$, whereas if the second stage is rate controlling, the transfer coefficient equal to 0.75 and the corresponding measurable rate constant is $k^*_{h2,app} = k_{h2,app}\sqrt{\rho}$, with $\sqrt{\rho}$, $= \exp[(F/4RT)(E^0_{1,app} - E^0_{2,app})]$. The same formulas are valid for both heterogeneous and surface reactions.

Determination of the intrinsic electron transfer rate constants k_{ei} ($i = 1-6$) is thus possible provided that a minimal set of pK_a values and standard potentials is known. Unfortunately, this condition is not frequently fulfilled, and kinetic analyses of two electron−two proton sequences are scarce.

The kinetics of the *p*-benzoquinone/quinone couple on a platinum electrode was analyzed long ago on the basis of this theoretical framework.[111] Experimental values of $k^*_{h1,app}$ and $k^*_{h2,app}$ as a function of pH were obtained from Vetter's data.[110] A fitting with theoretical formulas using pK_a values and standard potentials from the literature leads to reasonable values for the k_{ei} values ($i = 3-5$). k_{e1} and k_{e6} cannot be determined, whereas k_{e2} seems too high. The adsorption of the protonated quinone at the platinum surface may cause the apparent acceleration. The reaction sequence can be determined from all constants:[117] the path of electron transfer is defined by the largest of the rate constants in each column of Scheme 17. If all of the elementary rate constants of electron transfer for a given scheme are known, the sequence of electron and proton transfer steps can be predicted. In the case of benzoquinone, the k_{ei} values show that QH_2^{2+} and Q^{2-} are not involved and that at low pH the reduction sequence (for oxidation simply reverse the sequences given) is $H^+e^-H^+e^-$, then followed by $e^-H^+H^+e^-$ at intermediate pH (around 4) and finally $e^-H^+e^-H^+$ at higher pH (neutral).

The same kinetic analysis was carried out on oxidation of three catechols (4-methylcatechol, 3,4-dihydroxybenzylamine, and 3,4-dihydroxyphenylacetic acid) at a carbon paste electrode.[112] All three catechols have the same behavior, despite the differences in their side chains, and the same observations as for hydroquinone result: reaction sequences are identical, and k_{e2} seems too high. This feature calls for a further comment on the magnitude of elementary rate constants. Electron transfers are assumed to be heterogeneous, that is, to involve freely diffusing reactant. However, as already mentioned, if the adsorption film is sufficiently mobile, the electrode electron transfer reaction is apparently the same as a typical heterogeneous reaction, but it has an apparent rate constant higher than a typical heterogeneous rate constant (Scheme 18b).[96,97] The resulting apparent rate constant $k_{h,app,ad}$ is given by $k_{h,app,ad} = mk_e$, where k_e is the heterogeneous electron transfer constant and m is given by eq 15

Scheme 17

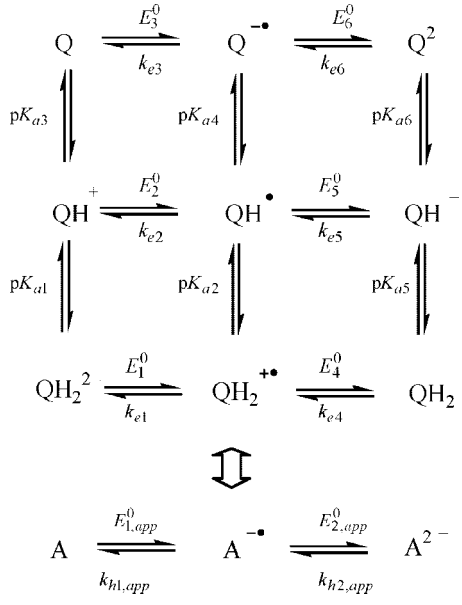

$$m = 1 + \frac{k_{surf}\Gamma_m/k_e C}{\left(C\sqrt{b_O b_R}\right)^{-1} + 0.5\left(\sqrt{\frac{b_O}{b_R}} + \sqrt{\frac{b_R}{b_O}}\right)} \quad (15)$$

in which k_{surf} is the surface electron transfer rate constant, Γ_m is the maximum surface concentration, C is the solution concentration, and b_O and b_R are the oxidant and reducing agent adsorption coefficients. The apparent rate constant is thus higher than the real heterogeneous rate constant because $m > 1$. To get the m value, and thus the contribution of adsorption reaction, k_{surf} has to be known. An example of such an analysis is afforded by the reduction of aromatic nitro compounds in water, which involves four electrons and four protons to give hydroxylamine and takes place via two successive nine-membered square schemes linked by the dehydration of the intermediate dihydroxylamine (Scheme 16). Focusing on dihydroxylamine formation, the rate-determining step and its apparent rate constant are obtained from a study of variations of anodic and cathodic peak potentials with scan rate. The rate-determining step is always the second electron transfer, that is, reduction of $RNO_2H^{\bullet}$. The variation of the peak potential with scan rate also allows determination of whether a "pure" surface reaction or a heterogeneous (be it real or only apparent from the presence of a mobile adsorption film) reaction occurs.[118] A "pure" surface reaction takes place in the case of $PhCOPhNO_2$, 1,4-dinitrobenzene, and 4-nitrobenzophenone.[119] In the case of nitropyridine[105] and 4-nitropyridine *N*-oxide,[106] although a heterogeneous reaction occurs at low scan rate, a surface reaction occurs at high scan rate. Note that the global scheme is complicated by protonation of the N or NO group, leading to cubic schemes. A study of the variation of the rate constants (surface or heterogeneous) with pH allows an estimation of elementary rate constants provided a reasonable guess has been made at the pK_a values. On the one hand, the values obtained for the surface rate constants k_{surf} seem to be correct because application of an empirical relationship proposed by Brown and Anson ($k_{surf} = 6 \times 10^8 k_e$)[120] to those k_{surf} values leads to reasonable values of the corresponding heterogeneous rate constants (i.e., $k_e = 0.35$ cm s^{-1}). On the other hand, the experimental values obtained for heterogeneous rate constants k_e are several orders of magnitude higher than any reasonable value. This is attributed to a surface reaction parallel to the heterogeneous reaction, which

Scheme 18

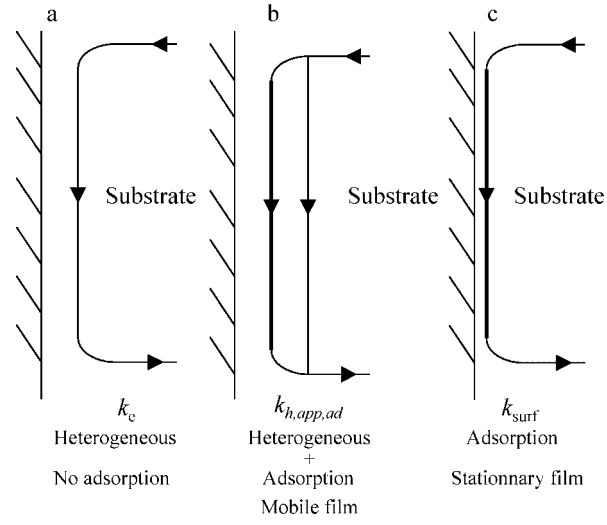

increases the apparent reversibility of the electrochemical reactions by the factor m given above (Scheme 18b). Consequently, the high value obtained for k_{e2} in the case of quinone can probably be interpreted in the same way, but this remains an ad hoc explanation because no experimental evidence is given for the existence of an adsorbed film. Moreover, one has to point out that no experimental evidence can rule out a concerted route. The second two electron−two proton sequence for the nitro group reduction, corresponding to nitroso reduction leading to hydroxylamine, has also been analyzed within the same framework,[108] and reaches the very same conclusions.

Because required pK_a values are usually not known, such determinations of elementary electron transfer rate constants for organic systems involving an even number of electrons transferred are usually not possible. The availability of simulation software,[50,121] gives an opportunity to simulate experimental data and thus test different reaction mechanisms. An attempt has been made to analyze flavin adenine dinucleotide reduction in this way.[122,123] However, in the absence of reliable experimental values for reduction potentials and acid dissociation constants, the selection of values for so many parameters does not seem to be reasonable.

Treatment based on Laviron's formalism (i.e., square schemes with protonation steps at equilibrium) should be easier to apply to the metal−ligand systems mentioned in section 2.2.2 and involving one electron−one proton transfer. Surprisingly, such kinetic studies have not been done except for a very few examples, one of which concerns the $Ru^{III}OH$ oxidation[71] already discussed in section 2.2.2 and another of which involves a substrate attached to an electrode as detailed in section 2.3.[124]

Another type of system, polyoxometalate anions, may involve proton-coupled electron transfer in water. Electrochemical methods have been used to quantitatively study and interpret PCET for both Keggin and Dawson systems, such as $[\alpha\text{-}H_2W_{12}O_{40}]^{6-}$, $[\alpha\text{-}P_2W_{18}O_{62}]^{6-}$,[125] and $[\gamma^*\text{-}S_2W_{18}O_{62}]^{4-}$.[126] Substituted forms have also been generated in which one of the tungsten cations is replaced by another metal ion that occupies a distorted six-coordinate site comprising five bridging oxo ligands from the metalate framework and a terminal ligand, typically water.[127] This water molecule may be deprotonated or protonated when the metal ion is oxidized or reduced, potentially leading to proton-coupled electron transfer. $[\alpha\text{-}Fe^{III}(OH_2)_2P_2W_{17}O_{61}]^{7-}$ reduction has been investigated using cyclic voltammetry in buffered aqueous media.[128] The experimental results can be well-described by the square scheme mechanism, and therefore a full thermodynamic description as well as a kinetic characterization was possible. Such investigations are useful because the influence of the medium (pH, for example) on the redox chemistry of polyoxometalate has important consequences for their catalytic properties. Other structures such as $[\alpha\text{-}SiW_{12}O_{40}]^{4-}$, $[\alpha\text{-}PW_{12}O_{40}]^{3-}$, $[\alpha\text{-}SiW_{11}O_{39}]^{8-}$, and $[\alpha\text{-}PW_{11}O_{39}]^{7-}$, leading to more complex mechanistic schemes, have also been investigated recently by voltammetry.[129,130] Two single pH-independent waves are first observed (A/B and B/P couples) followed by a third pH-dependent two-electron wave. The general scheme considered is shown in Scheme 19.

Because two electron−two proton pathways are involved, full thermodynamic and kinetic characterization is again difficult. Indeed, many parameters are not known. However, a set of parameters chosen on physically and chemically

Scheme 19

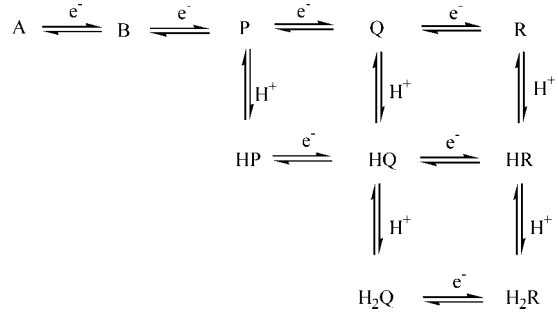

Scheme 20

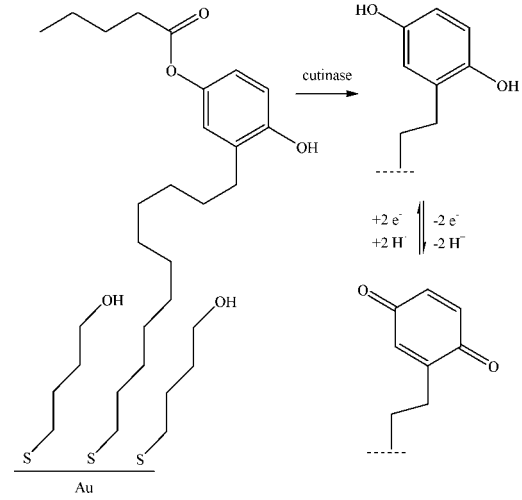

mimicked experimental voltammograms over a wide range of scan rates and pH values as well as rotating disk experiments. Nevertheless, the authors stressed the difficulty of ensuring that a unique solution has been achieved.

2.3. PCET Involving Substrate Attached to an Electrode

Redox couples tethered to an electrode afford an excellent means of observing surface electron transfer kinetics with no complications caused by mass transfer effects.[131] Moreover, self-assembled monolayers (SAMs) allow the preparation of a chemical interface, which is a stable and structurally well-defined monolayer with a controllable thickness and with desirable functionality. Two beneficial effects of SAMs as spacers between the metal and the redox center can be obtained. These are slowing of the electron transfer rates to experimentally accessible ranges by requiring tunneling across the monolayer and minimization of double-layer effects in the kinetic measurements by the low dielectric constant of the monolayer.[131] Therefore, this tool can be applied to decipher mechanistic pathways for redox couples in which proton transfer is coupled to electron transfer. There is also an increasing parallel development of methods that use an interface to transduce a biological activity to an electrical signal. Those interfaces may involve a PCET. Among the wide range of strategies, an approach developed by Mrksich and co-workers relies on the enzymatic conversion of a redox inactive molecule to generate a redox active product. This has been implemented with the enzyme cutinase and 4-hydroxyphenyl valerate as the substrate tethered to a SAM (Scheme 20).[132,133] Cyclic voltammetry is employed to monitor the enzymatic reaction in real time.

The observed waves are due to the oxidation of the enzymatically generated hydroquinone group and the corresponding reduction of the benzoquinone. To quantitatively make the most of this monitoring of enzyme activity, the PCET has to be well characterized.

Another example illustrates the analytical use of PCET from a substrate attached to a SAM. 3,4-Dihydroxyphenethyl mercaptans (DHPM) immobilized on a gold surface are used as chelating ligands for the extraction of metal ions. The overall goal is then to trigger the release of the metal ions by transforming DHPM oxidatively into a weaker ligand.[134] After the metal ions have been removed, reduction of the quinone groups would regenerate the catechol chelating agent. Cyclic voltammetry has, again, been used to assess the electroactivity of the pendant catechol after immobilization.

Both of these examples show that an accurate analysis of PCET involving substrate attached to an electrode is required. Besides, as already mentioned, attachment of the substrate to the electrode is a convenient tool to investigate PCET. Prior to getting mechanistic information on PCET through such systems, characterization of the self-assembled monolayer is necessary. SAMs have been extensively studied during the past 20 years, and their characterization is routine using spectroscopic methods. However, several parameters have to be taken into account when one aims at deciphering electron transfer kinetics through the monolayer, for example, the type of attachment of the redox couple and the effects of the chain length and bridging structure. Regarding the first aspect, that is, attachment of the redox couple, several synthetic strategies have been developed to incorporate molecules such as quinones when they are to be used as the terminal redox center. Most methods lead to a covalently bonded quinone. However, in the specific case of the use of quinones' reactivity toward amines to modify surface molecular chains, it has been established that quinone molecules can be attached in three different forms, each with well-distinguished redox potential.[135] This result shows that attachment of the redox molecule to the thiol chain prior to SAM formation seems to be a better strategy than using a coupling reaction on the already formed monolayer. Moreover, a common approach to overcoming problems arising from intermolecular interactions between functional groups in the SAM consists of dilution of the redox species in the layer by forming a mixed monolayer.[136] Mixed monolayers have been shown to be significantly more stable than a pure monolayer.[137] A second important factor is the effect of chain length on electrochemical behavior of a redox molecule attached to a self-assembled monolayer. This effect was investigated long ago for single outer-sphere electron transfer species.[138] The dependence of the electron transfer rate constant (k) on the electrode−redox species distance (d) is described by eq 16

$$k = k_0 \exp[-\beta d] \tag{16}$$

in which β is the electron tunneling constant. The reported value of β is close to 1 $Å^{-1}$ for a ferrocene-[138] or $Ru(NH_3)_5Py$-[139] tethered molecule on an alkyl chain. A series of thiol-functionalized hydroquinone (H_2Q) derivatives with different alkyl chain lengths have been investigated by cyclic voltammetry.[140] The H_2Q SAMs typical voltammetric responses in aqueous solution are pH dependent with a slope of 58.5 mV/pH for surface formal potential in the pH range from 1.3 to 12.1, which corresponds to the two electron−two proton process of hydroquinone. Complete kinetic characterization of each elementary step was not performed, but an apparent rate constant for overall bielectronic reaction was extracted using Laviron's procedure[55,56,116,117,141] by measuring variation of peak potential splitting with scan rate. Rate constants were obtained in acidic solutions as a function of the number of methylene groups of H_2Q SAMs on gold. The experimental value of $\beta = 1.04$ $Å^{-1}$ is in good agreement with the values previously reported for reversible redox center tethered monolayer systems. However, the electron transfer kinetics shows remarkably different behavior in basic solution.[142] At the same scan rate for which a large peak separation was obtained in acidic solution, a small peak separation value was obtained in basic solution, and it remained the same despite an increase in the alkyl chain length. In highly basic conditions, the hydroquinone moiety is totally deprotonated and a dianion (Q^{2-}) is the major species in SAMs undergoing a bielectronic transfer reaction consisting of two monoelectronic steps uncoupled with proton transfer. It is assumed that in these highly basic conditions, there is a smaller apparent structural change, which makes the apparent rate constant higher. Nonetheless, this effect, if present, would increase the value of k_0 in eq 16, but it cannot explain the extremely small β value observed. Indeed, when high scan rates are reached, large peak separations can be measured, which allows determination of apparent rate constants, but it is remarkable that these large peak separations are independent of the chain length leading to $\beta = 0$ $Å^{-1}$. To date, there is no explanation for this behavior. This study confirms only that solution pH plays an important role in the electron transfer kinetics of a H_2Q-terminated SAM. Besides chain length, the chemical properties of the chain may also influence electron kinetics and thus affect PCET. Electron transfer kinetics of the hydroquinone functionality attached through delocalized tethers, such as oligo(phenylene vinylene)s, are 100-fold faster between pH 4 and 9 than for the same functionality confined to the surface via alkane tethers. This suggests that the rate-limiting step in the two electron−two proton process has a significant electron tunneling component. Also, in this same pH range apparent rate constants are independent of the length of the bridge.[143] No clear interpretation of this feature in terms of the interplay between the electron tunneling and the proton-coupled steps has been given. A possible involvement of counterion movements in the rate-limiting step[144] cannot be excluded.

Assemblies other than SAMs have been used to attach redox couples to an electrode. Poly(vinyl hydroquinone)s[145] and poly(vinyl benzoquinone)s[146] have been coated on glassy carbon electrodes. This last redox polymer exhibits an electrochemical behavior corresponding to a two electron−two proton transfer, with the formal potential having a linear pH dependence with a slope of 59 mV/decade up to pH 6. An apparent electron transfer for overall bielectronic reaction can be determined according to Laviron's procedure,[55,56,116,117,141] and was found to be small (2.1 s^{-1}). This slowness was attributed to the hydrophobic nature of the film, which affects the accessibility of protons.

The effect of buffering on the redox behavior of substrate tethered to a SAM and involving PCET has been investigated. The behavior is more complex than in buffered solution and, in the case of adsorbed mercaptohydroquinone, for example,[147] two redox waves are observed. When the new reduction peak and its corresponding oxidation peak appear (at a more positive potential), both anodic and

cathodic peaks of the original wave become smaller. This new wave is observed when proton concentration in solution is high and the scan rate is low. This has been interpreted as the new wave corresponding to an HeeH or HeHe sequence, whereas the original wave corresponds to an eHeH sequence. The supply of protons is more limited in a solution of lower proton concentration and at a higher scan rate. Studies on anthraquinone-2,7-disulfonic acid SAMs also show the very same behavior.[148]

In all of the above-mentioned studies in buffered solutions, kinetic information is given as an apparent electron transfer rate constant for the overall bielectronic reaction. This results from Laviron's analysis as described in the previous section for freely diffusing species, but it is also valid for attached substrates. It is based on the nine-member square scheme under the assumption that protonation reactions are at equilibrium in the absence of disproportionation and dimerization. In this description, apparent electron transfer rate constants are related to elementary electron transfer rate constants, pK_a values, and proton concentration (eqs 1 and 2). Therefore, determination of reorganization energy from the temperature dependence of this apparent electron transfer rate constant has no chemical meaning.[149] In principle, elementary rate constants may be determined from a kinetic analysis as a function of pH. However, there are many practical limits on using this theoretical treatment to analyze PCET reaction pathways. Those limits usually arise from the fact that information such as pK_a values is unknown. Nonetheless, this theoretical treatment has been implemented to take into account the potential dependence of the transfer coefficient[150,151] as predicted by Marcus theory,[152] whereas in Laviron's treatment, transfer coefficients for electron transfer are assumed to be 0.5 at all potentials. It has been shown that an empirical fifth-order polynomial expression accurately yields the potential dependence of the transfer coefficient, which is theoretically a function of reorganization energies associated with oxidation and reduction processes. The polynomial coefficients are given for a range of reorganization energies. In the framework of PCET, five cases have been considered: 1e1H, 1e2H, 2e, 2e1H, and 2e2H.[151]

There are two distinctive characteristics introduced by the potential-dependent transfer coefficient: (i) deviation of the apparent transfer coefficient from 0.5 in the 1e1H and 1e2H cases and (ii) dependence of the path of electron transfer on electrode potential. Otherwise, the behavior of the apparent rate constant versus pH and the Tafel plots is qualitatively similar to the predicted behavior when all transfer coefficients are equal to 0.5 (Figure 10).

As in the case of freely diffusing substrates, attempts to analyze PCET of substrate attached to electrodes using Laviron's treatment or Finklea's implementation to analyze are very scarce. In the case of two electron−two proton systems, a W-shaped curve with two minima is expected for the logarithm of the apparent rate constant as a function of pH (Figure 10b). Azobenzene SAMs on gold show voltammetric responses in a pH range of 3.2−8.6 that correspond to two electron−two proton oxidation but exhibit a V-shaped dependence of apparent rate constant on pH.[153] The lack of information represented by the missing minimum has prevented more detailed investigation. Hydroquinone SAMs recently studied in alkaline solutions also do not match Laviron's prediction.[154]A simple rate law containing one equilibrium constant and two apparent rate constants (Scheme 21) is able to describe the dependence of the apparent rate constant as a function of pH, but this phenomenological treatment leads to rate constants (k_{QH_2} and k_{QH}) with no obvious chemical meaning. Thus, it appears that a systematic study of the kinetics of systems attached to SAM and involving two electron−two proton-coupled transfer remains challenging.

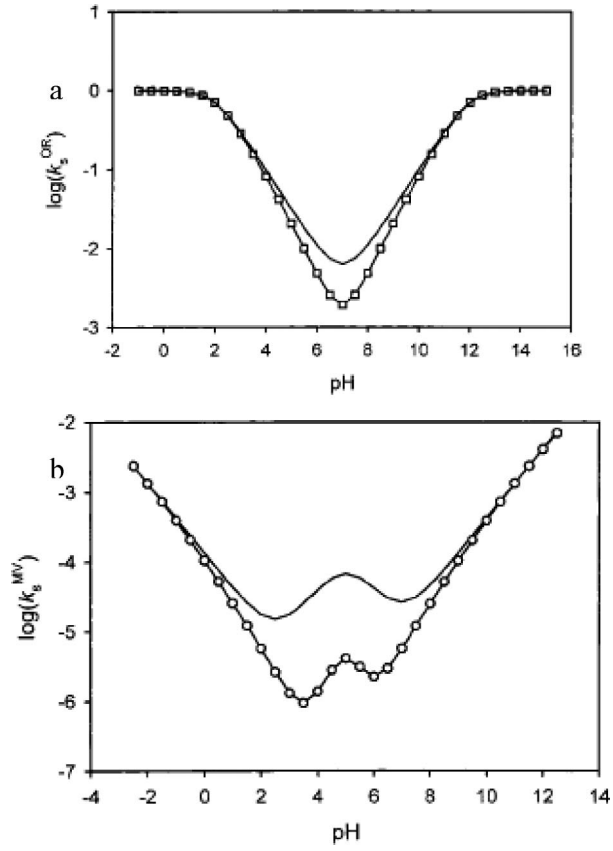

Figure 10. (a) Apparent standard rate constant versus pH for the 1e-1H case, with pK_{a1} = 2, pK_{a2} = 12, and E^0_2 = 0 V: (squares) potential-dependent α; (line) α = 0.5. (b) Apparent standard rate constant versus pH for the 2e-2H case, with pK_{a1} = −12, pK_{a2} = 0, pK_{a3} = −5, pK_{a4} = 10, pK_{a5} = 14, pK_{a6} = 20, E^0_2 = 0 V, and E^0_5 = −0.8 V: (circles) potential-dependent α; (line) α = 0.5. Reprinted with permission from ref 151. Copyright 2001 American Chemical Society.

Scheme 21

$$Q + 2e^- + 2H^+ \overset{k_{QH2}}{\rightleftharpoons} QH_2$$

$$QH_2 \overset{K_{QH2}}{\rightleftharpoons} QH^- + H^+$$

$$Q + 2e^- + H_2O \overset{k_{QH}}{\rightleftharpoons} QH^- + OH^-$$

When incorporated in a phospholipid layer adsorbed on a mercury electrode[155] or incorporated in a supported lipid bilayer and reacting at a gold electrode,[156] ubiquinone-10 (UB) behaves as an adsorbed substrate. Although it is located in a lipidic environment, water and its ions are able to participate in the chemical steps involved in the redox conversion, and the quinone exhibits a typical aqueous two electron−two proton-coupled transfer behavior. A full kinetic characterization has been performed within the framework of Laviron's nine-member square scheme analysis recalled previously.[156] Besides the fact that it is a rare example of a complete application of this theoretical treatment, the most

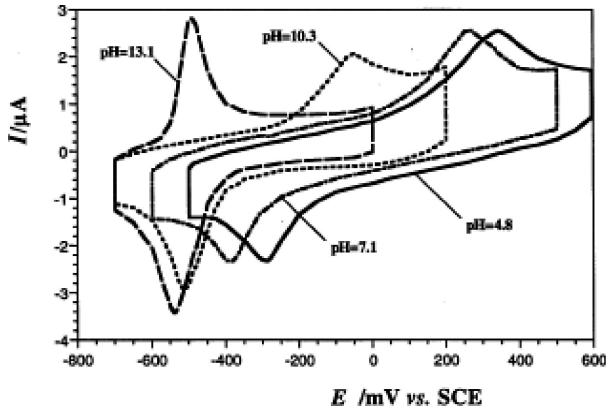

Figure 11. Cyclic voltammograms of ubiquinone in a supported bilayer structure at various pH values. Scan rate: 0.1 V/s. Reprinted with permission from ref 156. Copyright 1998 Elsevier.

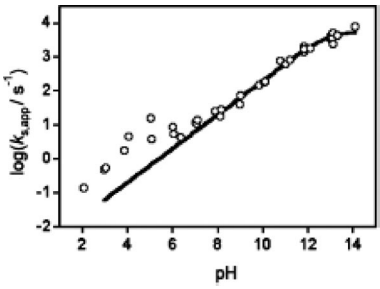

Figure 12. Log(k_s) versus pH plot. The solid line represents the least-squares fit of the data at pH >7 to a model with $\alpha = 0.5$ at all potentials. Reprinted with permission from ref 162. Copyright 2003 Elsevier.

interesting result is that it allows a justification of the striking change affecting the shape of the cathodic peak when the cyclic voltammograms at pH <7.5 are compared with those at pH >7.5 (Figure 11). This reflects a change in the kinetic control of the cathodic process from the first apparent heterogeneous rate constant $k^*_{h1,app}$ at low pH to the second one, $k^*_{h2,app}$ at high pH (Scheme 17).[157] Most elementary surface rate constants (k_{si} $i = 2-6$) have been determined from the pH dependence of the apparent rate constants and reasonable pK_a values. As in the case of freely diffusing benzoquinone,[111] k_{s2} seems too high. The adsorption of the protonated quinone at the gold surface probably causes this apparent acceleration.

Turning to one electron−one proton systems, kinetic analysis should be easier. Among several examples of such systems,[158,159] there are only a few systems for which a full analysis has been performed. The galvinol/galvinoxyl redox system[160] was investigated for pH values between 7 and 13. The apparent formal potential of the redox couple shows a pH dependence (−60 mV per pH unit) in the pH range of 2−11 and a break toward a pH-independent value above pH 12.[161] A nonlinear least-squares fit of the data to the one electron−one proton model described previously (Scheme 11 and Figure 7) yields p$K_{a2} = 11.3$ and $E^0_2 = -0.06$ V versus SCE.[162] pK_{a1} is not measurable, but it is believed to be negative. Measuring the apparent rate constant as function of pH and fitting the data with the one electron−one proton stepwise model at pH >7 yields $k_{s2} = 5600$ s^{-1},[157] independent of whether the transfer coefficient is fixed at 0.5 or potential-dependent (Figure 12). Note, however, that Tafel plots show that anodic and cathodic transfer coefficients are not equal and that the averaged value is above 0.5 over a wide range of pH, thus indicating that transfer coefficient is potential-dependent. Figure 12 shows a substantial deviation of measured rate constants above the predicted rate constants of the models at pH <7. The causes of the deviations have been discussed.[162] Neither a second proton/electron step nor kinetic limitation by proton transfer is a viable explanation. It has thus been suggested that the assumption of stepwise proton−electron transfer is invalid and that a concerted mechanism is involved. Because the low-pH behavior is inaccessible for the galvinol redox center, this possibility has been studied on another model system (e.g., metal complex with an ionizable ligand) that affords access to the entire pH range of behavior.[124,163] This is described in detail in the next section.

3. Concerted Pathway in PCET?

3.1. Introduction

Several experimental features observed in PCET reactions do not fit square schemes (stepwise) mechanism: the second voltammetric cathodic wave of 3,5-di-*tert*-butyl-1,2-benzoquinone being too large,[12] the large potential shift in hydroquinone oxidation in presence of a nearby carboxylate group,[38] the kinetic isotope effect in $[(bpy)_2(py)(HO)Ru^{III}]^{2+}$ oxidation,[77] and the galvinol kinetic deviation from Laviron's stepwise model.[162] These have been attributed to a concerted proton−electron transfer (CPET) mechanism as discussed later in this review. There is indeed a growing interest in the possibility that the electron transfer and proton transfer steps might be concerted, because such a mechanism has a possible role in many natural processes. An important example is photosystem II, which functions to split water and in which CPET could be involved at several levels.[85,164] In PSII, the oxidized chlorophyll P_{680}^+ oxidizes a tyrosine, Y_Z, which functions as a charge transfer interface, and the electron transfer appears to be concerted with proton transfer to a histidine. Moreover, CPET is not limited to charge transport at the terminus of the photosystem: it has been proposed that the oxidation of water at the oxygen-evolving complex (OEC) proceeds by a series of CPET of an oxo-bridged cluster of manganese. Extensive studies have also been done on CPET in cytochrome *c* oxidase[165] and ribonucleotide reductase.[166] Therefore, there have been important recent theoretical and experimental efforts aimed at a systematic study of the concerted proton−electron transfer.[167] The issues to be resolved have been summarized as follows:[2] (i) What factors distinguish the stepwise processes from a concerted pathway? (ii) What structural/electronic features of the proton interface are important in governing the coupling between the electron and the proton? (iii) How will the energetics for charge transfer in an electron transfer or a proton transfer be different in CPET? (iv) How will the CPET rate compare in magnitude with the electron transfer rate? Electrochemical methods appear to be suitable tools to contribute to answering these questions. A key step in getting information from electrochemical data is providing a derivation of potential-dependent rate constant $k(E)$ corresponding to an electrochemical CPET because a typical potential−current density I law would be as given in eq 17

$$\frac{I}{F} = k(E)\left([\mathrm{Red}]_0 - [\mathrm{Ox}]_0 \exp\left[-\frac{F(E - E^0_{\mathrm{CPET}})}{RT}\right]\right) \quad (17)$$

in which $[\mathrm{Red}]_0$ and $[\mathrm{Ox}]_0$ are the CPET reactant concentra-

tions at the electrode surface, E is the electrode potential, and E^0_{CPET} is the standard potential. This key step is detailed in the following section.

3.2. Theory

A quite detailed theoretical framework for homogeneous CPET exists and has been mainly developed by Cukier,[2,168–171] Hammes-Schiffer, [3,172–184] and their co-workers along with contributions from others.[185–187] This theory has proven to be useful in understanding many features of CPET and has been applied to many homogeneous systems. However, the simpler form of Marcus theory, originally devised for outer-sphere electron transfers,[152] has been preferred for analyzing most CPET reactions. The reason is presumably that this CPET theoretical framework, requiring as it does calculation of multiple mixed electronic/vibrational states, is not in a suitable form for easy analysis of the data. Moreover, its application to electrochemical CPET, in which the electron donor or acceptor is an electrode, requires averaging the rate constant over the Fermi levels of the electron in the electrode (as in conventional electron transfer reaction treatments of electrochemical processes[188]).

Electrochemical CPET has been recently investigated theoretically by several groups.[189–192] The main point of CPET theories is the double adiabatic approximation, which treats the electron as a fast subsystem with respect to the proton and treats the proton as a fast subsystem with respect to the degrees of freedom of the medium, as in proton transfer theories.[193–197]

In the early approach[189] the electron transfer was assumed to be nonadiabatic and was treated as a two-level system with the environment approximated by harmonic baths. One of these baths represented the medium, and its interaction with electrons described the long-range electrostatic interaction with a polarizable continuum. The other bath represented a local dispersion mode, which is typically the proton donor−acceptor vibration (Q mode) coupled to additional vibrations (Scheme 22).

It follows that the medium and local mode interactions contribute to the reaction rate independently. The medium is treated classically and appears as a reorganization energy in the expression of the reaction activation energy. The role of the dispersion mode depends on the temperature regime. At low temperature, the local vibration (Q mode) is frozen in the ground state. This vibration is referred to as a gating

Scheme 22

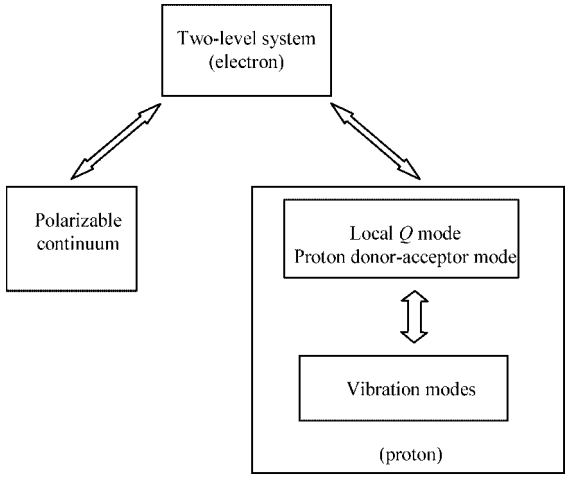

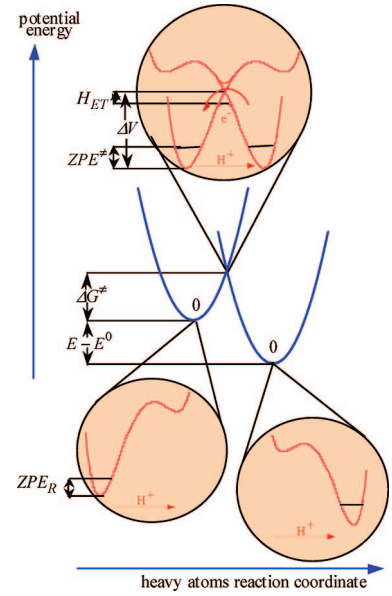

Figure 13. Schematic representation of the potential energy profiles in the case where the CPET reaction involves only the proton vibrational ground states: (upper inset) at the transition state, the system is described by two electronic states, each of them being obtained from a pair of proton diabatic states; (lower insets) proton diabatic state for reactant and products.

mode. An expression for the rate constant is obtained from the Golden Rule formula once the Hamiltonian has been described as

$$H = \Delta E + C_C + H_I + H_{II} + H_C$$

where ΔE is the energy difference between both levels of the two-level system, C_C is the coupling operator, H_C is the linear coupling term between the two-level system and both baths, and H_I, H_{II} are the harmonic Hamiltonian of the two baths. Rate constants have been given in various limiting situations. At high temperatures with respect to the local mode and strong coupling (i.e., large values of reorganization energies), $k(E)$ is given by eq 18

$$k(E) = C^2 \sqrt{\frac{\pi}{RT(\lambda_0 + \lambda_Q)}} \exp\left[\frac{-(\Delta E + \lambda_0 + \lambda_Q)^2}{4RT(\lambda_0 + \lambda_Q)}\right] \quad (18)$$

in which λ_0 and λ_Q are the reorganization energies of both baths. This expression coincides with the Marcus formula for a simple nonadiabatic electron transfer. At low temperatures with respect to the local mode, the activation energy is determined by the "polar" bath and $k(E)$ is as given in eq 19

$$k(E) = C^2 \exp\left[-\frac{\lambda_Q}{h\nu_Q}\right] \sqrt{\frac{\pi}{RT\lambda_0}} \exp\left[\frac{-(\Delta E + \lambda_0)^2}{4RT\lambda_0}\right] \quad (19)$$

in which ν_Q is the local mode vibration. The tunneling matrix element C is very sensitive to the proton donor−acceptor distance as shown in similar models in the context of homogeneous proton transfer[195,198,199] and PCET.[2,3] These rate constants must be averaged over E, the electron energy in the electrode.

For this theory to be useful in analyzing experimental data, two terms have to be specified: λ_0, the reorganization energy

of the "polar" bath, that is, the solvent, and C, the tunneling matrix element. Moreover, this theory has been developed in the nonadiabatic limit, and one must consider what happens when the coupling constant is high and adiabatic conditions are approached. This issue has been discussed in a theoretical contribution from Kuznetsov and Ulstrup.[187] The concerted mechanism is referred to as synchronous and is treated in the framework of the double-adiabatic approximation. Three regimes, fully nonadiabatic, partially adiabatic, and fully adiabatic, are considered. The first case is similar to the theoretical description given above, but the tunneling matrix element is detailed in eq 20

$$C = H_{ET}\langle\chi_i|\chi_f\rangle \tag{20}$$

where H_{ET} is the electron coupling constant and $\langle\chi_i|\chi_f\rangle$ the overlap between the initial and final proton vibrational wave functions. A partially adiabatic transition takes place when the electron coupling constant H_{ET} is sufficiently large, whereas the resonance splitting of the proton levels remains small. The rate constant remains the same, but the coupling constant C is now described by a tunneling probability for the proton through a potential barrier. For a fully adiabatic transfer, the transmission coefficient is 1. The link between these limiting cases is given by the Landau−Zener transition probability.[200,201]

These theoretical formulations of rate constants are difficult to apply to experimental data analysis. The theoretical treatment developed by Schmickler and co-workers,[190,191] the basis of which is very similar to that of the early approach described above, is even more difficult to apply to experimental data analysis.

A simpler model that is formed on the same basis but overcomes these difficulties has been proposed.[192] The relationships expressing the electrochemical rate constant as a function of the electrode potential have been derived initially in the nonadiabatic limit,[192] and they have been extended to other regimes using the Landau−Zener model.[202] The model is based on the double-adiabatic approximation under which the electron and proton both act as light particles, so that their transfer requires a reorganization of the solvent and of heavy atoms to reach a transition state in which both reactants and products have the same configuration. Note that proton transfer is electronically adiabatic because the system is described by two electronic states, each obtained from a pair of proton diabatic states (Figure 13). Consequently, the reaction coordinate for a CPET pathway is made up of three ingredients: (i) an internal coordinate representing all interatomic distance and angle changes involving heavy atoms, (ii) a fictitious charge number representing solvent reorganization upon electron transfer, and (iii) a dipole variation index representing solvent reorganization upon proton transfer. Separation of the solvent coordinates into two independent coordinates has been established using an electrostatic model sketched in Scheme 23.[192] The two reorganization energies noted, λ_0^{ET} and λ_0^{PT}, are defined according to eqs 21 and 22, respectively,

$$\lambda_0^{ET} = \frac{e^2}{4\pi\varepsilon_0}\left(\frac{1}{\varepsilon_{op}} - \frac{1}{\varepsilon_S}\right)\frac{1}{2a} \tag{21}$$

$$\lambda_0^{PT} = \frac{1}{4\pi\varepsilon_0}\left[\left(\frac{\epsilon_S - 1}{2\varepsilon_S + 1}\right) - \left(\frac{\epsilon_{op} - 1}{2\varepsilon_{op} + 1}\right)\right]\frac{(\mu_R - \mu_P)^2}{a^3} \tag{22}$$

in which ε_0 is the vacuum permeability, ε_{op} and ε_S are the optical and static dielectric constants of the solvent, a is the radius of the reactant equivalent sphere, and μ_R and μ_P are the dipole moments of the reactant and product, respectively. Equation 22 is similar to the Lippert−Mataga equation that accounts for change in dipole moment between ground and excited states.[203,204]

The classical quadratic Marcus−Hush term for the activation energy based on harmonic approximation for the free energy of diabatic states is given in eq 23, with the potentials in volts and the energies in electron volts.

$$\Delta G^{\neq} = \frac{\lambda}{4}\left(1 + \frac{\Delta G^0}{\lambda}\right)^2 - \frac{\Delta ZPE}{RT} \tag{23}$$

In eq 23, λ, the total reorganization energy during the reaction, is given by $\lambda = \lambda_i + \lambda_0^{ET} + \lambda_0^{PT}$ in which λ_i is the intrinsic reorganization energy. ΔZPE is the difference between the transferring proton zero point energies at the transition state and at the reactant state, and ΔG^0 is the standard free energy of the CPET reaction. Z, the pre-exponential factor of the rate constant, is the product $Z = Z_{el}\chi$ of the collision frequency $Z_{el} = \sqrt{RT/2\pi M}$, in which M is the reactant molar mass and the transmission coefficient χ is given in eq 24.

$$\chi = \frac{2p}{1+p} \tag{24}$$

In eq 24, p is the probability of proton tunneling and electron transfer, which occurs at the transition state as sketched in the upper inset of Figure 13 and is obtained from the Landau−Zener expression as in eq 25.

$$p = 1 - \exp\left[-\pi\left(\frac{C}{RT}\right)^2\sqrt{\frac{\pi RT}{\lambda}}\right] \tag{25}$$

In eq 25, the constant Cmeasures the coupling between the reactant and product proton vibrational states. (Note that in this approach vibronic states are the product of electronic and vibrational states so that this is a subset of more general theories.[168−187]) The transmission coefficient χ is a measure of the deviation from adiabatic behavior. If transfer is adiabatic, then Z is equal to the collision factor Z_{el} or, equivalently, in the framework of transition state theory, the ratio of the partition functions of the transition state and the initial state of the reactant. If transfer is nonadiabatic, $0 < \chi$

Scheme 23. Electrostatic Model for Solvent Reorganization in Electrochemical CPET Reduction[a]

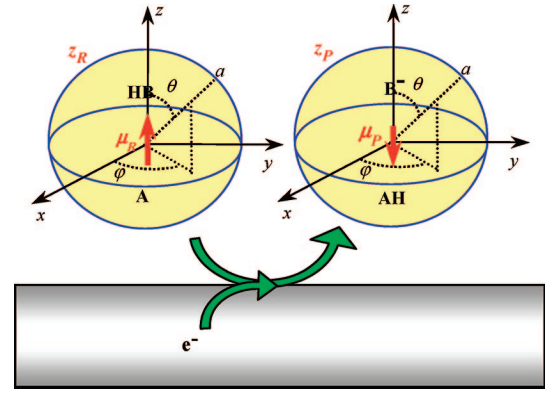

[a] Reactant A···HB is a spherical cavity (of radius a and of charge z_R) with a point dipole (μ_R) at the center of the cavity. Product AH···B$^-$ is a spherical cavity (of radius a and of charge z_P) with a point dipole (μ_P) at the center of the cavity.

< 1. The double-adiabatic approximation implies that the electron is transferred at the avoided crossing intersection of the potential energy profiles of the resulting two states while the proton tunnels through the barrier thus formed, leading to the potential energy profiles sketched in Figure 13, in which a proton transfer occurs between two proton vibrational ground states. In an initial simple approach, it is assumed that this, rather than transfers involving proton vibrational excited states, is the most important contribution to the rate constant. The modeling of the barrier skeched in Scheme 24 has been proposed. It allows an estimation of C_{eq} (i.e., the coupling constant corresponding to the equilibrium distance between the proton donor and acceptor atoms) as a function of the barrier height, ΔV, depending on the distance between the donor and acceptor atoms, Q.

Within this model, the coupling constant is given by eqs 26 and 27 as

$$C(Q) = h\nu_0^{\neq} \exp\left[-\frac{8\sqrt{2}}{3}\sqrt{\frac{h\nu_0^{\neq}}{\Delta V^{\neq}}}\left(\frac{\Delta V^{\neq}}{h\nu_0^{\neq}} - \frac{1}{2}\right)^{3/2}\right] \quad (26)$$

with

$$\Delta V^{\neq}(Q) = \frac{f_0^{\neq}}{4}\left(\frac{Q - d_{AH}^0 - d_{DH}^0}{2}\right)^2 \quad (27)$$

where $f_0^{\pm} = 4\pi^2\nu_0^{\pm 2}m_P$ is the force constant of the proton well and d_{DH}^0 and d_{AH}^0 are the proton equilibrium distances in the reactant and product, respectively. Finally, the transmission coefficient is averaged in the classical mechanical Q motion limit. Indeed, mere consideration of the equilibrium coupling constant is not sufficient for an accurate description of the reaction kinetics. The actual coupling constant, C, is a function of Q, the distance between the donor and acceptor atoms, so proton tunneling between the reactant and product states is a function of the donor−acceptor vibration with the shorter distance yielding easier proton tunneling. In a classical mechanical description, the contribution of each distance Q to proton tunneling is obtained by weighting the transmission coefficient by the Boltzmann probability $P(Q)$ that the donor and acceptor atoms are at a distance Q from one another, as in eq 28

$$\chi = \int_{-\infty}^{+\infty} \chi(Q)P(Q)\,dQ \quad (28)$$

where $P(Q)$ is the normalized Boltzmann distribution function for a classical harmonic oscillator, as in eq 29

Scheme 24. Modeling of Tunneling Barrier[a]

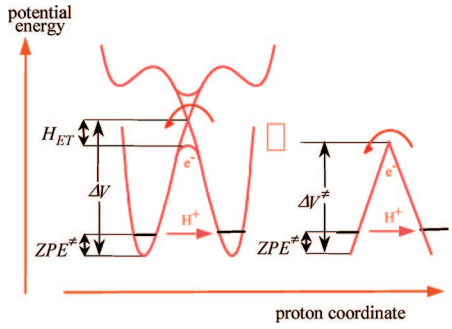

[a] The barrier is approximated by an isosceles triangle.[202]

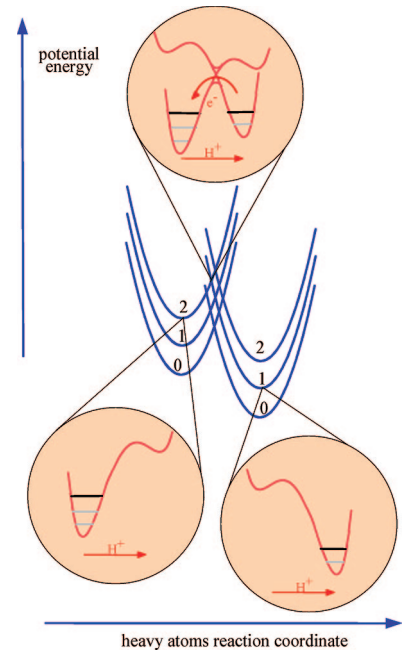

Figure 14. Schematic representation of the potential energy profiles in the case where the CPET reaction involves the proton vibrational excited states.

$$P(Q) = \sqrt{\frac{f_Q}{2\pi RT}}\exp\left(-\frac{f_Q(Q - Q_{eq})^2}{2RT}\right) \quad (29)$$

in which $f_Q = 4\pi^2\nu_Q^2 m_Q$ with ν_Q being frequency and m_Q reduced mass. The end result is that estimation of the averaged transmission coefficient requires the values of a limited of number parameters (ν_Q, $\nu_0^{\pm}$, Q_{eq}, d_{DH}^0, and d_{AH}^0), which can be estimated in typical experimental cases.[202]

In dealing with electrochemical CPET reactions, all electrode electronic states, not only those that are close to the Fermi level, have to be taken into account. Once the expressions of the individual rate constants are obtained, they are summed over all electronic states, weighing each state's contribution according to the Fermi−Dirac distribution just as in the theory of electrochemical outer-sphere electron transfer.[188] Assuming that the individual transmission coefficient χ and the density of state are independent of the energy of the electronic states,[205] the resulting rate constant for an oxidation process is expressed by eq 30[202]

$$k(E) = Z\sqrt{\frac{RT}{4\pi\lambda}}\int_{-\infty}^{+\infty} \times \frac{\exp\left\{-\frac{w_R}{RT} - \frac{RT}{4\lambda}\left[\frac{\lambda}{RT} + \frac{F(E - E^0) - w_P + w_R}{RT} - \zeta\right]^2\right\}}{1 + \exp\zeta}d\zeta \quad (30)$$

with $\zeta = (\mathbf{E} - \mathbf{E}_F)/RT$, $w_R = z_R F\phi_S$, and $w_P = (z_R + 1)F\phi_S$, where $\mathbf{E}_F$ is the Fermi level energy and ϕ_S is the double-layer potential. The pre-exponential factor is $Z = Z_{el}\chi_m$, where the transmission coefficient χ_m in which m refers to a multistate model, involves the electronic interaction between the redox system and each level in the electrode. The equation for χ_m is analogous to that for χ in the case of two states (eq 24), but the probability of proton tunneling and electron transfer p_m now includes the density of states ρ, as in eq 31.

$$p_m = 1 - \exp\left[-\pi\left(\frac{C}{RT}\right)^2\sqrt{\frac{\pi RT}{\lambda}}\rho\right] \quad (31)$$

At zero driving force, that is, for $E = E^0$, this yields k_S as in eq 32.

$$k_S = Z\sqrt{\frac{RT}{4\pi\lambda}}\int_{-\infty}^{+\infty}\frac{\exp\left\{-\frac{w_R}{RT} - \frac{RT}{4\lambda}\left[\frac{\lambda}{RT} + \frac{w_R + w_P}{RT} - \zeta\right]^2\right\}}{1+\exp\zeta}d\zeta \quad (32)$$

The expression relating the CPET rate constant to the electrode potential is thus formally the same as for outer-sphere[206] and dissociative[207] electron transfer electrochemical reactions. It is characterized by three parameters, E^0, Z, and λ. Typical values of Z and λ are, however, different in each of these cases. With CPET reactions, slowness is mostly related to a small value of Z rather than to a large value of λ. It follows that individual rate constants pertaining to the inverted region may well be involved, which makes the consideration of all electrode electronic states mandatory. The pre-exponential factor $Z = Z_{el}\chi_m$ can be modified when the proton is replaced by a deuteron, but E^0 and λ are less sensitive. If the CPET reaction is fully adiabatic, that is, if $\chi_m = 1$ (and $p_m = 1$), the H/D kinetic isotope effect is expected to be small. Larger values of the H/D kinetic isotope effect are expected as nonadiabaticity increases (i.e., $\chi_m < 1$ and $p_m < 1$), because tunneling is expected to be slower in the deuterium case than in the hydrogen case.

So far, only the case when proton transfer occurs between two proton vibrational ground states has been considered. The effect of proton transfer between proton vibrational excited states has been addressed.[202] Such a situation is exemplified in Figure 14, which shows the case of proton transfer occurring between the vibrational excited states $\mu = 2$ and $\nu = 1$. As compared to the $\mu = 0$ to state $\nu = 0$ transfer, the situation is more favorable in terms of both driving force and proton tunneling. The corresponding contribution has, however, to be weighted by the Boltzmann probability of the system being in this excited state. In general, the rate constant appears as a sum of a series of individual rate constants, $k_{\mu\nu}$, with each contributing according to its Boltzmann weight according to eq 33

$$k(E) = \frac{\sum_{\mu=0}^{\mu=\infty}\sum_{\nu=0}^{\nu=\infty}k_{\mu\nu}(E)\exp\left(-\frac{\mu h\nu_0}{RT}\right)}{\sum_{\mu=0}^{\mu=\infty}\exp\left(-\frac{\mu h\nu_0}{RT}\right)} \quad (33)$$

where ν_0 is the frequency of the H vibration, which is assumed to be the same in the transition reactant and product electronic states.

To get information from electrochemical data, the typical potential−current density law (eq 17) can be used. Considering the fact that the potential excursion in cyclic voltammetric experiments (or in other electrochemical techniques) does not exceed a few hundreds of millivolts, the rate law may be linearized[202] leading to the applicability of Butler−Volmer rate law as shown in eq 34

$$\frac{I}{F} = k_S^{ap}\exp\left[\frac{\alpha F}{RT}(E - E^0_{CPET})\right]\left([Red]_0 - [Ox]_0 \times \exp\left[\frac{-F(E-E^0_{CPET})}{RT}\right]\right) \quad (34)$$

and to eqs 35–37 defining the apparent standard rate constant

$$k_S^{ap} \simeq Z\left[\sqrt{\frac{RT}{4\pi\lambda}}\pi\exp\left(-\frac{\lambda + 4(\alpha + z_R)F\varphi_S + 4\Delta ZPE}{4RT}\right)\right] \quad (35)$$

with

$$Z = Z_{el}\chi^{ap} \quad (36)$$

and

$$\chi^{ap} \approx \left[\frac{\sum_{\mu}\sum_{\nu}\chi_{\mu\nu}\exp\left[-\alpha\frac{(\nu-\mu)h\nu_0}{RT}\right]\exp\left(\frac{\mu h\nu_0}{RT}\right)\exp\left(\frac{-2\mu\Delta ZPE}{RT}\right)}{\sum_{\mu}\exp\left(-\frac{\mu h\nu_0}{RT}\right)}\right] \quad (37)$$

where $\chi_{\mu\nu}$ is the transmission coefficient for the μ to ν transition. The value of the transfer coefficient, α, is taken to be constant, although not necessarily equal to 0.5, over the relatively narrow potential excursion in standard cyclic voltammetric experiments.

This electrochemical expression for the CPET rate constant, like more general CPET rate constant expressions,[168–187] makes it possible to make progress on the issues listed previously, to wit:

(i) What structural/electronic features of the proton interface are important in governing the coupling between the electron and the proton?

The fundamental reason for potential nonadiabaticity of CPET is that the reactant and product proton vibrational wave functions are localized in different wells and may have very small overlap. In other words, as discussed earlier, the proton has to tunnel through a substantial barrier. Consequently, the proton donor−acceptor distance as well as its vibration frequency, also called "gating frequency", is the important factor in governing the coupling between the electron and the proton.

(ii) How will the energetics for charge transfer in an electron transfer or a proton transfer be different in CPET?

Coupling of a follow-up protonation with an electron transfer reaction offers an additional driving force regardless of whether the two steps are successive or concerted. For the stepwise mechanisms, kinetic limitations on the gain in driving force are imposed by the electron transfer steps. In the concerted case, the kinetics responds directly to changes in the standard free energy of the global reaction. The price paid for this direct responsiveness is the next issue.

(iii) How will the CPET rate compare in magnitude with electron transfer rate?

This problem is somewhat similar to that for reactions in which electron transfer is concerted with the breaking of a bond linking two heavy atoms and, indeed, once it has been linearized, the expression relating the CPET rate constant to the electrode potential is formally the same as for outer-sphere or dissociative electron transfer electrochemical reactions. This equation is characterized by three parameters,

Scheme 26

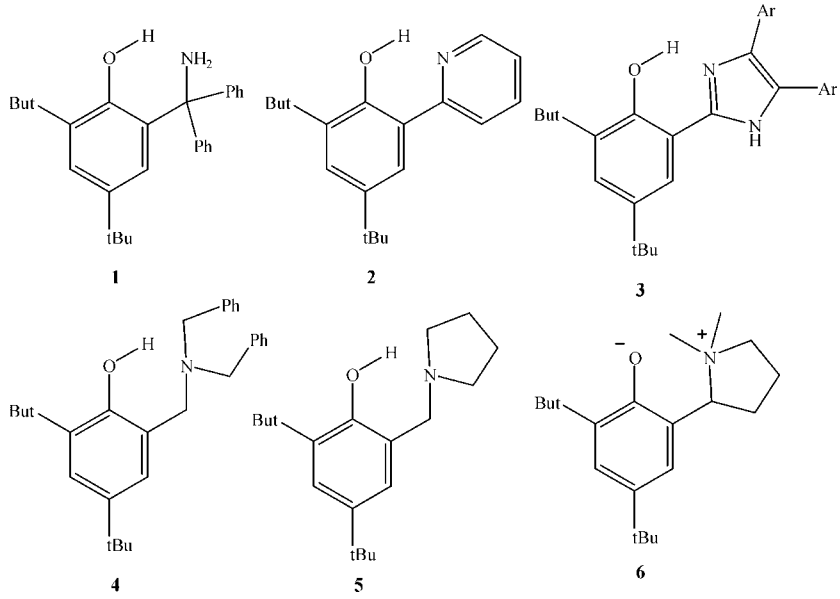

E^0, Z, and λ. In the case of dissociative electron transfer, the gain in driving force is partly compensated by the inclusion of the bond dissociation energy in the reorganization factors that control the intrinsic barrier. In CPET reactions, the trade-off is different and involves instead a decreased pre-exponential factor that originates from proton tunneling through a substantial barrier resulting from proton−electron coupling. Therefore, with CPET reactions, slowness is mostly related to a small value of Z rather than to a large value of λ.

All of these features have been investigated experimentally on various systems as described in section 3.3 with a view to illustrating the occurrence of CPET pathways, rather than competing stepwise pathways that involve the transfer of an electron followed by the transfer of a proton or vice versa. For the sake of simplicity, the two cases in which either CPET takes place within a hydrogen-bonded complex in aprotic solvent (subsection 3.3.1) or in which CPET takes place in water (subsection 3.3.2) are considered separately.

3.3. Experimental Illustrations

3.3.1. CPET through Hydrogen-Bonded Complexes

The effect of proton motion in the PCET reaction has been intensively investigated by Nocera and co-workers on donor/acceptor model systems with well-defined electron transfer distances and proton hydrogen bond geometries.[208] The reaction is initiated by laser excitation of the donor or the acceptor, and the reaction is monitored by a wide array of ultrafast and nanosecond spectroscopies. The electron and proton transfers are collinear and transferred through a amidinium−carboxylate salt bridge (Scheme 25).

Scheme 25

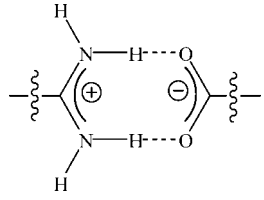

Such reactions are important in biology because electron transfer in many proteins and enzymes occurs along pathways that have hydrogen bond contacts between amino acid residues and polypeptide chains.[209] In the systems investigated, protons mediate electronic coupling between the electron donor and acceptor, and the mediating protons must deviate from their equilibrium positions to optimize electronic coupling for electron transfer. However, from an experimental point of view, these studies show that it is difficult to measure PCET reaction kinetics directly by time-resolved methods because proton networks retard charge transfer rates, thus resulting in low yields of PCET intermediates.[210] They also show that kinetic isotope effects (KIE) and their temperature dependence are key observables to characterize photoinduced CPET.[211] Other systems have been investigated by spectroscopic methods with a photochemical initiation of CPET as in, for example, the oxidation of phenol by C_{60} triplet in the presence of pyridine, in which a significant deuterium kinetic isotope effects is observed, indicating a CPET reaction.[212] The same argument has been used to prove that oxidation of disubstituted α-hydroxy radical is concerted with its deprotonation.[213] The KIE appears as the main experimental criterion for assigning a CPET pathway.

Thermal initiation of PCET reactions, such as intramolecularly amine driven phenol oxidations (**1**−**3** in Scheme 26), have also been reported. The homogeneous electron acceptor is a cation radical, and the kinetics has been determined by stop-flow experiments. Stepwise pathways are ruled out on thermochemical considerations, and the concerted nature of the mechanism is confirmed by KIE.[214–216] A third argument for the CPET mechanism is the dependence of activation barrier on driving force. Indeed, the variation of the rate constant for oxidation of **1** by a series of triarylamine cation radicals leads to $\Delta\Delta G^{\neq}/\Delta\Delta G^0 = 0.53$, a value not compatible with a stepwise mechanism, which would have $\Delta\Delta G^{\neq}/\Delta\Delta G^0 \approx 0$ for a proton transfer limiting step and $\Delta\Delta G^{\neq}/\Delta\Delta G^0 \approx 1$ for an initial electron transfer limiting step.[215] Analysis of the rate constant as a function of temperature and driving force was done in the framework of Marcus theory, and it is concluded that the reaction is adiabatic but endowed with a larger reorganization energy than that for electron transfer reactions of aromatic com-

Scheme 27

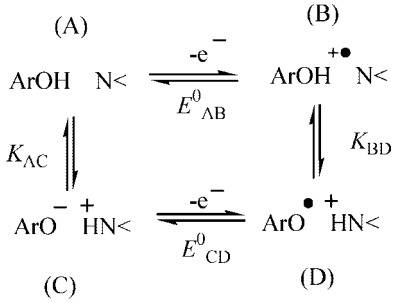

pounds. On systems similar to compound **2**, in which the phenol is conjugated with the basic nitrogen atom, CPET is faster due to this conjugation.[217]

Although reversible cyclic voltammetry has been reported in several cases,[218–220] only one electrochemical mechanistic study of this family of compounds has concluded that the reaction follows the same CPET mechanism.[221,202] Another electrochemical mechanistic study has appeared on **4**, concluding that the reaction occurs via a square scheme mechanism that would involve both of the stepwise branches shown in Scheme 27.[222] However, this proposal has been considered to be unlikely.[223] The electrochemical approach consists of two steps: first, establishment of the mechanistic pathway as being stepwise or concerted and, second, if a concerted mechanism is followed, comparison of the kinetic experimental data (rate constant, reorganization energy, pre-exponential factor, KIE) obtained from cyclic voltammetry to theoretical values obtained from application of a model[192,202] in which only a few parameters are estimated from literature data or quantum mechanical ab initio or density functional theory calculations. This strategy was applied to 2,4-di-*tert*-butyl-6-(1-pyrrolidino)phenol **5**. At low scan rates, the cyclic voltammogram shows a wave that is electrochemically reversible. At a higher scan rate, the kinetics of electron transfer starts to interfere. Comparison of experiments in the presence of 2% methanol and 2% CD_3OD indicates the existence of a small but definite kinetic isotope effect ($Z_H/Z_D = 1.8$). Although the observed KIE is a good indicator for the occurrence of a CPET reaction, the possibility that the cyclic voltammetric data could be interpreted in terms of the square scheme mechanism involving the electron−proton (EP) and/or proton−electron (PE) pathways shown in Scheme 27 was tested. The standard potentials and equilibrium constants defined in Scheme 27 were estimated for this purpose. As a first approximation, E^0_{CD} can be equated with the standard potential of the zwitterionic phenolate: 2-(3,5-di-*tert*-butyl-2-oxyphenyl)-1,1-dimethylpyrrolidinium **6**. Similarly, E^0_{AB} can be equated with the standard potential of tri-*tert*-butylphenol, that is, 1.59 V versus SCE.[41] Simulation[121] of the voltammogram expected at 0.2 V/s (blue line in Figure 15) is clearly incompatible with the experimental data. Note that these estimates of the E^0 values and consequently K values implicitly assumed that the electrostatic and H-bonding stabilization of C equates the electrostatic stabilization of the zwitterionic phenolate **6** and that the H-bonding stabilizations of A and B are approximately the same. Such approximations may lead to an underestimation of the contributions of the PE and EP pathways. If an average value of H-bond energy is taken into account, the simulation (green line in Figure 15) is clearly incompatible with the experimental data (red line in Figure 15).

Scheme 28

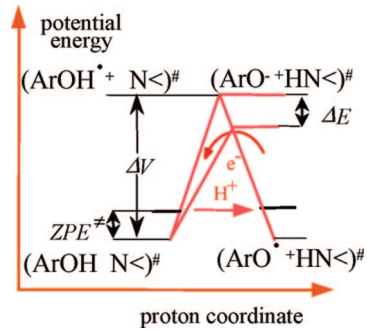

To resolve the question of the degree of adiabaticity of the reaction, a separate determination of the pre-exponential factor and of the reorganization energy from an examination of the rate constant variations with temperature has been done.[202] This was derived from the variation of the cyclic voltammogram with temperature. Linearization of the activation−driving force laws simplifies the treatment of the kinetic data, notably by allowing the use of Arrhenius plots to treat the temperature dependence of the rate constant. The electrochemical reaction appears to be adiabatic. In contrast, application of this procedure and a careful determination of the variation of the driving force with temperature led to the conclusion, unlike those previously reported,[215] that the homogeneous reaction between **1** and cation radicals is nonadiabatic with a transmission coefficient on the order of 0.005 and that the self-exchange reorganization energy is about 1 eV lower than previously estimated. The value of the transmission coefficient is in agreement with a value calculated from a model using reasonable estimated parameters. The difference in behavior of the electrochemical and homogeneous reactions is deemed to derive from the effect of the strong electric field within which the electrochemical reaction takes place, which stabilizes a zwitterionic form of the reactant at the transition state in which the proton has been transferred from oxygen to nitrogen as in Scheme 28. Taking this difference in adiabaticity into account, the magnitudes of the reorganization energies of the two reactions appear to be quite compatible one with the other as revealed by an analysis of the solvent and intramolecular contributions in both cases.

As already mentioned, a large potential shift in hydroquinone oxidation is observed in aprotic media in the presence of a nearby carboxylate group.[38] A strategy comparable to that described above was used to interpret this feature. The 2,5-dicarboxy-1,4-benzoquinone/2,5-dicarboxylate 1,4-hydrobenzoquinone couple exhibits a quasi-Nernstian behavior at low scan rate, whereas the anodic and

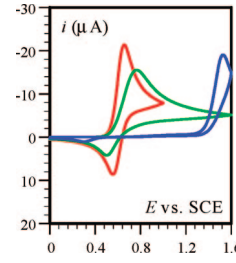

Figure 15. Cyclic voltammetry of **5** in acetonitrile + 0.1 M n-NBu_4PF_6: (red) experimental data; (blue, green) simulation of the square scheme mechanism. Temperature: 20 °C. Scan rate: 0.2 V/s. Reprinted with permission from ref 221. Copyright 2006 American Chemical Society

Scheme 29

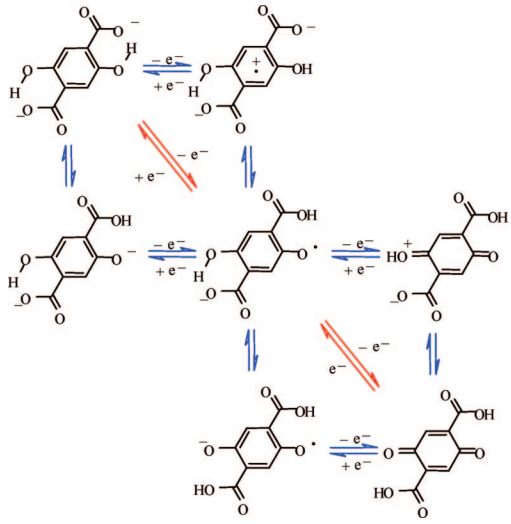

cathodic peaks tend to separate upon raising the scan rate as electron transfer kinetics starts to interfere. These observations point to two successive reactions in which the transfer of each successive electron is coupled with proton transfer from the phenolic to the carboxylate position. The mechanism (Scheme 29) of these two successive proton-coupled electron transfers may be stepwise (square scheme marked in blue) or concerted (CPET marked in red). There is a small but definite hydrogen/deuterium kinetic isotope effect on both waves, which appears, as expected, only when the scan rate is large enough for electron transfer kinetics to interfere.

This observation is a good indication that a CPET mechanism is followed for the two successive proton-coupled electron transfers. The stepwise square scheme mechanism is ruled out because it is predicted to be slower than observed and because it is also predicted to show no H/D kinetic isotope effect. For the CPET mechanism, approximate predictions based on the theory of electrochemical concerted proton−electron transfers[192] led to a predicted value of the standard rate constant compatible with the experimental values. This is also the case with the value of the H/D kinetic isotope effect predicted on the same basis. This is an additional demonstration that carboxylate groups may serve as proton-accepting sites in concerted proton−electron transfer reactions.

Oxidation of a phenol group has also been shown to be facilitated by a hydrogen-bonded external base, for example, pyridine.[224] The oxidation was mediated with a ferrocene acting as an intramolecular antenna (Scheme 30). The intramolecular electron transfer has been suggested to be concerted with deprotonation.

The proton-coupled reduction of oxygen to water powers aerobic organisms. On the one hand, the design of catalysts that promote the selective reduction of oxygen to water requires the management of both electrons and protons and has attracted attention for a long time.[225] The role of proton-coupled electron transfer in O−O bond activation has been recently reviewed.[226] On the other hand, direct reduction of dioxygen at various electrodes has also been extensively studied.[227] Platinum, for example, has well-known electrocatalytic properties in the presence of proton donors.[228] In nonaqueous media the reduction of dioxygen leads to superoxide on various electrode surfaces. In the presence of sufficiently strong proton donors, a proton-coupled electron

Scheme 30

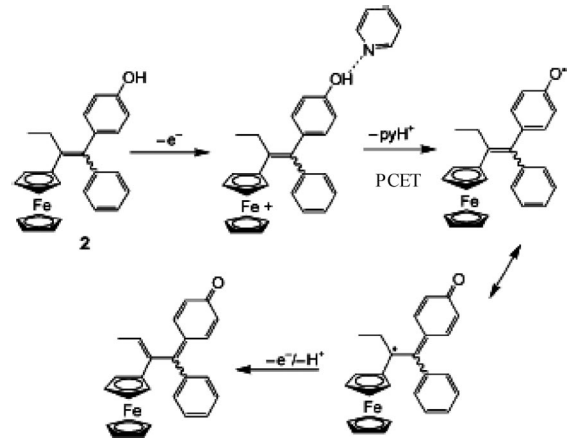

transfer is triggered, as it is for the quinone discussed previously, and the one-electron reduction of dioxygen is converted to an overall two-electron process producing hydroperoxide anion.[229] Attention has been recently directed to the reduction of superoxide in nonaqueous media in the presence of weak proton donors.[230,231] This is indeed the first case in which the occurrence of an electrochemical CPET reaction was unambiguously proved.[232] The cyclic voltammetries of dioxygen in acetonitrile and in dimethylformamide (DMF) are similar. In both cases, the second wave corresponds to the reduction of a water−superoxide ion complex. Figure 16 shows an example of cyclic voltammetric response obtained in DMF. The peak width of the second wave indicates a remarkably small value of the transfer coefficient (symmetry factor), α. It is much smaller than the value typical of outer-sphere electron transfer, 0.5, and is more reminiscent of dissociative electron transfers.[207] However, the reasons behind these small α values are different in the two cases. With dissociative electron transfers, reorganization energies are large because they include the dissociation energy of a bond linking two heavy atoms. The reaction therefore takes place at a potential that is far more negative than the standard potential, thus causing α to be small. With CPET, the driving force is also large, but this is now because the pre-exponential factor is small, whereas λ is not particularly large.

One of the reasons for the nonadiabaticity is that the proton has to tunnel through a substantial barrier. A kinetic isotope effect in agreement with a CPET pathway was measured. Similarly, the second reduction wave of 3,5-di-*tert*-butyl-1,2-benzoquinone is very large.[11] A detailed analysis[12] showed that a 1:1 complex between water and semiquinone anion radical is the reactant, and the large width of the wave has been interpreted as an indication of a very small transfer

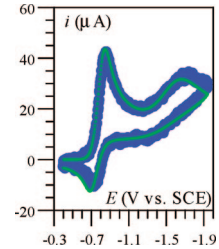

Figure 16. Cyclic voltammetry of dioxygen in DMF + 0.1 M *n*-NBu_4PF_6: (green) experimental data; (blue) simulation. Scan rate: 0.2 V/s. Reprinted with permission from ref 232. Copyright 2005 American Chemical Society.

Scheme 31

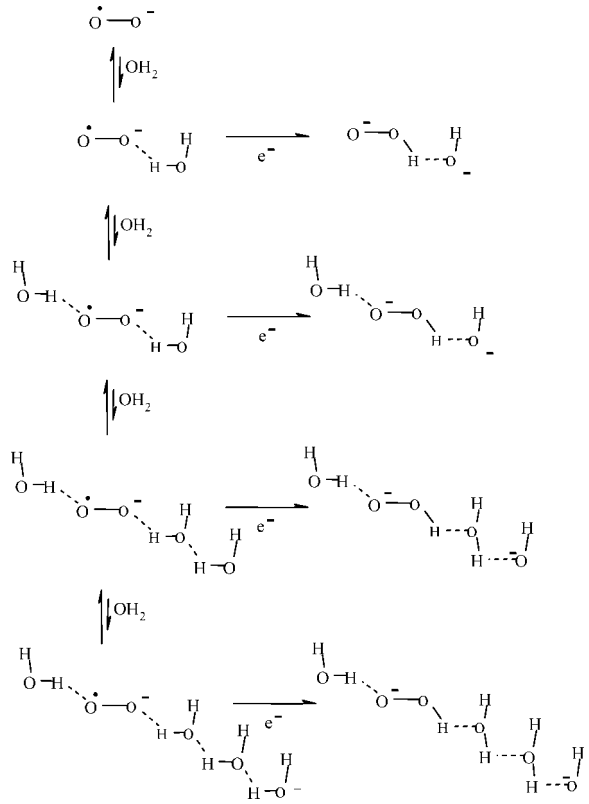

coefficient, thus confirming a concerted mechanism. Again, with CPET, the reorganization energy λ is not expected to be particularly large, thus contrasting with concerted dissociative electron transfer. Therefore, the smallness of the transfer coefficient α given by $\alpha = 0.5[1 + \Delta G^0/\lambda]$ is rather because of the very negative value of the standard free energy $\Delta G^0 = F(E_p - E^0)$ resulting from nonadiabaticity of the reaction. Indeed, because of this nonadiabaticity, the preexponential factor of the rate constant and hence the standard rate constant is small. Because in cyclic voltammetry the peak is reached when the electron transfer kinetics equals the diffusion kinetics, a small standard rate constant induces, for a reduction, a peak potential much more negative than the standard potential. Consequently, $\Delta G^0 = F(E_p - E^0)$ is very negative and the transfer coefficient α is much smaller than 0.5.

A subsequent more detailed study[230] revealed additional important features of the effect of water on the reduction of superoxide ion including very large peak potential shifts associated with the water−superoxide complex reduction upon the addition of water, methanol, or 2-propanol and also an increase of KIE with water concentration. This has been interpreted as being a consequence of the change in the formal potential with water concentration.[230] However, the formal potential and hence the driving force of the reaction are independent of the reactant concentration.[231] Instead, it has been proposed[231] that short hydrogen-bonded water chains involving approximately three water molecules (Scheme 31) are involved in the CPET process, thus providing a preliminary picture of the mechanisms that operate in pure water.

3.3.2. CPET in Water

When a CPET reaction takes place in water, water itself may act as the proton acceptor or donor. This role may also be played by OH^- or H_3O^+ and by the components of buffers in which the experiments are often carried out (Scheme 32). In the case when water is the proton acceptor, the CPET pathway may compete favorably with the stepwise pathway. The main parameter of the competition is whether the pK of the oxidized form of the substrate being smaller or larger than 0.[74] At high pH values, CPET reactions involving OH^- as proton acceptor may likewise compete favorably with stepwise pathways, but the overall reaction rate constant is an increasing function of pH only because OH^- is a reactant, not because the driving force depends on pH per se. In buffered media, association of the substrate with the basic components of the buffer offers an alternative CPET route. An increase of buffer couple pK entails an increase of the driving force offered to the reaction and therefore a potential increase of the rate constant. Although this change in driving force is, besides the buffer base component concentration, the second main factor of an increase of the rate constant with pH when going from a buffer to a more basic buffer, one should also take into account that the standard rate constant (or equivalently the intrinsic barrier) and the two association constants may also vary. As to the latter factor we note that the variations of the association constants (Scheme 32) upon passing from one buffer to the other tend to compensate each other. In all cases, the variations with pH are indirect, being caused either by an increase of the concentration of a reactant or by an increase of the buffer pK.

In this connection, the oxidation of the phenol group of tyrosine, among other reactions,[233] has attracted particular attention.[75,234–240] Whereas in all cases the contribution of the CPET pathway is deemed to be important, conflicting evidence has been reported concerning the respective roles of water[236] and of the basic component of the buffer[237] as proton acceptors. In the initial experiments reported by Hammarström and co-workers,[75] the CPET reaction between tyrosine and Ru(III) in an intramolecular complex is initiated by a "flash-quench" method. The reaction kinetics is followed by monitoring the recovery of Ru^{II} adsorption. The reaction is shown to follow a CPET mechanism characterized by a pH-dependent rate constant, a large reorganization energy, and the presence of a KIE. A parallel stepwise mechanism also occurs. The results, in particular the variation of the CPET observed rate constant with pH, were rationalized initially by considering that the driving force of the CPET reaction is an increasing function of pH.[75,241] Note that similar results have been obtained by Nocera and coworkers[234] using initiation of a CPET reaction from an MLCT excited states of a rhenium polypyridyl complex. Introduction of the pH-dependent driving force into the Marcus relationship between activation and driving force, which is assumed to be applicable to CPET reactions, would then account for the increase of the rate constant with pH. This appears to be not correct. Indeed, as already mentioned, the driving force, that is, the negative of the standard free energy obtained from standard (or formal) redox potentials does not depend on pH despite the equilibrium redox potential of the proton−electron system being a function of pH (see eqs 6–9).[74] Moreover, when Marcus' quadratic equation is considered, standard free energy has indeed to be considered.[242,243] However, in buffered media, the association of the substrate with the basic components of the buffer offers an alternative CPET route:[74] the rate constant is predicted to increase with the base concentration, and

Scheme 32

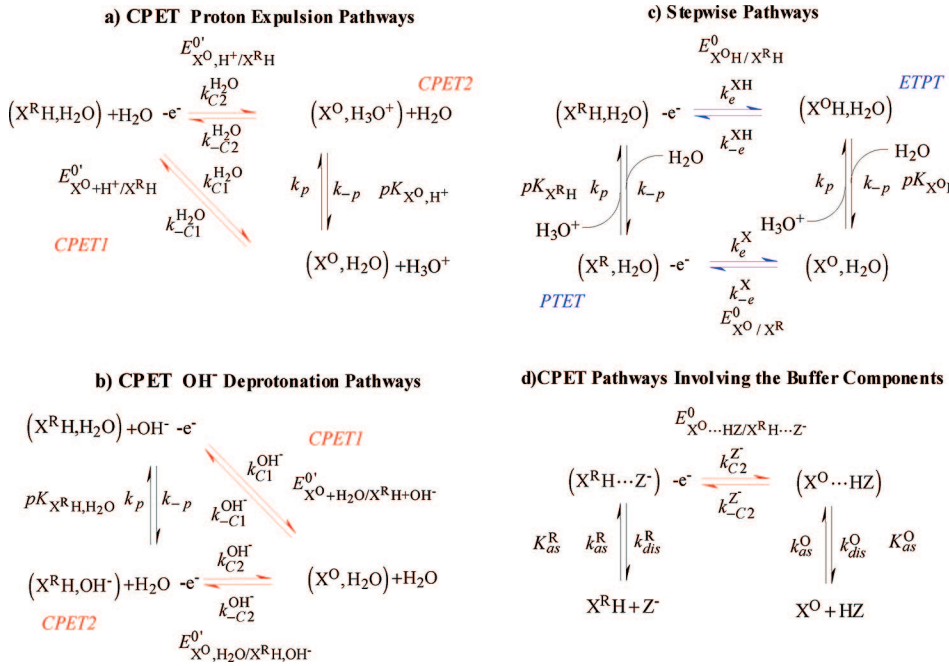

therefore this association could be one reason for its increase with pH in experiments in which pH variations around the buffer pK_a are obtained by increasing the concentration of base. Results on rhenium polypyridyl complexes have been thus recently interpreted in terms of the titration between the two forms of the phosphate buffer that serves as the proton acceptor.[244] The second main factor for an increase of the rate constant with pH is that when going from a buffer to a more basic buffer, there is an increase of the driving force, but in experiments describing this initial work and in recent additional experiments,[245] the pH dependence of the rate constant is observed even at low buffer concentration or in the absence of buffer. However, dependence of the rate constant on buffer concentration is observed at higher buffer concentration as well as in other experiments[240] on a comparable, although not identical, system, that is, tyrosine. In the tyrosine work, the CPET reaction is studied by an indirect electrochemical method, that is, redox catalysis, where a catalyst, here $Os(bpy)_3^{2+}$, is oxidized at the electrode at a potential that is less anodic than the potential at which the direct oxidation of tyrosine occurs. The oxidized form of the catalyst then oxidizes tyrosine, and catalysis appears as an increase in the catalyst wave accompanied by a loss of reversibility.[246] The reaction of tyrosine with $Os(bpy)_3^{2+}$ was investigated over a range of buffer concentrations, and the data were analyzed by digital simulation[50] of voltammograms. The results demonstrate that the reaction goes through a hydrogen-bonded complex between tyrosine and the basic component of the buffer and that a CPET mechanism occurs in parallel with a stepwise mechanism proceeding via a rate-limiting proton transfer followed by oxidation of the phenoxide anion (Scheme 33). However, at low concentration or in the absence of buffer, the CPET mechanism remains unclear and requires further examination.

Redox catalysis and stopped-flow experiments have also been used to investigate proton-coupled electron transfer in the oxidation of guanine and its derivatives (Chart 6) in water. The mechanism was deemed to be concerted on the bases that a kinetic isotope effect was observed and that a slope of 0.8 for the variation of ln(k), the logarithm of the

Scheme 33

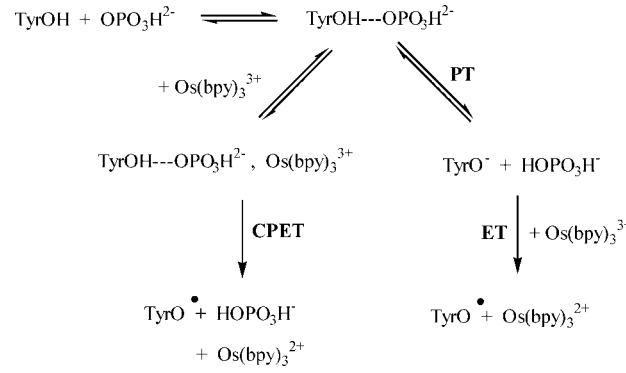

Chart 6

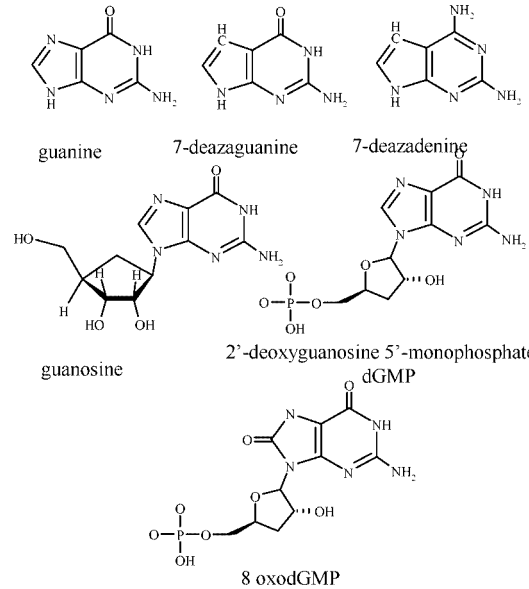

observed rate constant k, with the driving force was 0.8.[247] However, one can suppose that a mixed kinetic control of both electron transfer and deprotonation in the framework

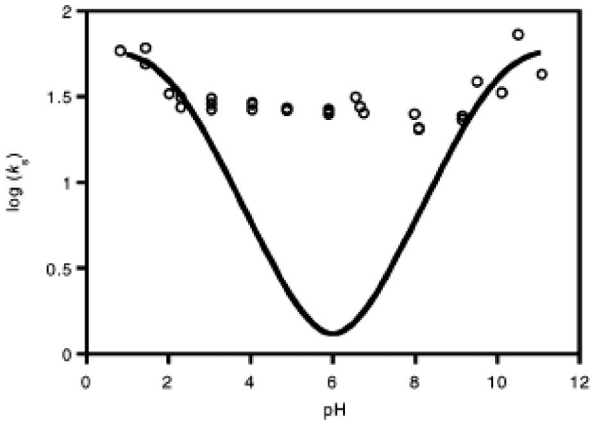

Figure 17. Log(k_s) versus pH plot. The solid line is the expected pH dependence for the stepwise model. Reprinted with permission from ref 124. Copyright 2004 American Chemical Society.

of a stepwise mechanism could lead to the same observations. dGMP-photoinduced oxidation experiments supported a coupled mechanism but gave no information on the stepwise versus concerted nature of the pathway.[248] A subsequent more detailed study[249] indicates that the KIE observed for dGMP oxidation supports a concerted mechanism because within the framework of a stepwise mechanism, 8-oxodGMP, being easier to oxidize and leading to a less acid cation radical, should be driven to a proton transfer rate-determining step and should exhibit KIE, which it does not. On the contrary, pulse radiolysis experiments show that the radical cation of deoxyguanosine is produced by oxidation with $SO_4^{\bullet-}$ at pH 7 and is rapidly deprotonated with a rate constant of 1.8×10^7 s^{-1}, thus indicating that a stepwise mechanism is followed.[250] This apparent contradiction between a stepwise mechanism in pulse radiolysis and a concerted mechanism in redox catalysis may in fact be explained by a shift from the stepwise and the concerted pathway upon decreasing the driving force dependent on the different oxidizing powers of $SO_4^{\bullet-}$ ($E^0_{SO_4^{\bullet-}/SO_4^{2-}} \approx 2.5-3.1$ V vs NHE[251]) and $Ru(bpy)_3^{3+}$ ($E^0_{Ru(bpy)_3^{3+}/Ru(bpy)_3^{2+}} = 1.28$ V vs NHE). Such a mechanistic shift is a well-documented fact, both theoretically and experimentally, in the case of bond breaking between heavy atoms.[252–256] The same behavior, even if somehow different, is thus a reasonable possibility in the case of deprotonation.

As mentioned in a previous section, myriad metal−ligand complexes exhibit proton-coupled electron transfer behavior in water. Surprisingly, kinetic analysis of only a few examples has been done. Among them, deviations from Laviron's stepwise model have been reported and interpreted as the occurrence of a concerted mechanism.[124,162] As an example, the kinetic behavior of an osmium aquo complex, $[Os^{II}(bpy)_2(4\text{-aminomethylpyridine})(H_2O)]^{2+}$, attached to a SAM has been fully investigated.[163] In both H_2O and D_2O, the standard rate constant is weakly dependent on pH, which is not in agreement with a stepwise mechanism (Figure 17), and the KIE is around 2, suggesting a concerted mechanism. Concerted pathways are described with water as the proton donor or acceptor rather than with H_3O^+ or OH^- in those roles, thus making the CPET independent of pH. The slight variation of the standard rate constant with pH is also accompanied by a variation of the Os^{III} reorganization energy. However, no explanation is given for such a behavior. One might also argue that the buffer component acting as proton donor or acceptor may contribute to a pH dependence of the apparent standard rate constant. A recent study on the same complex but not attached on a SAM reached the conclusion that a stepwise mechanism was operational.[257] The occurrence of CPET pathways requires either an exceptionally large concentration of a proton acceptor or the close proximity of proton-accepting group of intermediate pK, as is the case for the osmium aquo complex attached to a SAM imbedded in carboxylate-terminated long-chain thiol.

The presence of a kinetic isotope effect remains the major reason for invoking a concerted proton−electron transfer. A kinetic isotope effect of a magnitude of 4.6 has been measured for reduction of the di-μ_2-oxo-$Mn^{III}Mn^{IV}$ complex $[(bpy)_2Mn(O)_2Mn(bpy)_2]^{3+}$, which suggests a concerted proton−electron transfer pathway.[93] However, the activation enthalpy determined from the temperature dependence of the standard rate constant is consistent with a stepwise mechanism proceeding via an initial slow proton transfer. Larger KIE, even greater than 60, have been reported for $Ru^{III}(OH)$ complex oxidation both coated on an electrode or in a solution.[77] The range of the KIE observed is higher for highly loaded surface than for dilute surface in the presence of $[(tpy)(bpy)(H_2O)Ru^{II}]^{2+}$ added to the external solution. This is interpreted as an indication that a concerted electron and proton transfer reaction requiring specific orientations between reactants for tunneling of the proton to occur (Scheme 14) is involved, in accord with the theoretical description of a concerted mechanism which predicts that the distance between proton donor and acceptor is the most crucial parameter in determining the magnitude of the CPET rate constant.

4. Voltammetric Studies of the Kinetics and Energetics of PCET in Biological Systems

Proton transfer and its coupling to catalytic electron transfer in proteins are integral features of bioenergetics and are fundamental to the conservation of biological energy. Protein film voltammetry (PFV) has been used to establish at the molecular level how individual proton transfer occurs or is coupled to electron transfer. Armstrong and co-workers have shown that protein film voltammetry is a powerful approach to the study of the kinetics of protein redox function.[258] For example, recently PFV was found to be very useful for determining the reduction potential of the catalytic heme of cytochrome c nitrite reductase and thus demonstrating that proton transfer is coupled to electron transfer at an active site.[259] It has also been suggested that PCET events play important roles in determining the activity of the enzyme.[260]

4.1. Principle

When a protein film is adsorbed onto an electrode and a simple reversible electron-transfer process occurs, it gives rise to a "trumpet"-shaped plot because oxidation and reduction peaks are increasingly separated at high scan rate. This trumpet plot is altered when electron transfer is coupled to proton transfer. It is then possible to derive particularly detailed information on the kinetics and energetics of the PCET. In interpreting the voltammetry of coupled systems, several deviations from ideal behavior have been described for simple uncoupled systems.[261] (For a more detailed discussion, see the contribution of Christophe Léger and Patrick Bertrand on this issue in their paper "Direct

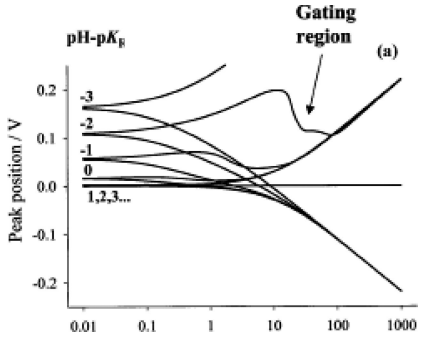

Figure 18. Modeled "trumpet" plots (peak positions as a function of the logarithm of the scan rate) for the gated electron transfer reaction by a proton transfer at different pH values. pK_R is the pK_a of the reduced form. Reprinted with permission from ref 261 (http://dx.doi.org/10.1039/b002290j). Copyright 2000 The Royal Society of Chemistry.

Electrochemistry of Redox Enzymes as a Tool for Mechanistic Studies".)

A square scheme represents the most elementary model to describe PCET. In proteins, the redox center is buried inside the protein so that proton transfer is sufficiently slow to control kinetics, contrary to the situation for PCET in water. Consider the situation starting from the oxidant species. Figure 18 shows the calculated peak positions for hypothetical experiments undertaken at different pH values relative to the pK_a of the reduced form (denoted pK_R). As expected from the Pourbaix diagram (see Figure 7), at pH values much higher than this pK_a, only simple electron transfer occurs. As the pH is lowered the features change significantly and the peak positions are no longer distributed symmetrically around the reduction potential. In addition, the relative peak heights show that, at intermediate scan rates, the anodic wave vanishes as the pH decreases. This effect is called "gating" and occurs because the protonated reduced species is formed but cannot be reoxidized as the deprotonation is too slow. At very high scan rate, the data sets converge for all pH values because in this case the protonation of the reduced species cannot occur in the forward reaction, so the electron is withdrawn in the backward scan and regenerates the oxidant. Electron transfer is thus uncoupled from proton transfer in this time domain. This behavior parallels the well-described journey through the kinetic zone diagram taken by the EC mechanism as it goes from reversible behavior in the DE zone to reversible behavior in the DO zone as the scan rate is increased.[262] It should be noted that the proximity of enzyme to an electrode in PFV may influence PCET processes as is illustrated by cytochrome *c* electrostatically bound to SAM on a Ag electrode.[263] At the Ag/SAM interface, the energy barrier for the proton transfer processes of the adsorbed Cyt-*c* is raised by the electric field; this effect increases upon reducing the distance to the electrode.

4.2. Experimental Illustrations

Ferredoxin I from *Azotobacter vinelandii* (*Av*FdI) is one of the proteins for which proton transfer has been the most studied. It is indeed considered to be a simple proton-transferring module. The sequence has been established as consisting first of an electron transfer to the cofactor, a [3Fe-4S] cluster, followed by proton transfer from bulk water, and then in the reverse reaction, electron transfer off the cluster does not occur until after the proton has been released

Scheme 34

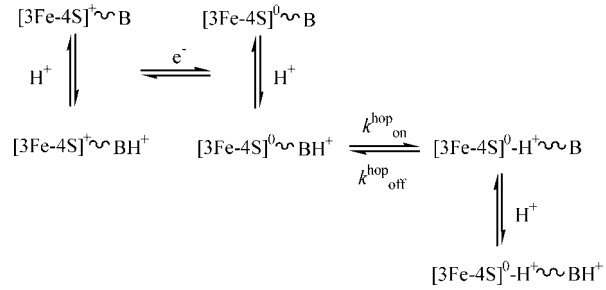

Scheme 35

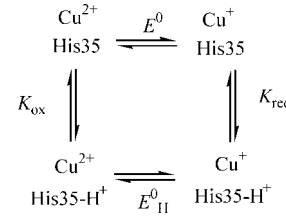

to solvent.[264] The proton transfer is mediated by a mobile carboxylate of an adjacent surface aspartate residue (Scheme 34).[265] It has been shown that a proline residue in the same region is not involved.[266] This information was obtained by comparison of the native *Av*FdI and mutants. Note that a concerted mechanism can be ruled out by observation of the "uncoupled" behavior at high scan rates.

Deconvolution of PCET has also been possible using protein film voltammetry with the blue copper protein azurin from *Pseudomonas aeruginosa*.[267] The electron transfer on the copper ion redox site is coupled to slow protonation of a nearby histidine. Another histidine, for which (de)protonation is rapid, also influences the redox behavior. This can be taken into account by considering an apparent pH dependent standard potential in the square scheme (Scheme 35). Contrary to the first case (*Av*FdI), in which electrochemical kinetics and structures at atomic resolution lead to a mechanism involving a single "swinging arm" carboxylate, deviation from modeling suggests that in azurin other protonation sites in addition to both histidines are coupled to electron transfer. This is actually the case with many proton transfer pathways studied to date in which a chain of closely spaced proton donors, acceptors, and sometimes also water molecules are involved.[268]

It thus appears that there is a diversity of mechanisms of proton and electron coupling in proteins having cofactors, including protein-ligated iron−sulfur clusters and hemes, that cannot bind protons to completely cancel the charge changes occurring during the redox process and thus compensates charge through proton exchange involving the protein medium that supports the redox center. One approach for clarifying the effects of proton binding to the protein scaffold on the redox activity of the cofactor is to design de novo proteins or "maquettes".[269] This has been done to get insights into proton coupling to heme reduction in cytochrome *c* oxidase.[270] By modulating the thermodynamic affinity of designed protein scaffold to the heme, it was possible to change the mechanism of proton-coupled electron transfer on the heme. In one case, proton transfer occurs on glutamate (Scheme 36A), whereas in the other case proton transfer is associated with ligand loss on the heme (Scheme 36B). Nearby glutamate has also been shown to participate using a cytochrome *b* maquette. [271]

Scheme 36

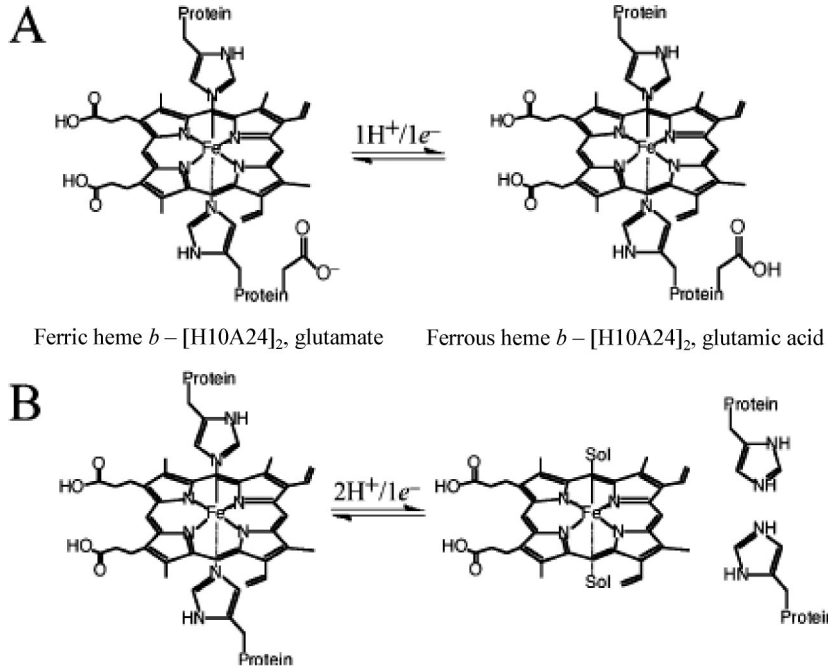

Ferric heme *b* – $[H10A24]_2$, glutamate Ferrous heme *b* – $[H10A24]_2$, glutamic acid

Ferric heme *b* – $[\Delta 7\text{-His}]_2$, imidazole Ferrous heme *b* – $[\Delta 7\text{-His}]_2$, imidazolium

Scheme 37

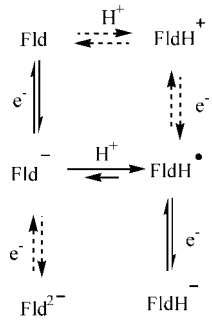

Whereas most PFV studies have been performed on pyrolytic graphite-"edged" or alkanethiol-modified gold electrodes, another approach based on immobilization of protein on nanocrystalline mesoporous SnO_2 electrodes has been employed. The high surface area and optical transparency of this electrode allow the combine use of optical spectroscopy and electrochemistry. This was applied to the study of PCET of flavodoxin belonging to the class of flavoprotein, that is, with a flavin as redox cofactor.[272] Contrary to the previously described class of redox cofactors, including protein-ligated iron−sulfur clusters and hemes, flavin redox cofactor can bind proton to its moiety to fully compensate the introduced charge. Two waves are thus observed in cyclic voltammetry, and the thermodynamics of both the quinone/semiquinone and semiquinone/hydroquinone couples was determined. The second is pH-independent whereas the first is pH-dependent. A kinetics study done by increasing the scan rate can be interpreted within the framework of a square scheme mechanism going through the deprotonated semiquinone (Scheme 37) with a slow rate-limiting deprotonation in the oxidation pathway, thus exhibiting the gating region described in Figure 18.

Thin lipid film voltammetry has also been used to investigate redox biological hemic systems.[273] The same method has recently been applied to spinach photosystem II. For the first time a direct electron transfer between an

Scheme 38

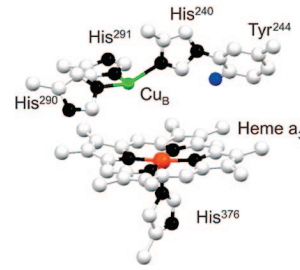

Scheme 39

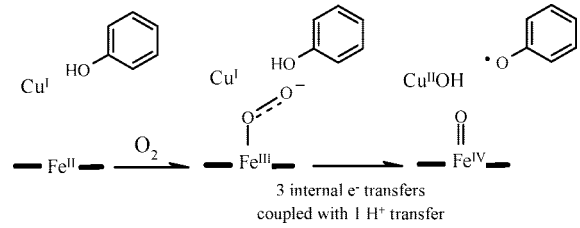

electrode and the PSII reaction center has been claimed to be observed.[274] Note, however, that a large surface concentration is measured (1.2×10^{-10} mol cm^{-2}), making highly likely a multilayer structure and thus a very difficult kinetic analysis. Several waves are observed. One is attributed to quinone cofactors. It is pH-dependent and exhibits a quite high standard rate constant as compared to ubiquinone incorporated in a bilayer.[156] Another wave, not observed with PSII depleted of the Mn_4 complex, is assigned to the manganese cluster. Its behavior with scan rate and pH is interpreted as an EC/CE mechanism with an electron transfer gated by deprotonation on the oxidation reaction. However, other electron transfers must occur because the wave corresponds to more than a one-electron wave. Therefore, interpretation of these experiments remains speculative.

As in the case of PSII converting H_2O into O_2, proton transfers are intimately coupled to electron transfer in the catalytic center of cytochrome *c* oxidase converting O_2 into

H_2O. The four-electron reduction is essential to avoid the production of toxic partially reduced oxygen species, such as $O_2^{\bullet -}$, H_2O_2, $OH^{\bullet}$. As shown in Scheme 38, a copper complex and a heme act as electron relays to mediate electron transfer between cytochrome *c* and the heme−Cu catalytic site, which contains besides a heme and a copper center a tyrosine residue able to transfer one proton and one electron (Scheme 39).[275–280] Despite a beautiful study demonstrating that the presence of both the copper center and the tyrosine residue is required under biological condition,[281] there is as yet no information on whether the intimate coupling of proton and electron transfer in this catalytic center is concerted or not.

5. Conclusions

Electrochemical techniques such as cyclic voltammetry have proved to be very useful in characterizing electron transfer associated with proton transfer and have also contributed to the growing attention paid to these mechanisms in view of their involvement in many natural processes. Theoretical tools are available that allow deciphering intimate mechanisms such as two-step proton-coupled electron transfer or one-step concerted proton−electron transfer whether in aprotic media or in water.

In aprotic media, the effect of hydrogen bonding is distinguished from that of proton transfer, and there is a mechanistic shift from hydrogen bonding to proton transfer coupled to electron transfer when the acidic or basic properties of the reactants are changed.

In water, myriad systems involving PCET are thermodynamically characterized through pH-dependent equilibrium potentials. However, despite available theoretical tools, kinetic analyses are scarce and the roles of water itself, of its ions, and of buffer components in the intimate mechanism remain unclear, in particular when a concerted pathway is followed. Contradictory results exist on this issue, and debate is still open.

Attachment of the redox substrate to the electrode allows the preparation of a stable interface and its use in an increasing number of methods for transducing a biological activity into an electrochemical signal. Many of them involve a proton-coupled electron transfer characterized by the same electrochemical and theoretical methods as a freely diffusing reactant. In turn, the beneficial effects of self-assembled monolayers as spacers between metal and redox center, that is, tunneling across the monolayer, slowing the electron transfer rates to experimentally accessible ranges, and the low dielectric constant of the monolayer minimizing double-layer effects in the kinetic measurements, have been used to get insights into PCET pathways.

Analyzing PCET pathways in biological systems is challenging, but protein film voltammetry has contributed to establishing at the molecular level how individual proton transfers occur and how they may be coupled to electron transfer. However, with such complicated systems as proteins, the distinction between stepwise or concerted remains unexplored by electrochemical approaches. Actually, the electrochemical approach to concerted proton-coupled electron transfer is quite recent. Theoretical tools are now available, but exploration of new experimental molecular systems is needed to fully determine intrinsic factors important in governing the coupling between the electron and the proton. Having this knowledge in hand will, in turn, be valuable in uncovering PCET in natural processes.

6. References

(1) Huynh, M. H. V.; Meyer, T. J. *Chem. Rev.* **2007**, *107*, 5004.
(2) Cukier, R. I.; Nocera, D. G. *Annu. Rev. Phys. Chem.* **1998**, *49*, 337.
(3) Soudackov, A.; Hammes-Schiffer, S. *J. Chem. Phys.* **1999**, *111*, 4672.
(4) Kolthoff, I. M.; Lingane, J. J. In *Polarography*, 2nd ed.; Interscience: New York, 1952; Vol. I, Chapters XIV and XV; Vol. II, Chapter XL.
(5) Pourbaix, M. In *Atlas of Electrochemical Equilibria in Aqueous Solution*, 2nd ed. (English translation); Franklin, J. A., Ed.; Pergamon Press: New York, 1974.
(6) Chambers, J. Q. In *The Chemistry of the Quinonoid Compounds*; Patai, S., Rappoport, Z., Eds.; Wiley: New York, 1974; Vol. I, Chapter 14, pp 737−791; 1988; Vol. II, Chapter 12, pp 719−757.
(7) Swallow, A. J. In *Function of Quinones in Energy Conserving Systems*; Trumpower, B. L., Ed.; Academic Press: New York, 1982; Chapter 3, p 66.
(8) Peover, M. E. In *Electroanalytical Chemistry*; Bard, A. J., Ed.; Dekker: New York, 1967; pp 1−51.
(9) Mastragostino, M.; Nadjo, L.; Savéant, J.-M. *Electrochim. Acta* **1968**, *13*, 721.
(10) Gupta, N.; Linschitz, H. *J. Am. Chem. Soc.* **1997**, *119*, 6384.
(11) Lehmann, M. W.; Evans, D. H. *J. Electroanal. Chem.* **2001**, *500*, 12.
(12) Lehmann, M. W.; Evans, D. H. *J. Phys. Chem. B* **2001**, *105*, 8877.
(13) Savéant, J.-M. In *Elements of Molecular and Biomolecular Electrochemistry*; Wiley-Interscience: Hoboken, NJ, 2006; p 85.
(14) Salas, M.; Gomez, M.; Gonzalez, F. J.; Gordillo, B. *J. Electroanal. Chem.* **2003**, *543*, 73.
(15) Salas, M.; Gordillo, B.; Gonzalez, F. J. *ARKIVOC (Gainesville, FL, U.S.)* **2005**, 172.
(16) Ge, Y.; Miller, L.; Ouimet, T.; Smith, D. K. *J. Org. Chem.* **2000**, *65*, 8831.
(17) Ge, Y.; Smith, D. K. *Anal. Chem.* **2000**, *72*, 1860.
(18) Stallings, M. D.; Morrison, M. M.; Sawyer, D. T. *Inorg. Chem.* **1981**, *20*, 2655.
(19) Savéant, J.-M. In *Elements of Molecular and Biomolecular Electrochemistry*; Wiley-Interscience; Hoboken, NJ, 2006; pp 96−102.
(20) Greaves, M. D.; Niemz, A.; Rotello, V. M. *J. Am. Chem. Soc.* **1999**, *121*, 266.
(21) Eggins, B. R.; Chambers, J. Q. *J. Electrochem. Soc.* **1970**, *117*, 186.
(22) Garza, J.; Vargas, R.; Gomez, M.; Gonzalez, I.; Gonzalez, F. J. *J. Phys. Chem. A* **2003**, *107*, 11161.
(23) Savéant, J.-M. In *Elements of Molecular and Biomolecular Electrochemistry*; Wiley-Interscience: Hoboken, NJ, 2006; p 7.
(24) Savéant, J.-M. In *Elements of Molecular and Biomolecular Electrochemistry*; Wiley-Interscience: Hoboken, NJ, 2006; p 100.
(25) Gómez, M.; González, I.; González, F. J.; Vargas, R.; Garza, J. *Electrochem. Commun.* **2003**, *5*, 12.
(26) Gomez, M.; Gonzalez, F. J.; Gonzalez, I. *J. Electroanal. Chem.* **2005**, *578*, 193.
(27) Inbaraj, J. J.; Ganghidasan, R.; Murugesen, R. *Free Radical Biol. Med.* **1999**, *26*, 1072.
(28) Frigaard, N. V.; Tokita, S.; Matsuura, K. *Biochim. Biophys. Acta* **1999**, *1413*, 108.
(29) Goulart, M. O. F.; Zani, C. L.; Tonholo, J.; Freitas, L. R.; de Abreu, F. C.; Oliveira, A. B.; Raslan, D. S.; Starling, S.; Chiari, E. *Bioorg. Med. Chem. Lett.* **1997**, *7*, 2043.
(30) Ferraz, P. A. L.; de Abreu, F. C.; Pinto, A. V.; Gleze, V.; Tonholo, J.; Goulart, M. O. F. *J. Electroanal. Chem.* **2001**, *507*, 275.
(31) Frontana, C.; González, I. *J. Electroanal. Chem.* **2007**, *603*, 155.
(32) Amatore, C.; Capobianco, G.; Farnia, G.; Sandoná, G.; Savéant, J.-M. *J. Am. Chem. Soc.* **1985**, *107*, 1815.
(33) Parker, V. D.; Eberson, L. *J. Chem. Soc., Chem. Commun.* **1970**, 1289.
(34) Eggins, B. R.; Chambers, J. Q. *J. Chem. Soc., Chem. Commun.* **1969**, 232.
(35) Astudillo, P. D.; Tiburcio, J.; González, F. J. *J. Electroanal. Chem.* **2007**, *604*, 57.
(36) Savéant, J.-M. In *Elements of Molecular and Biomolecular Electrochemistry*; Wiley-Interscience: Hoboken, NJ, 2006; p 88.
(37) Amatore, C.; Savéant, J.-M. *J. Electroanal. Chem.* **1977**, *85*, 27.
(38) Costentin, C.; Robert, M.; Savéant, J.-M. *J. Am. Chem. Soc.* **2006**, *28*, 8726.
(39) Hammerich, O.; Svensmark, B. In *Organic Electrochemistry*, 3rd ed.; Lund, H., Baizer, M. M., Eds.; Dekker: New York, 1991; Chapter 16.
(40) Webster, R. D. *Acc. Chem. Res.* **2007**, *40*, 251.
(41) Richards, J. A.; Whitson, P. E.; Evans, D. H. *J. Electroanal. Chem.* **1975**, *63*, 311.
(42) Speiser, B.; Rieker, A. *J. Electronal. Chem.* **1979**, *102*, 373.
(43) Groves, J. T.; Boxer, S. G. *Acc. Chem. Res.* **2002**, *35*, 149.
(44) Williams, L. L.; Webster, R. D. *J. Am. Chem. Soc.* **2004**, *126*, 12441.

(45) Dürckheimer, W.; Cohen, L. A. *J. Am. Chem. Soc.* **1964**, *86*, 4388.
(46) Lee, S. B.; Yeh Lin, C.; Gill, P. M. W.; Webster, R. D. *J. Org. Chem.* **2005**, *70*, 10466.
(47) Savéant, J.-M. In *Elements of Molecular and Biomolecular Electrochemistry*; Wiley-Interscience: Hoboken, NJ, 2006; pp 96−102.
(48) Anne, A.; Hapiot, P.; Moiroux, J.; Neta, P.; Savéant, J.-M. *J. Phys. Chem.* **1991**, *95*, 2370.
(49) Amatore, C.; Gareil, M.; Savéant, J.-M. *J. Electroanal. Chem.* **1984**, *176*, 377.
(50) Digisim software package for example. Rudolph, M.; Reddy, D. P.; Feldberg, S. W. *Anal. Chem.* **1994**, *66*, 589A
(51) Shouji, E.; Buttry, D. A. *J. Phys. Chem. B* **1999**, *103*, 2239.
(52) Oyama, N.; Tatsuma, T.; Sato, T.; Sotomura, T. *Nature* **1995**, *373*, 598.
(53) Laviron, E. J. *J. Electroanal. Chem.* **1981**, *124*, 1.
(54) Slattery, S. J.; Blaho, J. K.; Lehnes, J.; Goldsy, K. A. *Coord. Chem. Rev.* **1998**, *174*, 391.
(55) Laviron, E. *J. Electroanal. Chem.* **1983**, *146*, 1.
(56) Laviron, E. *J. Electroanal. Chem.* **1983**, *146*, 15.
(57) Gilbert, J. A.; Eggleston, D. S.; Murphy, W. R., Jr.; Geselowitz, D. A.; Gersten, S. W.; Hodgson, D. J.; Meyer, T. J. *J. Am. Chem. Soc.* **1985**, *107*, 3855.
(58) Binstead, R. A.; Chronister, C. W.; Ni, J., Jr.; Hartshorn, C. M.; Meyer, T. J. *J. Am. Chem. Soc.* **2000**, *122*, 8464.
(59) Lebeau, E. L.; Adeyemi, S. J.; Meyer, T. J. *Inorg. Chem.* **1998**, *37*, 6476.
(60) Liu, F.; Cardolaccia, T.; Hornstein, B. J.; Schoonover, J. R.; Meyer, T. J. *J. Am. Chem. Soc.* **2007**, *129*, 6968.
(61) Sens, C.; Romero, I.; Rodriguez, M.; Llobet, A.; Parella, T.; Benet-Buchholz, J. *J. Am. Chem. Soc.* **2004**, *126*, 7798.
(62) Rodriguez, M.; Romero, I.; Sens, C.; Llobet, A. *J. Mol. Catal. A: Chem.* **2006**, *251*, 215.
(63) Meyer, T. J.; Huynh, M. H. V. *Inorg. Chem.* **2003**, *42*, 8140.
(64) Rodriguez, M.; Romero, I.; Llobet, A.; Deronzier, A.; Biner, M.; Parella, T.; Stoeckli-Evans, H. *Inorg. Chem.* **2001**, *40*, 4150.
(65) Moyer, B. A.; Meyer, T. J. *J. Am. Chem. Soc.* **1978**, *100*, 3601.
(66) Takeuchi, K. J.; Thompson, M. S.; Pipes, T. J.; Meyer, T. J. *Inorg. Chem.* **1984**, *23*, 1845.
(67) Ho, C.; Che, C.; Lay, T. *J. Chem. Soc., Dalton Trans.* **1990**, 967.
(68) Dovletoglou, A.; Adeyemi, S. A.; Meyer, T. J. *Inorg. Chem.* **1996**, *35*, 4120.
(69) Masllorens, E.; Rodriguez, M.; Romero, I.; Roglans, A.; Parella, T.; Benet-Buchholz, J.; Poyatos, M.; Llobet, A. *J. Am. Chem. Soc.* **2006**, *1287*, 5306.
(70) Moyer, B. A.; Meyer, T. J. *Inorg. Chem.* **1981**, *20*, 436.
(71) McHatton, R. C.; Anson, F. C. *Inorg. Chem.* **1984**, *23*, 3935.
(72) Lebeau, E. L.; Binstead, R. A.; Meyer, T. J. *J. Am. Chem. Soc.* **2006**, *123*, 10535.
(73) Binstead, R. A.; Meyer, T. J. *J. Am. Chem. Soc.* **1987**, *109*, 3287.
(74) Costentin, C.; Robert, M.; Savéant, J.-M. *J. Am. Chem. Soc.* **2007**, *29*, 5870.
(75) Sjödin, M.; Styring, S.; Åkermark, B.; Sun, L.; Hammarström, L. *J. Am. Chem. Soc.* **2000**, *122*, 3932.
(76) Cabaniss, G. E.; Diamantis, A. A.; Murphy, W. R., Jr.; Linton, R. W.; Meyer, T. J. *J. Am. Chem. Soc.* **1985**, *107*, 1845.
(77) Trammell, S. A.; Wimbish, J. C.; Odobel, F.; Gallagher, L. A.; Narula, P. N.; Meyer, T. J. *J. Am. Chem. Soc.* **1998**, *120*, 13248.
(78) Rocha, R. C.; Rein, F. N.; Toma, H. E. *J. Braz. Chem. Soc.* **2001**, *12*, 234.
(79) Takeuchi, K. J. G. J.; Gersten, S. W.; Gilbert, J. A.; Meyer, T. J. *Inorg. Chem.* **1983**, *22*, 1409.
(80) Dobson, J. C.; Takeuchi, K. J.; Pipes, D. W.; Geselowitz, D. A.; Meyer, T. J. *Inorg. Chem.* **1986**, *25*, 2357.
(81) Dobson, J. C.; Meyer, T. J. *Inorg. Chem.* **1988**, *27*, 3283.
(82) Pipes, T. J.; Meyer, T. J. *Inorg. Chem.* **1986**, *25*, 3256.
(83) Thorp, H. H.; Brudvig, G. W.; Bowden, E. F. *J. Electroanal. Chem.* **1990**, *290*, 293.
(84) Cheniae, G. M.; Martin, I. F. *Biochim. Biophys. Acta* **1970**, *197*, 219.
(85) McEvoy, J. P.; Brudvig, G. W. *Chem. Rev.* **2006**, *106*, 4455.
(86) Ferreira, K. N.; Iverson, T. M.; Maghlaoui, K.; Barber, J.; Iwata, S. *Science* **2004**, *303*, 1831.
(87) Manchanda, R.; Brudvig, G. W.; Crabtree, R. H. *Coord. Chem. Rev.* **1995**, *144*, 1.
(88) Lippard, S. *Angew. Chem., Int. Ed. Engl.* **1988**, *27*, 344.
(89) Mukhopadhyay, S.; Mandal, S. K.; Bhaduri, S.; Armstrong, W. H. *Chem. Rev.* **2004**, *104*, 3981.
(90) Thorp, H. H.; Sarneski, J. E.; Brudvig, G. W.; Crabtree, R. H. *J. Am. Chem. Soc.* **1989**, *111*, 9249.
(91) Manchanda, R.; Thorp, H. H.; Brudvig, G. W.; Crabtree, R. H. *Inorg. Chem.* **1991**, *30*, 494.
(92) Baldwin, M. J.; Gelasco, A.; Pecoraro, V. L. *Photosynth. Res.* **1993**, *38*, 303.
(93) Kalsberg, W. A.; Thorp, H. H.; Brudvig, G. W. *J. Electroanal. Chem.* **1991**, *314*, 335.
(94) Manchanda, R.; Thorp, H. H.; Brudvig, G. W.; Crabtree, R. H. *Inorg. Chem.* **1992**, *31*, 4040.
(95) Dubé, C. E.; Wright, D. W.; Pal, S.; Bonitatebus, P. J.; Armstrong, W. H. *J. Am. Chem. Soc.* **1998**, *120*, 3704.
(96) Laviron, E. *J. Electroanal. Chem.* **1981**, *124*, 19.
(97) Laviron, E. *J. Electroanal. Chem.* **1982**, *140*, 247.
(98) Laviron, E.; Meunier-Prest, R.; Mathieu, E. *J. Electroanal. Chem.* **1994**, *371*, 251.
(99) Meunier-Prest, R.; Gaspard, C.; Laviron, E. *J. Electroanal. Chem.* **1996**, *410*, 145.
(100) Mathieu, E.; Meunier-Prest, R.; Laviron, E. *Electrochim. Acta* **1997**, *42*, 331.
(101) Dion, D.; Meunier-Prest, R.; Laviron, E. *Acta Chem. Scan.* **1997**, *51*, 411.
(102) Mathieu, E.; Meunier-Prest, R.; Laviron, E. *Electrochim. Acta* **1997**, *42*, 2419.
(103) Dion, D.; Laviron, E. *Electrochim. Acta* **1998**, *43*, 2061.
(104) Vallat, A.; Meunier-Prest, R.; Laviron, E. *J. Electroanal. Chem.* **1997**, *428*, 11.
(105) Laviron, E.; Meunier-Prest, R.; Vallat, A.; Roullier, L.; Lacasse, R. *J. Electroanal. Chem.* **1992**, *341*, 227.
(106) Lacasse, R.; Meunier-Prest, R.; Laviron, E.; Vallat, A. *J. Electroanal. Chem.* **1993**, *359*, 223.
(107) Laviron, E.; Meunier-Prest, R.; Lacasse, R. *J. Electroanal. Chem.* **1994**, *375*, 263.
(108) Laviron, E.; Vallat, A.; Meunier-Prest, R. *J. Electroanal. Chem.* **1994**, *379*, 427.
(109) Meunier-Prest, R.; Laviron, E.; Gaspard, C.; Raveau, S. *Electrochim. Acta* **2001**, *46*, 1847.
(110) Vetter, K. J. *Elektrochem.* **1952**, *56*, 797.
(111) Laviron, E. J. *J. Electroanal. Chem.* **1984**, *164*, 213.
(112) Deakin, M. R.; Wightman, M. *J. Electroanal. Chem.* **1986**, *206*, 167.
(113) Deakin, M. R.; Kovach, P. M.; Stutts, K. J.; Wightman, M. *Anal. Chem.* **1986**, *58*, 1474.
(114) Wang, J.; Wang, L.; Wang, Y.; Yang, W.; Jiang, L.; Wang, E. *J. Electrocanal. Chem.* **2007**, *601*, 107.
(115) Quan, M.; Sanchez, D.; Wasylkiw, M. F.; Smith, D. K. *J. Am. Chem. Soc.* **2007**, *129*, 12847.
(116) Laviron, E. J. *J. Electroanal. Chem.* **1983**, *146*, 213.
(117) Laviron, E. J. *J. Electroanal. Chem.* **1981**, *130*, 23.
(118) Savéant, J.-M. In *Elements of Molecular and Biomolecular Electrochemistry*; Wiley-Interscience: Hoboken, NJ, 2006; pp 47, 53.
(119) Laviron, E.; Roullier, L. *J. Electroanal. Chem.* **1990**, *288*, 165.
(120) Brown, A. P.; Anson, F. C. *J. Electroanal. Chem.* **1978**, *92*, 133.
(121) Digielch software. Rudolph, M. *J. Electroanal. Chem.* **2003**, *543*, 23.
(122) Smith, E. T.; Davis, C. A.; Barber, M. J. *Anal. Biochem.* **2003**, *323*, 114.
(123) Cable, M.; Smith, E. T. *Anal. Chim. Acta* **2005**, *537*, 299.
(124) Haddox, R. A.; Finklea, H. O. *J. Phys. Chem. B* **2004**, *108*, 1694.
(125) Prenzler, P. D.; Boskovic, C.; Bond, A. M.; Wedd, A. G. *Anal. Chem.* **1999**, *71*, 3650.
(126) Richardt, P. J. S.; Gable, R. W.; Bond, A. M.; Wedd, A. G. *Inorg. Chem.* **2001**, *40*, 703.
(127) Hill, C. L. In *Comprehensive Coordination Chemistry II*; McCleverty, J. A., Meyer, T. J., Eds.; Elsevier: Amsterdam, The Netherlands, 2004; Vol. 4, pp 679−759.
(128) Guo, S.-X.; Feldberg, S. W.; Bond, A. M.; Callahan, D. L.; Richardt, P. J. S.; Wedd, A. G. *J. Phys. Chem. B* **2005**, *109*, 20641.
(129) Guo, S.-X.; Mariotti, A. W. A.; Schlipf, C.; Bond, A. M.; Wedd, A. G. *Inorg. Chem.* **2006**, *45*, 8563.
(130) Guo, S.-X.; Mariotti, A. W. A.; Schlipf, C.; Bond, A. M.; Wedd, A. G. *J. Electroanal. Chem.* **2006**, *591*, 7.
(131) Finklea, H. O. In *Electroanalytical Chemistry*; Bard, A. J., Rubinstein, I., Eds.; Dekker: New York, 1996; Vol *19*, p 109.
(132) Yeo, W. S.; Mrksich, M. *Angew. Chem. Int. Ed.* **2003**, *42*, 3121.
(133) Nayak, S.; Yeo, W. S.; Mrksich, M. *Langmuir* **2007**, *23*, 5578.
(134) Simmons, N. J.; Chin, K. O. A.; Harnisch, J. A.; Vaidya, B.; Trahanovsky, W. S.; Porter, M. D.; Angelici, R. J. *J. Electroanal. Chem.* **2000**, *482*, 178.
(135) Budavari, V.; Szücs, A.; Somlai, Cs.; Novak, M. *Electrochim. Acta* **2002**, *47*, 4351.
(136) Li, T. T.-T.; Weaver, M. J. *J. Am. Chem. Soc.* **1984**, *106*, 6107.
(137) Larsen, A. G.; Gothelf, K. V. *Langmuir* **2005**, *21*, 1015.
(138) Chidsey, C. E. D.; Bertozzi, C. R.; Putvinski, T. M.; Mujsce, A. M. *J. Am. Chem. Soc.* **1990**, *112*, 4301.
(139) Finklea, H. O.; Hanshew, D. D. *J. Am. Chem. Soc.* **1992**, *114*, 3173.
(140) Hong, H. G.; Park, W. *Langmuir* **2001**, *17*, 2485.
(141) Laviron, E. *J. Electroanal. Chem.* **1979**, *101*, 19.
(142) Hong, H. G.; Park, W. *Bull. Korean Chem. Soc.* **2005**, *26*, 1885.

(143) Trammell, S. A.; Seferos, D. S.; Moore, M.; Lowy, D. A.; Bazan, G. C.; Kushmerick, J. G.; Lebedev, N. *Langmuir* **2007**, *23*, 942.
(144) Amatore, C.; Maisonhaute, E.; Schöllhorn, B.; Wadhawan, J. *Chem. Phys. Chem.* **2007**, *8*, 1321.
(145) Funt, B. L.; Hoang, P. M. *J. Electroanal. Chem.* **1983**, *154*, 229.
(146) Takada, K.; Gopalan, P.; Ober, C. K.; Abruna, H. D. *Chem. Mater.* **2001**, *13*, 2928.
(147) Sato, Y.; Fujita, M.; Mizutani, F.; Uosaki, K. *J. Electroanal. Chem.* **1996**, *409*, 145.
(148) Forster, R. J.; O'Kelly, J. P. *Electroanal. Chem.* **2001**, *498*, 127.
(149) Hong, H. G.; Park, W. *Bull. Korean Chem. Soc.* **2006**, *27*, 381.
(150) Finklea, H. O. *J. Electroanal. Chem.* **2001**, *495*, 79.
(151) Finklea, H. O. *J. Phys. Chem. B* **2001**, *105*, 8685.
(152) Marcus, R. A. *J. Chem. Phys.* **1965**, *43*, 679.
(153) Yu, H.-Z.; Wang, Y.-Q.; Cheng, J.-Z.; Zhao, J.-W.; Cai, S.-M.; Inokuchi, H.; Fujishima, A.; Liu, Z.-F. *Langmuir* **1996**, *12*, 2843.
(154) Trammell, S. A.; Lowy, D. A.; Seferos, D. S.; Moore, M.; Bazan, G. C.; Lebedev, N. *J. Electroanal. Chem.* **2007**, *23*, 942.
(155) Gordillo, G. J.; Schiffrin, D. J. *Faraday Discuss.* **2000**, *116*, 89.
(156) Marchal, D.; Boireau, W.; Laval, J.-M.; Bourdillon, C.; Moiroux, J. *J. Electroanal. Chem.* **1998**, *451*, 139.
(157) Because adsorbed behavior is observed, elementary rate constants k_{ei} (in cm s^{-1}) have to be replaced by elementary surface rate constants k_{si} (in s^{-1}).
(158) Inomata, T.; Abe, M.; Kondo, T.; Umakoshi, K.; Uosaki, K.; Sasaki, Y. *Chem. Lett.* **1999**, 1097.
(159) Uehara, H.; Abe, M.; Hisaeda, Y.; Uosaki, K.; Sasaki, Y. *Chem. Lett.* **2006**, *35*, 1178.
(160) Shutlz, D. A.; Tew, G. N. *J. Org. Chem.* **1994**, *59*, 6159.
(161) Finklea, H. O.; Haddox, R. M. *Phys. Chem. Chem. Phys.* **2001**, *3*, 3431.
(162) Haddox, R. M.; Finklea, H. O. *J. Electroanal. Chem.* **2003**, *550*, 351.
(163) Madhiri, N.; Finklea, H. O. *Langmuir* **2006**, *22*, 10643.
(164) Meyer, T. J.; Huynh, M. H.; Thorp, H. H. *Angew. Chem., Int. Ed.* **2007**, *46*, 5284.
(165) Ferguson-Miller, S.; Babcock, G. T. *Chem. Rev.* **1996**, *96*, 2889.
(166) Chang, M. C. Y.; Yee, C. S.; Stubbe, J.; Nocera, D. G. *Proc. Natl. Acad. Sci. U.S.A.* **2004**, *101*, 6882.
(167) Mayer, J. M. *Annu. Rev. Phys. Chem.* **2004**, *55*, 363.
(168) Cukier, R. I. *J. Phys. Chem.* **1996**, *100*, 15428.
(169) Cukier, R. I. *J. Phys. Chem. A* **1999**, *103*, 5989.
(170) Cukier, R. I. *J. Phys. Chem. B* **2002**, *106*, 1746.
(171) Cukier, R. I. *Biochim. Biophys. Acta: Bioenerg.* **2004**, *1655*, 37.
(172) Decornez, H.; Hammes-Schiffer, S. *J. Phys. Chem. A* **2000**, *104*, 9370.
(173) Iordanova, N.; Decornez, H.; Hammes-Schiffer, S. *J. Am. Chem. Soc.* **2001**, *123*, 3723.
(174) Hammes-Schiffer, S. *Acc. Chem. Res.* **2001**, *34*, 273.
(175) Hammes-Schiffer, S. Proton-coupled electron transfer. In *Electron Transfer in Chemistry, Vol. I. Principles, Theories, Methods, and Techniques*; Balzani, V., Ed.; Wiley-VCH: Weinheim, Germany, 2001.
(176) Iordanova, N.; Hammes-Schiffer, S. *J. Am. Chem. Soc.* **2002**, *124*, 4848.
(177) Webb, S. P.; Iordanov, T.; Hammes-Schiffer, S. *J. Chem. Phys.* **2002**, *117*, 4106.
(178) Pak, M. V.; Swalina, C.; Webb, S. P.; Hammes-Schiffer, S. *Chem. Phys.* **2004**, *304*, 227.
(179) Hammes-Schiffer, S.; Iordanova, N. *Biochim. Biophys. Acta: Bioenerg.* **2004**, *1655*, 29.
(180) Hatcher, E.; Soudackov, A.; Hammes-Schiffer, S. *J. Phys. Chem. B* **2005**, *109*, 18565.
(181) Soudackov, A.; Hatcher, E.; Hammes-Schiffer, S. *J. Chem. Phys.* **2005**, *122*, 014505.
(182) Hatcher, E.; Soudackov, A.; Hammes-Schiffer, S. *Chem. Phys.* **2005**, *319*, 93.
(183) Hammes-Schiffer, S. Proton-coupled electron transfer reactions: theoretical formulation and applications. In *Handbook of Hydrogen Transfer. Vol. 1: Physical and Chemical Aspects of Hydrogen Transfer*; Hynes, J., Limbach, H.-H., Eds.; Wiley-VCH: Weinheim, Germany, 2006.
(184) Hatcher, E.; Soudackov, A.; Hammes-Schiffer, S. *J. Am. Chem. Soc.* **2007**, *129*, 187.
(185) Stuchebrukhov, A. A.; Georgievskii, Y. *J. Chem. Phys.* **2000**, *113*, 10438.
(186) Shin, S.; Cho, S.-I. *Chem. Phys.* **2000**, *259*, 27.
(187) (a) Kuznetsov, A. M.; Ulstrup, J. *Russ. J. Electrochem.* **2003**, *39*, 9. (b) Kuznetsov, A. M.; Ulstrup, J. *Elektrokhimiya* **2003**, *39*, 11.
(188) Levich, V. G. In *Advances in Electrochemistry and Electrochemical Engineering*; Delahay, P., Tobias, C. W., Eds.; Wiley: New York, 1955; pp 250−371.
(189) Benderskii, V. A.; Grebenshchikov, S. Y. *J. Electroanal. Chem.* **1994**, *375*, 29.
(190) Grimmiger, J.; Bartenschlager, S.; Schmikler, W. *Chem. Phys. Lett.* **2005**, *416*, 316.
(191) Grimmiger, J.; Schmikler, W. *Chem. Phys.* **2007**, *334*, 8.
(192) Costentin, C.; Robert, M.; Savéant, J.-M. *J. Electroanal. Chem.* **2006**, *588*, 197.
(193) Borgis, D.; Hynes, J. T. *J. Phys. Chem.* **1996**, *100*, 1118.
(194) Borgis, D.; Hynes, J. T. *J. Chem. Phys.* **1993**, *170*, 315.
(195) Borgis, D.; Lee, S.; Hynes, J. T. *Chem. Phys. Lett.* **1989**, *162*, 19.
(196) Borgis, D.; Hynes, J. T. *J. Chem. Phys.* **1991**, *94*, 3619.
(197) Lee, S.; Hynes, J. T. *J. Chim. Phys.* **1996**, *93*, 1783.
(198) Suárez, A.; Silbey, R. *J. Chem. Phys.* **1991**, *94*, 4809.
(199) Klochikhin, V. L.; Trakhtenberg, L. I. *Chem. Phys. Lett.* **1998**, *285*, 34.
(200) Landau, L. *Phys. Z. Sowjetunion* **1932**, *2*, 46.
(201) Zener, C. *Proc. R. Soc. London, Ser. A* **1932**, *137*, 696.
(202) Costentin, C.; Robert, M.; Savéant, J.-M. *J. Am. Chem. Soc.* **2007**, *129*, 9953.
(203) Lippert, E. Z. *Z. Naturforsch., A* **1955**, *10*, 541.
(204) Mataga, N.; Kaifu, Y.; Koizumi, N. *Bull. Chem. Soc. Jpn.* **1956**, *29*, 465.
(205) Gosavi, S.; Marcus, R. A. *J. Phys Chem. B* **2000**, *104*, 2057.
(206) Marcus, R. A. In *Special Topics in Electrochemistry*; Rock, P. A., Ed.; Elsevier: New York, 1977, pp 151−179.
(207) Savéant, J.-M. In *Advances in Physical Organic Chemistry*; Tidwell, T. T., Ed.; Academic Press: New York, 2000; Vol. 35, pp 117−192.
(208) Chang, C. J.; Brown, J. D.; Chang, M. C. Y.; Baker, E. A.; Nocera, D. G. In *Electron Transfer in Chemistry*; Balzani, V., Ed.; Wiley-VCH: Weinheim, Germany, 2001; Vol. 3, Chapter 2.4, pp 409−461.
(209) Beratan, D. N.; Onuchic, J. N.; Winkler, J. R.; Gray, H. B. *Science* **1992**, *258*, 1740.
(210) Damrauer, N. H.; Hodgkiss, J. M.; Rosenthal, J.; Nocera, D. G. *J. Phys. Chem. B* **2004**, *108*, 6315.
(211) Hodgkiss, J. M.; Damrauer, N. H.; Rosenthal, J.; Nocera, D. G. *J. Phys. Chem. B* **2006**, *110*, 6315.
(212) Biczók, L.; Gupta, N.; Linschitz, H. *J. Am. Chem. Soc.* **1997**, *119*, 12601.
(213) Shukla, D.; Young, R. H.; Farid, S. *J. Phys. Chem. A* **2004**, *108*, 10386.
(214) Rhile, I. J.; Mayer, J. M. *J. Am. Chem. Soc.* **2004**, *126*, 12718.
(215) Rhile, I. J.; Markle, T. F.; Nagao, H.; DiPasquale, A. G.; Lam, O. P.; Lockwood, M. A.; Rotter, K.; Mayer, J. M. *J. Am. Chem. Soc.* **2006**, *128*, 6075.
(216) Mayer, J. M.; Rhile, I. J.; Larsen, F. B.; Mader, E. A.; Markle, T. F.; DiPasquale, A. G. *Photosynth. Res.* **2006**, *87*, 3.
(217) Markle, T. F.; Mayer, J. M. *Angew. Chem., Int. Ed.* **2007**, *47*, 738.
(218) Maki, T.; Araki, Y.; Ishida, Y.; Onomura, O.; Matsumura, Y. *J. Am. Chem. Soc.* **2001**, *123*, 3371.
(219) Benisvy, L.; Blake, A. J.; Collison, D.; Davies, E. S.; Garner, C. D.; McInnes, E. J. L.; McMaster, J.; Whittaker, G.; Wilson, C. *J. Chem. Soc., Dalton Trans.* **2003**, 1975.
(220) Lachaud, F.; Quaranta, A.; Pellegrin, Y.; Dorlet, P.; Charlot, M.-F.; Un, S.; Leibl, W.; Aukauloo, A. *Angew. Chem., Int. Ed.* **2005**, *44*, 1536.
(221) Costentin, C.; Robert, M.; Savéant, J.-M. *J. Am. Chem. Soc.* **2006**, *128*, 4552.
(222) Thomas, F.; Jarjayes, O.; Jamet, H.; Hamman, S.; Saint-Aman, E.; Duboc, C.; Pierre, J.-L. *Angew. Chem., Int. Ed.* **2004**, *43*, 594.
(223) Rhile, I. J.; Mayer, J. M. *Angew. Chem., Int. Ed.* **2005**, *44*, 598.
(224) Hillard, E.; Vessières, A.; Thouin, L.; Jaouen, G.; Amatore, C. *Angew. Chem., Int. Ed.* **2006**, *45*, 285.
(225) Chang, C. K.; Liu, H. Y.; Abdalmuhdi, I. *J. Am. Chem. Soc.* **1984**, *106*, 2725.
(226) Rosenthal, J.; Nocera, D. G. *Acc. Chem. Res.* **2007**, *40*, 543.
(227) Tarasevich, M. R.; Sadkowski, A.; Yeager, E. In *Comprehensive Treatise of Electrochemistry*; Conway, B. E., Bockris, J. O'M., Yeager, E., Kahn, S. U. M., White, R. E., Eds.; Plenum: New York, 1983; Vol. 7, pp 301−398.
(228) Kinoshita, K. In *Electrochemical Oxygen Technology*; Wiley: New York, 1992.
(229) Andrieux, C. P.; Hapiot, P.; Savéant, J.-M. *J. Am. Chem. Soc.* **1987**, *109*, 3768.
(230) Singh, P. S.; Evans, D. H. *J. Phys. Chem. B* **2006**, *110*, 637.
(231) Savéant, J.-M. *J. Phys. Chem. C* **2007**, *111*, 2819.
(232) Costentin, C.; Evans, D. H.; Robert, M.; Savéant, J.-M.; Singh, P. S. *J. Am. Chem. Soc.* **2005**, *127*, 12490.
(233) Makarycheva-Mikhailova, A. V.; Stanbury, D. M.; McKee, M. L. *J. Phys. Chem. B* **2007**, *111*, 6942.
(234) Reece, S. Y.; Nocera, D. G. *J. Am. Chem. Soc.* **2005**, *127*, 9448.
(235) Reece, S. Y.; Stubbe, J.; Nocera, D. G. *Biochim. Biophys. Acta* **2005**, *1706*, 232.
(236) Sjödin, M.; Styring, S.; Åkermark, B.; Sun, L.; Hammarström, L. *Philos. Trans. R. Soc. London, Ser. B* **2002**, *357*, 1471.

(237) Sjödin, M.; Ghanem, R.; Polivka, T.; Pan, J.; Styring, S.; Sun, L.; Sundström, V.; Hammarström, L. *Phys. Chem. Chem. Phys.* **2004**, *6*, 4851.
(238) Sjödin, M.; Styring, S.; Wolpher, H.; Xu, Y.; Sun, L.; Hammarström, L. *J. Am. Chem. Soc.* **2005**, *127*, 3855.
(239) Sjödin, M.; Irebo, T.; Utas, J. E.; Lind, J.; Merenyi, G.; Åkermark, B.; Hammarström, L. *J. Am. Chem. Soc.* **2006**, *128*, 13076.
(240) Fecenko, C. J.; Meyer, T. J.; Thorp, H. H. *J. Am. Chem. Soc.* **2006**, *128*, 11020.
(241) Carra, N.; Iordanova, N.; Hammes-Schiffer, S. *J. Am. Chem. Soc.* **2003**, *125*, 10429.
(242) Marcus, R. A. *J. Chem. Phys.* **1956**, *24*, 966.
(243) Krishtalik, L. I. *Biophys. Biochim. Acta* **2003**, *1604*, 13.
(244) Ishikita, H.; Soudackov, A. V.; Hammes-Schiffer, S. *J. Am. Chem. Soc.* **2007**, *129*, 11146.
(245) Irebo, T.; Reece, S. Y.; Sjödin, M.; Nocera, D., G.; Hammarström, L. *J. Am. Chem. Soc.* **2007**, *129*, 15462.
(246) Savéant, J.-M. In *Elements of Molecular and Biomolecular Electrochemistry*; Wiley-Interscience: Hoboken, NJ, 2006; pp 106−119.
(247) Weatherly, S. C.; Yang, I. V.; Thorp, H. H. *J. Am. Chem. Soc.* **2001**, *123*, 1236.
(248) Kuzmin, V. A.; Dourandin, A.; Shafirovich, V.; Geacintov, N. E. *Phys. Chem. Chem. Phys.* **2000**, *2*, 1531.
(249) Weatherly, S. C.; Yang, I. V.; Armistead, P. A.; Thorp, H. H. *J. Am. Chem. Soc.* **2001**, *123*, 1236.
(250) Kobayasho, K.; Tagawa, S. *J. Am. Chem. Soc.* **2003**, *125*, 10213.
(251) Steenken, S. *Chem. Rev.* **1989**, *89*, 503.
(252) Andrieux, C. P.; Savéant, J.-M. *J. Electroanal. Chem.* **1986**, *205*, 43.
(253) Andrieux, C. P.; Robert, M.; Saeva, F. D.; Savéant, J.-M. *J. Am. Chem. Soc.* **1994**, *116*, 7864.
(254) Pause, L.; Robert, M.; Savéant, J.-M. *J. Am. Chem. Soc.* **1999**, *121*, 7158.
(255) Antonello, S.; Maran, F. *J. Am. Chem. Soc.* **1999**, *121*, 7158.
(256) Costentin, C.; Hapiot, P.; Médebielle, M.; Savéant, J.-M. *J. Am. Chem. Soc.* **1999**, *121*, 4451.
(257) Costentin, C.; Robert, M.; Savéant, J.-M.; Teillout, A.-L. *ChemPhysChem*, in press.
(258) Armstrong, F. A.; Heering, H. A.; Hirst, J. *Chem. Soc. Rev.* **1997**, *26*, 469.
(259) Almeida, M. G.; Silveira, C. M.; Guigliarelli, B.; Bertrand, P.; Moura, J. J. G.; Moura, I.; Léger, C. *FEBS Lett.* **2007**, *581*, 284.
(260) Gwyer, J. D.; Richardson, D. J.; Butt, J. D. *J. Am. Chem. Soc.* **2005**, *127*, 14964.
(261) Armstrong, F. A.; Camba, R.; Heering, H. A.; Hirst, J.; Jeuken, L. J. C.; Jones, A. K.; Léger, C.; McEvoy, J. P. *Faraday Discuss.* **2000**, *116*, 191.
(262) Savéant, J.-M. In *Elements of Molecular and Biomolecular Electrochemistry*; Wiley-Interscience: Hoboken, NJ, 2006; pp 80−92.
(263) Murgida, D. H.; Hildebrandt, P. *J. Am. Chem. Soc.* **2001**, *123*, 4062.
(264) Hirst, J.; Duff, J. L. C.; Jameson, G. N. L.; Kemper, M. A.; Burgess, B. K.; Armstrong, F. A. *J. Am. Chem. Soc.* **1998**, *120*, 7085.
(265) Chen, K.; Hirst, J.; Camba, R.; Bonagura, C. A.; Stout, C. D.; Burgess, B. K.; Armstrong, F. A. *Nature* **2000**, *405*, 814.
(266) Camba, R.; Jung, Y.-S.; Hunsicker-Wang, L. M.; Burgess, B. K.; Stout, C. D.; Hirst, J.; Armstrong, F. A. *Biochemistry* **2003**, *42*, 10589.
(267) Jeuken, L. J. C.; Wisson, L-J.; Armstrong, F. A. *Inorg. Chim. Acta* **2002**, *331*, 216.
(268) Pankhurst, K. L.; Mowat, C. G.; Rothery, E. L.; Hudson, J. M.; Jones, A. K.; Miles, C. S.; Walkinshaw, M. D.; Armstrong, F. A.; Reid, G. A.; Chapman, S. K. *J. Biol. Chem.* **2006**, *281*, 20589.
(269) Robertson, D. E.; Farid, R. S.; Moser, C. C.; Urbauer, J. L.; Mulholland, S. E.; Pidikiti, R.; Lear, J. D.; Wand, A. J.; DeGrado, W. F.; Dutton, P. L. *Nature* **1994**, *368*, 425.
(270) Reddi, A. R.; Reedy, C. J.; Mui, S.; Gibney, B. R. *Biochemistry* **2007**, *46*, 291.
(271) Chen, X.; Disher, B. M.; Pilloud, D. L.; Gibney, B. R.; Moser, C. C.; Dutton, P. L. *J. Phys. Chem. B* **2002**, *106*, 617.
(272) Astuti, Y.; Topoglidis, E.; Briscoe, P. B.; Fantuzzi, A.; Gilardi, G.; Durrant, J. R. *J. Am. Chem. Soc.* **2004**, *126*, 8001.
(273) Rusling, J. F. *Acc. Chem. Res.* **1998**, *31*, 363.
(274) Alcantara, K.; Munge, B.; Pendon, Z.; Frank, H. A.; Rusling, J. F. *J. Am. Chem. Soc.* **2006**, *128*, 14930.
(275) Tsukihara, T.; Aoyama, H.; Yamashita, E.; Tomizaki, T.; Yamaguchi, H.; Shinzawa-Itoh, K.; Nakashima, R.; Yaono, R.; Yoshikawa, S. *Science* **1995**, *269*, 1069.
(276) Tsukihara, T.; Aoyama, H.; Yamashita, E.; Tomizaki, T.; Yamaguchi, H.; Shinzawa-Itoh, K.; Nakashima, R.; Yaono, R.; Yoshikawa, S. *Science* **1996**, *272*, 1136.
(277) Yoshikawa, S.; Shinzawa-Itoh, K.; Nakashima, R.; Yaono, R.; Yamashita, E.; Inoue, N.; Yao, M.; Fei, M. J.; Libeu, C. P.; Mizushima, T.; Yamaguchi, H.; Tomizaki, T.; Tsukihara, T. *Science* **1998**, *280*, 1723.
(278) Iwata, S.; Ostermeier, C.; Ludwig, B.; Michel, H. *Nature* **1995**, *376*, 660.
(279) Ostermeier, C.; Harrenga, A.; Ermler, U.; Michel, H. *Proc. Natl. Acad. Sci. U.S.A.* **1997**, *94*, 10547.
(280) Yoshikawa, S.; Shinzawa-Itoh, K.; Tsukihara, T. *J. Inorg. Biochem.* **2000**, *82*, 1.
(281) Collman, J. P.; Devaraj, N. K.; Decreau, R. A.; Yang, Y.; Yan, Y.-L.; Ebina, W.; Eberspacher, T. A.; Chidsey, C. E. D. *Science* **2007**, *315*, 1565.

CR068065T